COLEGIO DE POSTGRADUADOS

INSTITUCIÓN DE ENSEÑANZA E INVESTIGACIÓN EN CIENCIAS AGRÍCOLAS

CAMPUS MONTECILLO

POSTGRADO EN CIENCIAS FORESTALES

ANÁLISIS ESPACIO-TEMPORAL DEL CRECIMIENTO, FISIOLOGÍA Y CONSTITUCIÓN QUÍMICA DE LA MADERA EN BOSQUES DE ALTA MONTAÑA

ARIAN CORREA DÍAZ

T E S I S
PRESENTADA COMO REQUISITO PARCIAL
PARA OBTENER EL GRADO DE:

DOCTOR EN CIENCIAS

MONTECILLO, TEXCOCO, ESTADO DE MÉXICO

2019

COLEGIO DE POSTGRADUADOS

INSTITUCIÓN DE ENSEÑANZA E INVESTIGACIÓN EN CIENCIAS AGRÍCOLAS

CARTA DE CONSENTIMIENTO DE USO DE LOS DERECHOS DE AUTOR Y DE LAS REGALÍAS COMERCIALES DE PRODUCTOS DE INVESTIGACIÓN

En adición al beneficio ético, moral y académico que he obtenido durante mis estudios en el Colegio de Postgraduados, el que suscribe, **Arian Correa Díaz**, Alumno de esta Institución, estoy de acuerdo en ser partícipe de las regalías económicas y/o académicas, de procedencia nacional e internacional, que se deriven del trabajo de investigación que realicé en esta institución, bajo la dirección del Profesor **Dr. Armando Gómez Guerrero**, por lo que otorgo los derechos de autor de mi tesis "**Análisis espacio-temporal del crecimiento, fisiología y constitución química de la madera en bosques de alta montaña**", y de los productos de dicha investigación al Colegio de Postgraduados. Las patentes y secretos industriales que se puedan derivar serán registrados a nombre del Colegio de Postgraduados y las regalías económicas que se deriven serán distribuidas entre la Institución, El Consejero o Director de Tesis y el que suscribe, de acuerdo a las negociaciones entre las tres partes, por ello me comprometo a no realizar ninguna acción que dañe el proceso de explotación comercial de dichos productos a favor de esta Institución.

Montecillo, Texcoco, Estado de México, a 08 de noviembre de 2019

Arian Correa Díaz

Vo. Bo. Dr. Armando Gómez Guerrero

La presente tesis titulada: ***"Análisis espacio-temporal del crecimiento, fisiología y constitución química de la madera en bosques de alta montaña***" realizada por el alumno: **Arian Correa Díaz** bajo la dirección del Consejo Particular indicado, ha sido aprobada por el mismo y aceptada como requisito parcial para obtener el grado de:

DOCTOR EN CIENCIAS
CIENCIAS FORESTALES

CONSEJO PARTICULAR

CONSEJERO (A)
DR. ARMANDO GÓMEZ GUERRERO

ASESOR (A)
DR. JESÚS VARGAS HERNÁNDEZ

ASESOR (A)
DR. WILLIAM R. HORWATH

ASESOR (A)
DR. JAVIER SUÁREZ ESPINOZA

ASESOR (A)
DR. JOSÉ VILLANUEVA DÍAZ

ASESOR (A)
DR. ALEJANDRO VELÁZQUEZ MARTÍNEZ

Montecillo, Texcoco, Estado de México, noviembre de 2019

ANÁLISIS ESPACIO-TEMPORAL DEL CRECIMIENTO, FISIOLOGÍA Y CONSTITUCIÓN QUÍMICA DE LA MADERA EN BOSQUES DE ALTA MONTAÑA

Arian Correa Díaz, Dr.

Colegio de Postgraduados, 2019

RESUMEN

El análisis retrospectivo de características en los anillos de crecimiento anual nos permite entender y anticipar los efectos de cambio climático en los ecosistemas forestales. Bajo un escenario de fenómenos climáticos extremos, temperaturas más cálidas y un aumento en las emisiones de gases de efecto invernadero, los bosques de alta montaña son ecosistemas vulnerables. Para avanzar en el conocimiento de este campo, se investigaron las respuestas espacio-temporales de *Pinus hartwegii* Lindl. en dos montañas del centro de México. Primero, se combinaron mediciones de anchura de los anillos con información de sensores remotos para cuantificar como los bosques responden a la variabilidad climática a través de gradientes altitudinales. Se encontró una disminución en el crecimiento a partir de mediados del siglo XX y un patrón divergente en las tendencias del índice de vegetación de diferencias normalizadas (NDVI). Sin embargo, se encontró una correlación significativa entre la anchura de los anillos y NDVI. Segundo, se probó el vínculo entre las respuestas fisiológicas de *P. hartwegii* y la actividad fotosintética (derivada de NDVI) a través de un gradiente altitudinal. Se observó una disminución en la composición de isótopos de carbono y oxígeno ($\delta^{13}C$, y $\delta^{18}O$), una discriminación contra carbono sin cambios ($\Delta^{13}C$), y un aumento en la eficiencia de uso de agua (EUAi). Sin embargo, todas las variables fisiológicas fueron afectadas por un evento de sequía extrema, independientemente de su posición espacial. Las composiciones de $\delta^{13}C$, y $\delta^{18}O$ estuvieron correlacionadas con NDVI, durante la estación de otoño-invierno del año anterior y el principio de la estación de crecimiento. Finalmente, se analizaron los ajustes en la densidad de la madera y los vínculos con información de sensores remotos. Se encontró un incremento en la densidad mínima y la presencia de anillos más densos después de 1950. El NDVI presento las correlaciones más altas con densidad máxima (MXD), sin embargo, las condiciones de micrositio modulan esta relación.

Palabras clave: Dendroecología, cambio climático, bosques de alta montaña, limite arbóreo, NDVI

SPATIO-TEMPORAL ANALYSIS OF TREE GROWTH, PHYSIOLOGY AND CHEMICAL COMPOSITION OF WOOD AT HIGH-MOUNTAIN FORESTS

Arian Correa Díaz, Dr.

Colegio de Postgraduados, 2019

ABSTRACT

The retrospective analysis of tree-ring traits allows to understand and foresee climate change effects on forest ecosystems. Under a scenario of extreme weather events, warmer temperatures and rising greenhouse gas emissions, the high-mountain forests are highly vulnerable ecosystems. To advance knowledge in this field, we focused on the spatio-temporal responses of *Pinus hartwegii* Lindl. at two mountains in central México. First, we combine tree-ring measurements to remotely sensed data to quantify how forests responded to climate variability across altitudinal gradients. We found a common growth trend decrease around the middle 20th century and divergent normalize difference vegetation index (NDVI) trends at high-elevations. However, a significant correlation was detected between tree-ring widths and NDVI. Second, we tested the link between physiological responses of *P.hartwegii* and the photosynthetic activity (NDVI-derived) across altitudinal gradients. We saw a decrease in carbon and oxygen isotopic ratios ($\delta^{13}C$, and $\delta^{18}O$), a stable carbon isotope discrimination ($\Delta^{13}C$), and a rising intrinsic water use efficiency (iWUE). Nevertheless, all physiological parameters unequivocally showed changes during an extreme drought event regardless of spatial position. Carbon and oxygen isotope ratios were correlated with NDVI mainly for the previous fall-winter season and for the beginning of the growing season. Finally, we analyzed tree-ring wood density adjustments and the links with remotely sensed variables. We found an increase in minimum wood density and denser rings after 1950. NDVI exhibited the strongest correlations with maximum latewood density (MXD), however, microsite conditions shape this relationship.

Keywords: Dendroecology, climate change, high-elevation forests, tree-line, NDVI

AGRADECIMIENTOS

Al **Consejo Nacional de Ciencia y Tecnología (CONACYT)** por el apoyo económico para el desarrollo de mis estudios de postgrado.

Al **Colegio de Postgraduados**, en especial al **Programa Forestal** por el respaldo y la oportunidad de estudiar en tan importante institución.

A la **Universidad de California, Davis**, en especial al personal del **Departament of Land, Air and Water Resources** por la experiencia de estudiar y desarrollar con éxito mi estancia de investigación en tan prestigiosa universidad.

Al **Proyecto ECOS-NORD México-Francia "Impacto del cambio climático en la adaptación y plasticidad fenotípica del crecimiento en árboles forestales"** por el apoyo logístico y económico para el desarrollo de una estancia de investigación en Francia.

Al personal de la **Unidad de Investigación de Genética y Fisiología Forestal del INRA Val de Loire en Orléans, Francia** por la capacitación y las facilidades otorgadas en el uso de sus instalaciones.

Al personal del **Laboratorio de Dendrocronología-INIFAP CENID-RASPA**, Durango por sus atenciones y apoyo para el procesamiento de muestras dendrocronológicas.

Al **Consejo Mexiquense de Ciencia y Tecnología (COMECYT)** por el financiamiento para la asistencia a un congreso internacional.

Al **Dr. Armando Gómez Guerrero**, por su respaldo, orientación, conocimientos y dedicación en la dirección de esta tesis. Profundamente agradecido por haberme permitido ser su alumno durante estos años

Al **Dr. Jesús Vargas Hernández**, por sus valiosas aportaciones y comentarios en el desarrollo de esta investigación. Así mismo, extremadamente agradecido por haberme considerado dentro del proyecto ECOS-NORD.

Al **Dr. William R. Horwath**, por sus excelentes aportes en la mejora sustancial de esta investigación. Además, por haberme permitido ser parte de su laboratorio y el respaldo económico otorgado para cumplir todas las metas planteadas.

Al **Dr. Javier Suarez Espinosa**, por sus valiosas lecciones en el campo de la estadística y útiles consejos para mi formación profesional.

Al **Dr. José Villanueva Díaz**, por sus amplios conocimientos y participación clave en esta investigación. Gracias por las facilidades en su laboratorio y su inagotable labor de investigación que nos impulsa a mejorar continuamente.

Al **Dr. Alejandro Velázquez Martínez**, por su experiencia, valiosos comentarios y aliento en no claudicar en la presente investigación.

A los **Dres. Lucas C. R. Silva** y **Philippe Rozenberg,** que, si bien no formaron parte de mi consejo particular, contribuyeron sustancialmente en la investigación y mi formación académica.

Al personal investigador del **INIFAP CENID-COMEF,** por la oportunidad de integrarme a tan importante centro de investigación.

DEDICATORIA

A mis padres, Víctor y Ana por su cariño, enseñanzas y consejos.

A mis hermanos, Omar y Erandy por su apoyo incondicional.

A Carmina por su amor y comprensión en estos años.

A Ana Eliette, por dar un nuevo sentido en mi vida.

A mis amigos y familia, muchas gracias.

CONTENIDO

LISTA DE CUADROS

LISTA DE FIGURAS

INTRODUCTION

The effects of climate change on forest ecosystems are reflected in different ways including variations in geographical distribution, tree growth, plant vigor, and physiological performance (Kullman, 2001; Parmesan, 2006; Peñuelas *et al.*, 2011). These environmental variations are becoming more frequent, especially along the ecosystem's edges, where plant communities are close to their physiological tolerance such as high-elevation forests (Holtmeier, 2009; Körner, 2012). In México, the high-elevation forests are inhabited by *Pinus hartwegii* Lindl., a fire-adapted tree species that grows from 3000 to 4100 m asl (Perry, 1991). Therefore, the natural distribution of *P. hartwegii* makes this ecosystem highly vulnerable to global warming due to habitat reduction (Gómez-Mendoza and Arriaga, 2007; Ricker *et al.*, 2007) and inherent physiological thresholds (Sáenz-Romero *et al.*, 2013).

Climate change is influencing several processes like increases atmospheric CO_2 concentrations, elevated temperatures, altered precipitation patterns, and the occurrence of more extreme weather events (IPCC, 2013; Blunden and Arndt, 2018). Under this climatic outlook, high-elevation forests are adjusting their physiology performance affecting tree growth, canopy vigor and wood structure traits (Körner, 2012). For example, some studies suggest an increase in gross primary productivity and a greening effect as CO_2 increases and soil water content remains stable (Keenan *et al.*, 2013; Zhu *et al.*, 2016). Other studies have reported a tree-line shift to upper elevations and a growth surge due to warmer conditions (Salzer *et al.*, 2009; Silva *et al.*, 2016). However, to understand how climate change will affect Mexican high-elevation forests, multi-proxy studies that allow us to understand the dynamics of tree species temporally and spatially are needed.

Traditionally, to study past climate variability impacts on forest ecosystems, tree-ring information has been used (i.e. dendrochronology). Tree-rings provide an excellent source of climatic information because they can be related to annual dominant climatic factors, reflecting major environmental changes (Fritts, 1976). Indeed, the chemical composition of wood, using stable isotopes (e.g. carbon and oxygen), is also a powerful

tool to investigate physiological responses associated with changes in the atmosphere. While stable isotope carbon ($\delta^{13}C$) in tree-rings has been related to hydric status and changes in water use efficiency (ratio of CO_2 fixation per unit of water) over time, the oxygen isotopic composition ($\delta^{18}O$) of tree-rings is expected to reflect the source water and evapotranspiration rates (McCarroll and Loader, 2004). In addition to that, wood structure traits such as wood density are also suitable to capture the historical plant responses to climate variations (Granda *et al.*, 2017). For example, maximum latewood density (MXD) is recognized to reconstruct past growing season temperatures while minimum earlywood density (MID) helps to understand water transport efficiency (Camarero *et al.*, 2014; Camarero and Gutiérrez, 2017). Finally, a complementary strategy to understand the effects of climate change on forest ecosystems is the use of vegetation indexes derived from remotely sensed information. A common vegetation index is the normalized difference vegetation index (NDVI, portion of red and near-infrared light reflected by a plant canopy). The NDVI is an indirect measure of photosynthetic activity at landscapes scales that shows a strong correlation with forest growth parameters (Tucker, 1979; Wang *et al.*, 2004).

In this work, we tested a novel multi-proxy approach, that incorporates variables related to physiological process (e.g. stable isotope ratios in tree-rings), spatial canopy status (e.g. remotely sensed variables) and anatomical wood properties (e.g. minimum earlywood or maximum latewood density) to customary dendrochronology techniques; presenting a new opportunity to assess and predict high-elevation forests responses in central Mexico to climate variability and potential biogeochemical changes over spatio-temporal scales (Castillo *et al.*, 2015; Maxwell *et al.*, 2018; Levesque *et al.*, 2019). This work was integrated by three chapters on a manuscript format where the first was focused to assess forest productivity changes and the link with remotely sensed information under warming conditions detected over the last decades. The second chapter relies on the physiological adjustment of *P. hartwegii* to rising CO_2 using stable isotope information and NDVI time series. The third chapter explored the wood density adjustment to climate variability and links with different remotely sensed variables. The first two chapters were developed at Tlaloc Mountain (Texcoco, State of México) whereas the last one was

carried out in two locations (Tlaloc Mountain and Jocotitlán, State of Mexico). Final remarks were included at the end of the text, to summarize important findings and highlights of the research.

General objective

To test a multi-proxy approach able to assess spatial and temporal responses in high-elevation forests in central México focused on a comprehensive understanding of their ecological performance under ongoing climate variability.

Specific objectives

i. To assess forest growth trends along an altitudinal gradient and to link with remotely sensed information in order to construct a robust vegetation trend analysis at a high-elevation forests in central México.

ii. To determine how altitude and aspect drive the *P. hartwegii* physiological behavior using tree-ring isotopic information and establish links with an NDVI time series from 2000 to 2016.

iii. To evaluate temporal trends and stability in tree-ring wood density profiles along an altitudinal gradient in two high-elevation forests and estimate links with different remotely sensed variables.

Hypothesis

i. Recent warming conditions coupled with rising CO_2 are traduced in forest growth increases mainly at the upper position of the tree line. Furthermore, a greening effect can be expected using an NDVI trend analysis. Finally, a robust link between tree-ring widths and NDVI allows reconstructing the canopy vigor for the last century.

ii. A topographic effect (altitude and aspect) on the physiological performance of *P. hartwegii* can be anticipated using the established patterns documented in other forests. Furthermore, the intrinsic water use efficiency (iWUE) is strongly correlated to NDVI, which allows a more comprehensive understanding of tree adaptation to climate variability.

iii. A temporal adjustment in tree-ring wood density is expected to be similar in two high-elevation forest closely located. Besides that, maximum latewood density (MXD) should tracks the NDVI behavior on the late growing season while the earlywood density (MID) is linked to previous year conditions.

References

Blunden, J. and D. S. Arndt. 2018. State of the climate in 2017. Bulletin American Meteorology Society 99: 332.

Camarero, J. J. and E. Gutiérrez. 2017. Wood density of silver fir reflects drought and cold stress across climatic and biogeographic gradients. Dendrochronologia 45: 101-112.

Camarero, J. J., V. Rozas, J. M. Olano and J. M. Fernández- Palacios. 2014. Minimum wood density of juniperus thurifera is a robust proxy of spring water availability in a continental mediterranean climate. Journal of Biogeography 41: 1105-1114.

Castillo, J. d., J. Voltas and J. P. Ferrio. 2015. Carbon isotope discrimination, radial growth, and ndvi share spatiotemporal responses to precipitation in aleppo pine. Trees: Structure and Function 29: 223-233.

Fritts, H. C. 1976. Tree rings and climate. Academic Press Inc, London. 567 pp.

Gómez-Mendoza, L. and L. Arriaga. 2007. Modeling the effect of climate change on the distribution of oak and pine species of mexico. Conservation Biology 21: 1545-1555.

Granda, E., J. J. Camarero, J. D. Galván, G. Sangüesa-Barreda, A. Q. Alla, E. Gutierrez, I. Dorado-Liñán, L. Andreu-Hayles, I. Labuhn, H. Grudd and J. Voltas. 2017. Aged but withstanding: Maintenance of growth rates in old pines is not related to enhanced water-use efficiency. Agricultural and Forest Meteorology 243: 43-54.

Holtmeier, F.-K. 2009. Mountain timberlines: Ecology, patchiness, and dynamics. Springer Science & Business Media. 421 pp.

IPCC. 2013. Climate change 2013: The physical science basis. Summary for policymakers. Cambridge University Press. London. 231 pp.

Keenan, T. F., D. Y. Hollinger, G. Bohrer, D. Dragoni, J. W. Munger, H. P. Schmid and A. D. Richardson. 2013. Increase in forest water-use efficiency as atmospheric carbon dioxide concentrations rise. Nature 499: 324.

Körner, C. 2012. Alpine treelines. Springer Basel. 220 pp.

Kullman, L. 2001. 20th century climate warming and tree-limit rise in the southern scandes of sweden. AMBIO: A Journal of the Human Environment 30: 72-80.

Levesque, M., L. Andreu-Hayles, W. K. Smith, A. P. Williams, M. L. Hobi, B. W. Allred and N. Pederson. 2019. Tree-ring isotopes capture interannual vegetation productivity dynamics at the biome scale. Nature Communications 10: 742.

Maxwell, T. M., L. C. R. Silva and W. R. Horwath. 2018. Integrating effects of species composition and soil properties to predict shifts in montane forest carbon–water relations. Proceedings of the National Academy of Sciences.

McCarroll, D. and N. J. Loader. 2004. Stable isotopes in tree rings. Quaternary Science Reviews 23: 771-801.

Parmesan, C. 2006. Ecological and evolutionary responses to recent climate change. Annual Review of Ecology, Evolution, and Systematics 37: 637-669.

Peñuelas, J., J. G. Canadell and R. Ogaya. 2011. Increased water-use efficiency during the 20th century did not translate into enhanced tree growth. Global Ecology and Biogeography 20: 597-608.

Perry, J. P. 1991. The pines of mexico and central america. Timber Press. Portland, Oregon. 231 pp.

Ricker, M., G. Gutierrez-Garcia and D. C. Daly. 2007. Modeling long-term tree growth curves in response to warming climate: Test cases from a subtropical mountain forest and a tropical rainforest in mexico. Canadian Journal of Forest Research 37: 977-989.

Sáenz-Romero, C., J.-B. Lamy, E. Loya-Rebollar, A. Plaza-Aguilar, R. Burlett, P. Lobit and S. Delzon. 2013. Genetic variation of drought-induced cavitation resistance among pinus hartwegii populations from an altitudinal gradient. Acta Physiologiae Plantarum 35: 2905-2913.

Salzer, M. W., M. K. Hughes, A. G. Bunn and K. F. Kipfmueller. 2009. Recent unprecedented tree-ring growth in bristlecone pine at the highest elevations and possible causes. Proceedings of the National Academy of Sciences 106: 20348-20353.

Silva, L. C. R., G. Sun, X. Zhu-Barker, Q. Liang, N. Wu and W. R. Horwath. 2016. Tree growth acceleration and expansion of alpine forests: The synergistic effect of atmospheric and edaphic change. Science Advances 2.

Tucker, C. J. 1979. Red and photographic infrared linear combinations for monitoring vegetation. Remote Sensing of Environment 8: 127-150.

Wang, J., P. M. Rich, K. P. Price and W. D. Kettle. 2004. Relations between ndvi and tree productivity in the central great plains. International Journal of Remote Sensing 25: 3127-3138.

Zhu, Z., S. Piao, R. B. Myneni, M. Huang, Z. Zeng, J. G. Canadell, P. Ciais, S. Sitch, P. Friedlingstein, A. Arneth, C. Cao, L. Cheng, E. Kato, C. Koven, Y. Li, X. Lian, Y. Liu, R. Liu, J. Mao, Y. Pan, S. Peng, J. Peñuelas, B. Poulter, T. A. M. Pugh, B. D. Stocker, N. Viovy, X. Wang, Y. Wang, Z. Xiao, H. Yang, S. Zaehle and N. Zeng. 2016. Greening of the earth and its drivers. Nature Climate Change 6: 791.

CHAPTER I. LINKING REMOTE SENSING AND DENDROCHRONOLOGY TO QUANTIFY CLIMATE-INDUCED SHIFTS IN HIGH-ELEVATION FORESTS OVER SPACE AND TIME[1]

1.1. Resumen

Es bien sabido que el crecimiento arbóreo es afectado fuertemente por el clima a altas elevaciones, pero aún permanece desconocido como la variabilidad climática influye en la distribución y funcionamiento de ecosistemas forestales de alta montaña. Para avanzar en el conocimiento de este campo, se combinaron datos temporales (series de anillos de crecimiento de árboles) y datos espaciales (variables de sensores remotos) para cuantificar como los bosques han respondido a la variabilidad climática a lo largo de un gradiente altitudinal en el centro de México. El índice de vegetación de diferencia normalizada (NDVI), series dendrocronológicas de anchura de anillo y datos climáticos a nivel sitio se utilizaron en un análisis de tendencia del verdor en la vegetación, y la reconstrucción del vigor del dosel para el último siglo. A pesar de desarrollar una cronología de anchura de anillo común a nivel montaña (Tláloc – Estado de México), se encontraron diferencias significativas a nivel sitio en crecimiento arbóreo, donde árboles jóvenes (<100 años) presentaron tendencias de crecimiento sin un patrón altitudinal. Sin embargo, los árboles maduros (100-200 años) presentaron una disminución común en el crecimiento a mediados del siglo XX, independientemente de su altitud. El análisis de tendencia en las anomalías máximas anuales de NDVI no mostró un efecto generalizado de enverdecimiento a mayores altitudes. Por tanto, el bosque presentó ambas tendencias (*greening* y *browning*) denotando variabilidad espacial en el vigor arbóreo. Además, la temperatura del año previo tuvo un efecto positivo tanto en NDVI como en el índice de anchura de anillo (IAA), aunque negativo al inicio de la estación de crecimiento. La relación significativa entre el NDVI de invierno-primavera (diciembre a marzo) e IAA ($r = 0.64$, $p < 0.05$), fue útil para reconstruir el vigor del dosel para los últimos 151 años. Por lo anterior, el efecto de enverdecimiento derivado del análisis de NDVI debe ser cautelosamente interpretado como un incremento en el crecimiento arbóreo. Estos resultados resaltan el potencial de integrar información de sensores remotos y métodos

[1] Artículo publicado en Journal of Geophysical Research: Biogeosciences. 2019. 124:1-18

dendrocronológicos para mejorar las predicciones de la distribución y funcionamiento de los ecosistemas forestales.
Palabras clave: Bosques de alta montaña, *Pinus hartwegii*, dendroecología, NDVI

1.2. Abstract

It is well known that tree growth is strongly affected by climate at high-elevations, but it is still unclear how climate variability influences the distribution and function of montane forest ecosystems. To advance knowledge in this field, we combined temporal (tree-ring measurements) and spatial data (remotely-sensed variables), to quantify how forests responded to climatic variability across altitudinal gradients in Central Mexico. Normalized difference vegetation index (NDVI), tree-ring chronologies and site-level climatic data were used in a vegetation trend analysis of greenness and browning, and to reconstruct the canopy vigor for the last century. Although a common ring-width chronology was developed (Tláloc – State of México), we found significant site-depended forest growth response, where young trees (<100 years) exhibited heterogeneous growth trends, without an altitudinal pattern. However, mature trees (100-200 years) showed a common growth decline during the mid-20th century, regardless of their altitude. Annual maximum NDVI anomalies did not show a general greening effect at high-elevations. The forest showed both, greening and browning zones denoting spatial variability in tree vigor. Furthermore, temperature from the previous year had a positive effect on both NDVI and ring-width index (RWI), but negative at beginning of the growing season. The significant relationship between winter-spring NDVI (December to March) and RWI ($r=0.64$, $p<0.05$), was useful to reconstruct the canopy vigor for the last 151 years. Thus, the greening effect derived from NDVI should be carefully interpreted as a direct forest growth increase. These results highlight the potential of integrating remotely-sensed and dendrochronological methods to improve predictions of forest ecosystem distribution and function.
Keywords: High-elevation forests, *Pinus hartwegii*, dendroecology, NDVI

1.3. Introduction

The spatio-temporal analysis of tree growth and its relationship with remotely-sensed ecosystem parameters can be a powerful tool to assess the status of forest resources and to understand the ongoing effects of climate change. Tree-line ecotones in high-elevation forests are especially sensitive to climate variations effects (Salzer *et al.*, 2009; Körner, 2012) which exert dominant control over forest productivity and tree water status (Körner, 2017; Silva, 2017; Maxwell *et al.*, 2018). Previous studies have shown that variation in precipitation, temperature, and atmospheric CO_2 concentration can result in unexpected changes in tree growth for many montane species, causing measurable ecosystem transformations (Körner, 2012; Gómez-Guerrero *et al.*, 2013; Silva *et al.*, 2016; Matías *et al.*, 2017). To evaluate whether and how such ecosystem transformations can be anticipated from a combination of tree ring data and remote sensing tools, we carried out a study in a high-elevation forest in Central Mexico. We tested the potential for connecting dendrochronological information to remotely-sensed variables in a forest dominated by *Pinus hartwegii* Lindl., a tree species that grows at elevations between 3,000 and 4,100 m above the sea level, on volcanic soils (Perry, 1991).

The natural distribution of *P. hartwegii* makes this species vulnerable to climate variation effects as the shallow and coarse-textured soils where it grows, are critical to assure water availability for tree growth (Biondi *et al.*, 2005). Negative effects from climate change might reduce the habitat of high-elevation forests because the colonization toward higher altitudes is limited for soil depth and by their biological range limit (Ricker *et al.*, 2007; Saenz-Romero *et al.*, 2013; Villanueva-Díaz *et al.*, 2015).

The rationale for this study comes from the need for long-term and geographical trends of vegetation response to climate variation in remote and high-altitude forests. These trends can be built by natural archives of tree-rings and remotely-sensed data (Vicente-Serrano *et al.*, 2016; Shunsuke and Atsuko, 2018). Connecting spatial (from remote sensing) and temporal (from tree-rings) information is essential to understand regional changes in forest productivity and carbon sequestration as climate change occurs. Because historical and instrumental records for climate variables are limited in high-

elevation forest sites, the combination of tree-ring and proxies of the ecosystem functionality might be useful to reconstruct changes in forest growth, distribution and function. For example, Silva *et al.* (2016) found that under certain conditions changes in tree growth can be used to anticipate the expansion of forest ecosystems in alpine ecotones in response to the effect of increasing CO_2 and warming-induced permafrost thaw. However, changes in productivity, are often negative in alpine ecotones when soil nutrients and water regimes become progressively limited under warmer climates (Gómez-Guerrero *et al.*, 2013; Silva and Anand, 2013; Maxwell *et al.*, 2018). In either scenario, changes in tree growth can be used to generate early warning signals of climate-induced ecosystem change.

To use tree-ring data as a proxy for forest expansion or decline, remotely-sensed metrics of ecosystem productivity, i.e. Normalized Difference Vegetation Index (NDVI), can be used to assess forest responses to climate in terms of magnitude and direction of changes in ecosystem distribution. The NDVI, derived from the ratio between red and near-infrared light reflected by a plant canopy, is an indirect measurement of photosynthesis and forest productivity (Miyeni *et al.*, 1995). The NDVI also correlates with leaf area index, photosynthesis, plant phenology, carbon isotope indices and more recently used for vegetation trend analysis (Lopatin *et al.*, 2006; Leavitt *et al.*, 2008; Liang *et al.*, 2009; Baird *et al.*, 2012; Karkauskaite *et al.*, 2017). These dynamics reflect NDVI trends which could be positive (greenness effect) or negative (browning trend), implying either stimulation or decline on photosynthetic activity and productivity (Goetz *et al.*, 2005; Beck and Goetz, 2011). However, despite the potential of the NDVI to assess seasonal changes and vegetation dynamics at regional scales (Eastman *et al.*, 2013; Krishnaswamy *et al.*, 2014), it is not until recent decades that a promising research field have related remotely sensed parameters to direct field dendrochronological measurements (Babst *et al.*, 2010; Berner *et al.*, 2013; Bunn *et al.*, 2013; Vicente-Serrano *et al.*, 2016; Bhuyan *et al.*, 2017; Coulthard *et al.*, 2017; Wang *et al.*, 2017; Brehaut and Danby, 2018); but notably, none did so in high-elevation regions of temperate forest. Moreover, these previous investigations have been focused in high-latitude forests at regional scales, so that there is still a large gap in relating remotely-sensed information

to tree ring variables using local specific conditions to improve our mechanistic understanding and ability to quantify the impact of climate on montane forest and their essential functions.

In this study, we correlate tree-ring information of *P. hartwegii*, a tree-line species, from Iztaccíhuatl-Popocatépetl National Park to both remote sensing (NDVI, and LAI) and climatic variables (temperature, precipitation, and growing-days) to yield a robust vegetation trend analysis and reconstruct canopy vigor for the last century. Canopy vigor here understood as an expression of photosynthetic activity reflected by foliar index (Xu *et al.*, 2012). We hypothesize that due to warmer conditions detected for the study site in the last decades (Lobato-Sánchez and Altamirano-del-Carmen, 2017) the following responses should occur: (i) high-elevation forest growth has increased in tandem with temperature such that a greening effect is expected in NDVI and tree basal area increments (BAI), especially at North facing high altitudinal sites where low temperatures can limit tree growth, (ii) the influence of climatic variables (such as maximum and minimum temperature) on NDVI can be anticipated based on tree-ring growth according to the geographic position of samples across the landscape, (iii) the combined information from tree-rings and remote sensing is statistically significant and sufficiently robust to reconstruct stand-level sensitivity for high-elevation *P. hartwegii* forests during the last century.

1.4. Materials and Methods

1.4.1. Study area

The study site is at the Tlaloc Mountain, in central Mexico with coordinates of 19.39° N and -98.74°W and 4,125 m of elevation (Figure 1.1). This Mountain belongs to the Iztaccíhuatl-Popocatépetl National Park, which is an important forest ecosystem in the basin of the State of Mexico. The climate is classified as temperate, sub-humid, mild to cool with mean annual temperature and annual rainfall ranging from 7 to 9°C and 800 to 1,200 mm, respectively. Thus, the climate can be characterized as *C* (w^2)(*w)* according to Köppen climate classification as modified by García (2004). However, according to the reconstructed values by Wang *et al.* (2016), average increases of 1.4°C and 150 mm

have been detected for the last century in the study site (Figure 1. 2). Forest ecosystems are distributed as follows: from 2800-3200 masl, the vegetation is represented by *Abies religiosa* (Kunth) Schtdl and above of 3,500 m of elevation, a pure stand of *Pinus hartwegii* is the dominant tree vegetation. For the dendrochronological information, we selected *P. hartwegii* undisturbed stands at two elevations and aspects. Field sites were carefully chosen in each of two altitudinal levels: (i) 3500 m representing the middle distribution range for *P. hartwegii* and (ii) 3900 m, at the upper distribution range, where the species is assumed to be close to its physiological tolerance (Acosta Mireles *et al.*, 2014; Alfaro-Ramírez *et al.*, 2017). At each elevation, two aspects of contrasting humidity and temperature were considered (NW and SW). The study site area has the same type of soil, a humic Andosol, with melanic epipedon, no subsurface horizon and soil horizons sequence of O, A, AC and C horizons (Marín *et al.*, 2002).

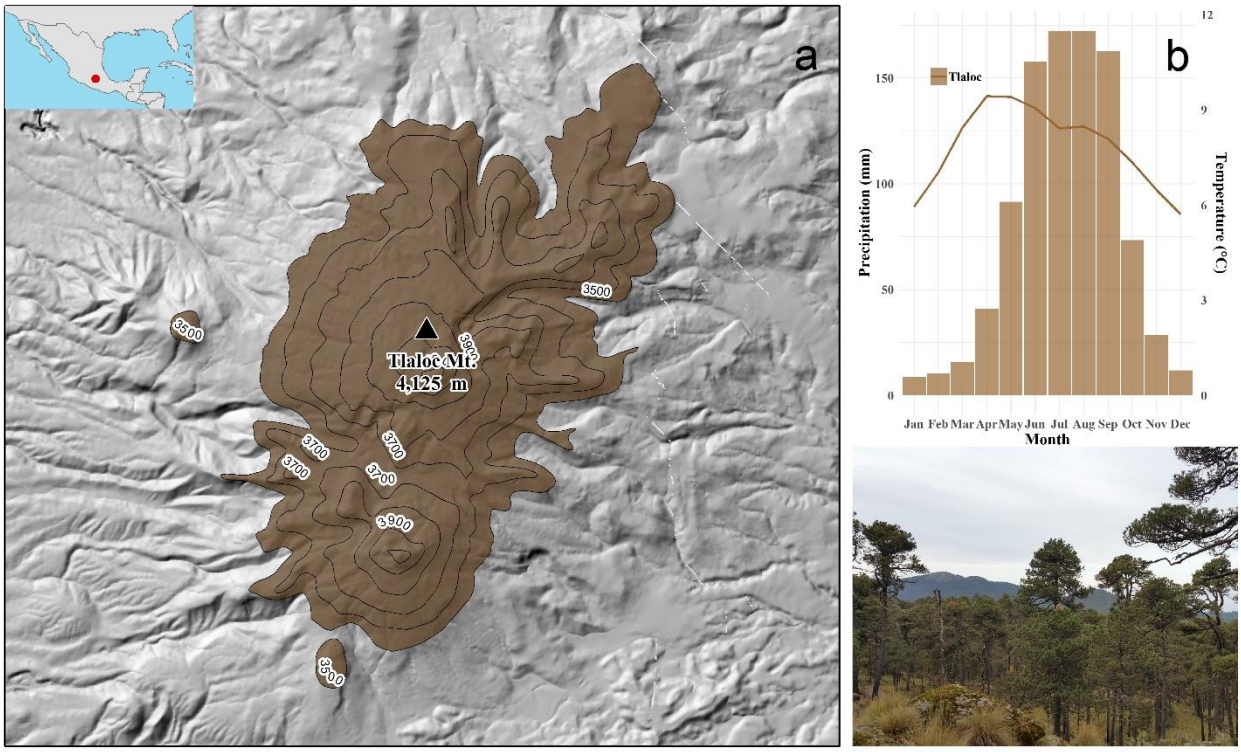

Figure 1. 1 (a) Localization of the study area (Tlaloc-TLA), (b) Climograph of the mean monthly temperature and precipitation values according to climatic data extracted using ClimateNA (Wang et al., 2016), and (c) General view of Mexican high-elevation forest.

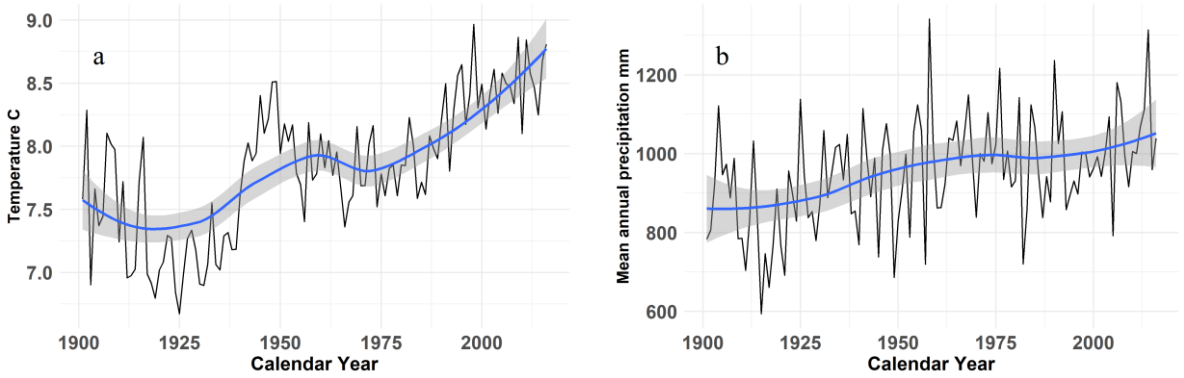

Figure 1. 2 (a) Average mean temperature (°C) and (b) Mean annual precipitation (mm) estimated at Tlaloc Mountain according to downscaled technique based on Climate Research Unit data (CRU ts4.01) (Harris *et al.*, 2014; Wang *et al.*, 2016). Both variables represent the average of all conditions analyzed.

1.4.2. Dendrochronological sampling and growth measurements

For each sampled tree, a single wood core bark to bark was sampled at 1.3 m above the ground in a parallel direction to slope using a Haglöf increment borer of 12 mm diameter and 24-inch long. The wood core samples were mounted on wood pieces, polished with sandpaper until tree rings were clearly visible and then, measured with a Velmex measuring system with a 0.001 mm accuracy (Robinson and Evans, 1980). Then, standard dendrochronology techniques were followed to process the increment cores (Stokes and Smiley, 1968). The quality control of dating and the removal of biological trends no related to climate were done using the Dendrochronology Program Library in R (dplR)(Bunn, 2008). At each site, a ring width index (RWI) was calculated by standardizing the total ring widths series dividing the raw measurements with a fitted value according to a spline function. The expressed population signal (EPS) was used to determine the most statistically reliable period of the ring-width chronology using a threshold of 0.85 (Wigley *et al.*, 1984). A Principal Component Analysis (PCA) was used to detect a common signal between study sites and to build a comprehensive chronology for the study area. Then, Gini coefficients, a quantitative measure of heterogeneity, were used to test inter-annual variability over time considering 10-year moving periods (Biondi and Qeadan, 2008a). Furthermore, to detect changes in productivity, a basal area increment (BAI) series was calculated. BAI correlates with RWI, however, unlike ring

width, BAI is a two-dimensional variable (cm^2 $year^{-1}$) that does not decline with age after trees reach maturity (Biondi and Qeadan, 2008b). To test growth trends, two-segment piecewise linear regression was performed by segmented package in R at each condition, this was done by finding an optimal break point with the lowest residual sum of squares (Muggeo, 2008). The analysis was performed dividing all trees into three age classes (<100 years, 100-200 years, >200 years).

1.4.3. Pre-processing data and NDVI trend analysis

At first, we considered using the Advanced Very High-Resolution Radiometer (AVHRR) NDVI dataset, which is the most common source of data (1981-2015), nevertheless, its relatively low spatial resolution (8 km) makes it unsuitable for application at local scales. For this reason, we chose to use instead data from these ecosystems NDVI based on Moderate Resolution Imaging Spectro-radiometer (MODIS), with a composited in 7-day intervals and a 250-meter spatial resolution, produced by U.S. Geological Survey's (USGS) Earth Resources Observation and Science Center (EROS) (Jenkerson *et al.*, 2010), and complemented with MODIS Leaf Area Index (LAI) (MCD15A2H) (Myneni and Park, 2015) with 8-day intervals and 500-meter spatial resolution, obtained from Oak Ridge National Laboratory (Collection 6) (ORNL DAAC, 2017). Pre-processing data included pixel quality analysis (QA=0, good quality), harmonic interpolation, maximum value composite and avoiding disturbed areas with a high-resolution forest cover change raster (Holben, 1986; Jenkerson *et al.*, 2010; Hansen *et al.*, 2013; Eastman, 2016). To assure an unbiased vegetation trend analysis, all remotely-sensed variables were converted to anomalies, calculating the deviation from the general mean. Afterward, either greenness or browning trends were tested by Theil-Sen slope (TS) and Mann-Kendall Trend (MK) using Earth Trend Modeler in IDRISI Terrset (Eastman, 2016). Theil-Sen slope, a robust non-parametric trend operator, is the median of the slopes between every pairwise combination (rate of change of NDVI per year), which is robust against outliers and rejecting odd values without affecting the slope (Sen, 1968; Neeti and Eastman, 2011). To test for a non-linear trend, the Monotonic Trend operator (Mann-Kendall) was performed. This operator allows measuring the degree to which a trend is consistently increasing or decreasing. It has a range from -1 to +1, values close to +1

indicates a trend continuously increasing and never decrease (Kendall, 1975). Finally, the Contextual Mann-Kendall (CMK) test was used for assessing significant trends (TS and MK). CMK test is highly recommended to detect significant trends in short and noisy time series using the principle of spatial autocorrelation (Neeti and Eastman, 2011). Here, we used Leaf Area Index trend to verify that the changes in NDVI were related to forest productivity rather than other features.

1.4.4. Climatic data relations with tree-rings and NDVI

Monthly temperature (maximum and minimum), chilling degree-days (DD < 0°C), growing degree-days (DD > 5°C), number of frost-free days (NFFD) and precipitation data were obtained by ClimateNA v550, a software package which allows estimates of climatic values for any location at North American continent at a scale-free resolution by downscale technique (Wang *et al.*, 2012; Wang *et al.*, 2016). The software uses the time series data generated by the Climate Research Unit (CRU ts4.01, climatic historical data from 1901-2016), at the University of East Anglia (Harris *et al.*, 2014). Then, at each site, relationships between monthly climatic data and either yearly tree-rings or maximum NDVI were investigated by R package treeclim using bootstrapped response function ($p<0.05$) (Zang and Biondi, 2015).

1.4.5. Canopy vigor reconstruction

A bootstrapped response function was performed between yearly RWI (master chronology) and monthly remotely-sensed data (NDVI and LAI). Then, using RWI as a proxy, an ordinary least square regression (OLS) was carried out to develop a canopy vigor reconstruction using each significant period detected by treeclim in R (Zang and Biondi, 2015). This procedure was carried out for every single pixel at study site, using 65% of the time span as a calibration period and the complement as verification. To assess the accuracy of reconstruction, root of mean square error (RMSE), reduction of error (RE) and coefficient of efficiency (CE) were computed. RE compares the MSE between the reconstruction with a hypothetical reconstruction with the mean for the calibration data. On the other hand, CE compares the MSE of a reconstruction constant

in time with a value equivalent to the sample mean for the validation data. Then, if the reconstruction has predictive skills both statistics are > 0, and RE>CE (Council, 2006).

1.4.6. Agreement between tree-growth and NDVI trends

In order to compare both approaches, pixel information was extracted at two different scales using altitude and aspect as factors. First, at each site, we extracted yearly values from either maximum NDVI or significant NDVI period detected using a single pixel (where increment cores were sampled) or a spatial window (3 x 3 pixels) to get their Theil-Sen slopes (TS). The spatial window was selected based upon similar forest conditions. Thus, considering the significance and slope direction as a referent (positive, negative or no trend) of concordance, slopes were compared to each condition.

1.5. Results

1.5.1. Growth dynamics of *Pinus hartwegii*

Principal Component Analysis (PCA) indicated a common response in tree-ring indexes for the first component, explaining almost 60% of the variance, which useful for a common ring-width chronology for the mountain. The series inter-correlation and average mean sensitivity were in the range expected with values of 0.486 and 0.447, respectively. These numbers indicate a reliable dating and detection of high and low-frequency events. The common ring-width chronology was created encompassing from 1664 to 2016 (353-year). Based upon the threshold of EPS >0.85, the statistically time span was from 1866-2016 (151-year) (Figure 1. 3). Remarkable low growth at stand level (> 60 % global response) were identify according to Cropper values (tree-growth normalization method) in 1867 (0.731), 1872 (0.002), 1887 (0.519), 1891 (0.333), 1897 (0.329), 1904 (0.499), 1908 (0.760), 1911 (0.464), 1914 (0.636), 1924 (0.435), 1929 (0.743), 1960 (0.583), and 1979 (0.524). On the other hand, the highest tree growth peaks were in 1885 (1.348), 1889 (1.216), 1919 (1.180), 1923 (1.119), 1940 (1.221), and 1997(1.297). Although Astudillo-Sánchez *et al.* (2017) developed a chronology in the same mountain, our new ring-width chronology is an updated series 50 years longer with a stronger sample depth support to describe the tree growth variation for this *P. hartwegii* forest. Gini coefficients calculated

over the 10-year moving period in the adjusted ring-width chronology (EPS-threshold), indicated a positive trend (increased inter-annual variability) until 1920 (R^2 = 0.64, p = 0.05), afterward, a lower tree-ring variation remains until present (R^2=0.62, p = 0.01).

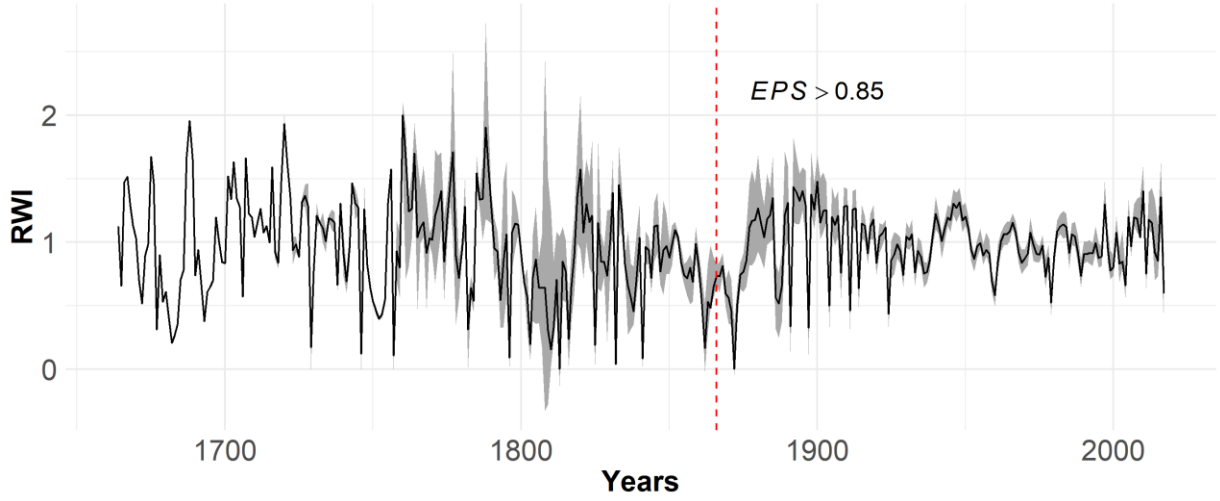

Figure 1. 3 Ring-width chronology of *Pinus hartwegii* at Tlaloc Mountain. The black line represents the mean value of the Ring Width Index (RWI), the gray shaded area is the 99% bootstrapped confidence interval. The red dashed line is the Expressed Population Signal (EPS > 0.85) threshold.

Tree age and size varied through altitudinal transects, the youngest and largest diameter for trees was at 3500 m. asl (84.3 ± 3.63 years and 64.57 ± 1.84 cm for diameter at breast height). This was also reflected into the productivity of *P. hartwegii* forest, where low-altitudinal sites showed higher productivity (BAI-cm^2 $year^{-1}$) than high-altitudinal sites. The 3500-SW site has an average BAI of 25.45 ± 10.64 cm^2 $year^{-1}$ while the same aspect at 3900 m, has only 5.57 ± 2.70 cm^2 $year^{-1}$. Regarding aspects, a factor interaction was seen, higher BAI was found in NW aspect (12.55 cm^2 $year^{-1}$), when the altitude was 3900 m, while higher BAI occurred in the SW aspect (25.45 cm^2 $year^{-1}$) at the altitude of 3500 m (Figure 1. 4). Here, an upward trend derived by an age-effect of trees was detected across altitudes and aspects, but notably at the same rate for each condition. All sites exhibited a shifting trend from increasing to decreasing growth rates (-0.66 cm^2 $year^{-1}$) for mature trees (> 100 years) during the mid-20^{th} (Table 1.1). On the other hand, young trees (<100 years) exhibited a different response for this second period, at 3900-NW, they reached a peak in BAI (after 50 years) and a steady trend in BAI was observed (Figure

1. 4a); conversely, at 3900-SW, they exhibited a downward trend after the peak (Figure 1. 4b). In the most productive sites at 3500 m asl, it took about 25 years to young trees to reach the peak of BAI but conversely to the 3900-sites, they increased their BAI at North, pushing values up higher than expected average peak (Figure 1. 4c), and decreased at South (Figure 1. 4d).

Table 1. 1 Determination of breakpoints for basal area increment (BAI) according to a 2-segment piecewise linear regression. BAI was stratified into age classes including an average of six trees by class. NS indicates a no significant slope and SE standard errors.

Site	Age class (years)	BAI cm^2 $year^{-1}$ (±SE)	Breakpoint year (±SE)	n (trees)	*p*-value	R^2	Slope 1	Slope 2
							(cm^2 $year^{-1}$)	
3500-SW	< 100	24.24 (±0.9)	1939 (±2.5)	9	<0.001	0.35	1.18	-0.11
	100-200	27.68 (±1.5)	1942 (±1.5)	5	<0.001	0.80	1.10	-0.66
3500-NW	< 100	25.28 (±1.1)	1940 (±3.0)	12	<0.001	0.65	1.16	0.13
	100-200	17.20 (±0.9)	1950 (±2.4)	5	<0.001	0.72	0.55	-0.24
3900-SW	< 100	5.04 (±0.3)	1967(±3.9)	4	<0.001	0.52	0.14	-0.04
	100-200	5.64 (±0.2)	1947(±4.0)	12	<0.001	0.62	0.11	-0.03
3900-NW	< 100	10.34 (±0.7)	1986 (±3.5)	6	<0.001	0.87	0.28	NS
	100-200	8.28 (±0.4)	1955 (±4.9)	4	<0.001	0.33	0.12	-0.17
	>200	11.92 (±0.5)	1900 (±4.2)	5	<0.001	0.26	0.44	-0.10

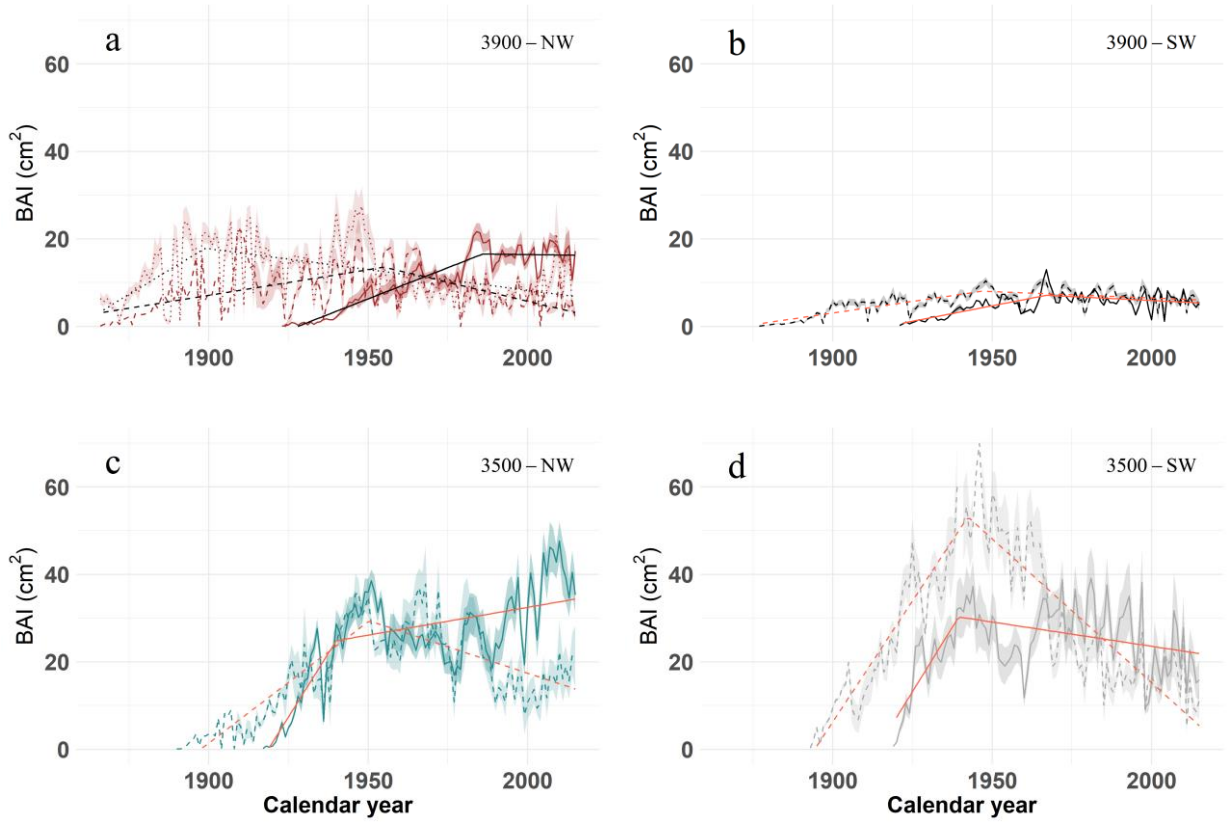

Figure 1. 4 Basal area increment chronologies of *Pinus hartwegii* at Tlaloc Mountain by site (a) 3900-NW, (b) 3900-SW, (c) 3500-NW and (d) 3900-SW. Trees were divided into three age classes: <100 years (solid line), 100–200 years (dashed line), >200 years (dotted line). Red and black lines represent a 2-segment piecewise linear regression. Shaded areas are standard errors. Note that the time span of chronologies was adjusted to EPS > 0.85.

1.5.2. NDVI time series

Average monthly NDVI values slightly decreased from January to a minimum in April (0.57 ± 0.08). The May NDVI value was higher than the April value, implying that at some point between months, *P. hartwegii* began to grow, then reached maximum values in September-October (0.69 ± 0.07) (Figure 1. 5a). Meanwhile, winter NDVI values decreased as the trees go into the dormant period and reduce photosynthetic activity. The higher variability detected from June to August (SD = 0.05) could be a reflection of increased leaf area and photosynthesis at different altitudes. Results indicate that low-altitude sites reach higher NDVI values likely due to a bigger canopy and better

edaphoclimatic conditions. This is confirmed by a statistical difference on average NDVI value across altitudinal levels (3500 vs 3900 m asl) ($p < 0.001$). The lower altitudinal belt showed 0.66 ± 0.06 and the upper belt 0.61 ± 0.05 in the mean NDVI from 2000 to 2016. North, (NW, and NE) aspects showed higher mean NDVI than South (S and SE) aspects ($p < 0.001$). This difference is more evident when the analysis is performed using both altitude and aspect, where a 0.09 difference in the mean value was found between North and South aspects at each altitudinal level ($p < 0.05$). The monthly NDVI values showed a pattern with maximum values in September 2007 and 2010 (0.74 ± 0.07) and minimum values in March 2004 and May 2009 (0.54 ± 0.08) (Figure 1. 5b). Spatially, the highest greenness in NDVI values were detected along the lower altitudes and decreased as *P. hartwegii* photosynthesis is constrained by the altitude factor (i.e. temperature, soil conditions, water availability, etc.). Above 4000 m asl, where the upper tree-line is located, NDVI values correspond to the mountain shrub ecosystem composed mainly by *Juniperus monticola* Martínez (Villanueva-Diaz *et al.*, 2016) (Figure 1. 6b).

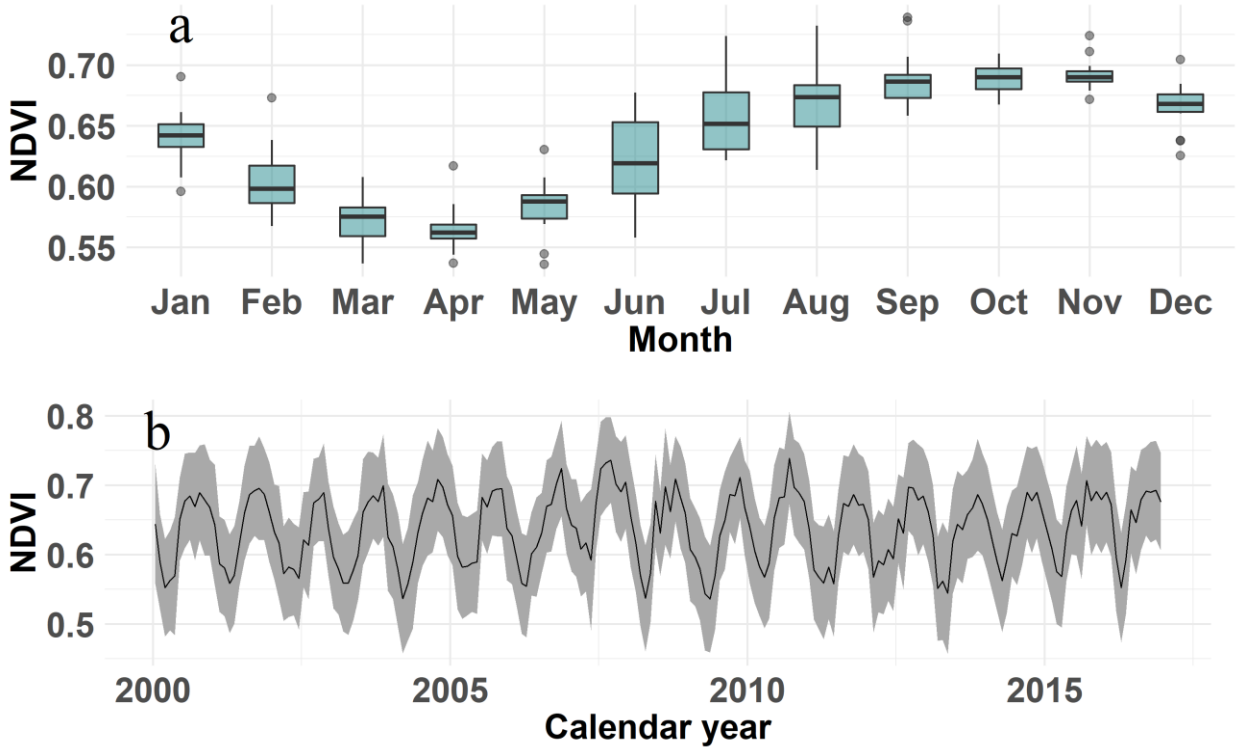

Figure 1. 5 (a) Monthly Box-Plot of maximum NDVI values during 2000-2016 and (b) Average maximum NDVI time series (black line) and 68% confidence interval (gray shaded area).

1.5.3. NDVI trend analysis

Once the seasonality trends were removed, the Theil-Sen slope (TS) showed a no-trend across years in the overall mean value, with a slightly negative slope of -0.00011 (± 0.002) per year. However, a general browning trend must not be considered since this value just represents a combination of gains and losses on NDVI across the whole Mountain. A carefully spatial-analysis shows a browning effect in the South zone, as well as sections of the mountain facing to NW. On the other hand, a greening effect was found nearby the top of the mountain and across different zones along the study area (Figure 1. 6a). Then, browning trends (< 0 NDVI $year^{-1}$) represented 4,500 ha and greening trends (> 0 NDVI $year^{-1}$) reached almost the same value (4,362.5 ha) (Table 1.2). Mann-Kendall test confirmed the results, showing a constantly increasing trend (greenness, closer to +1) at the top as well as different sections of the mountain, and a consistently decreasing trend (closer to -1) in the South of the study area. The TS and MK trends are significant (p <

0.1) in more than a half of Tlaloc Mountain (57.48%). This means a higher probability of change (at different rates) in the study site, though, insignificant trends were also detected scattered all over the Mountain, mainly in the Southeast. No relationship was detected between significant trends and altitude or aspects.

Table 1. 2 Area by NDVI trend categories in the Tlaloc Mountain from 2000-2016

Slope (NDVI year^{-1})	Category	Theil-Sen slope (TS)		Significance ($p < 0.1$)	
		Count (Pixels)	Area (ha)	Count (Pixels)	Area (ha)
<-0.004	High Browning	43	268.75	23	143.75
-0.004 - 0	Low Browning	677	4,231.25	292	1,825.00
0 – 0.004	Low Greening	671	4,193.75	473	2,956.25
>0.004	High Greening	27	168.75	27	168.75
		1418	8,862.50	815	5,093.75

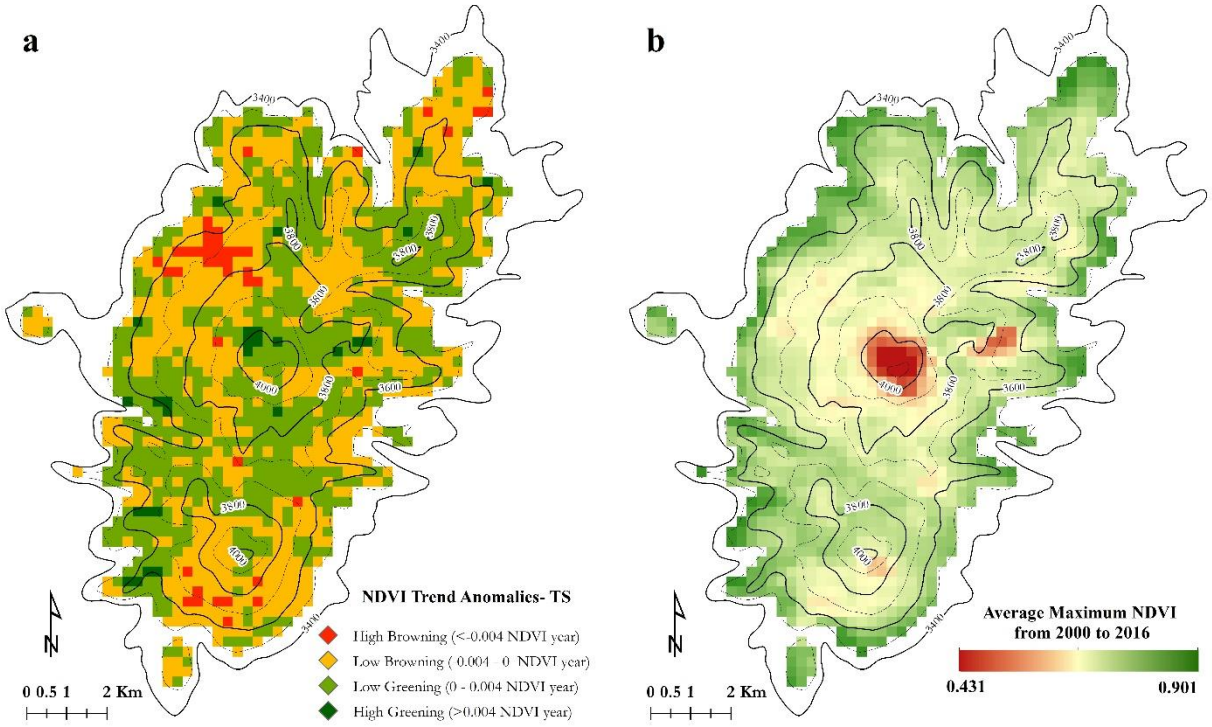

Figure 1. 6 (a) NDVI trend analysis according to Theil-Sen slope (TS), and (b) Average Maximum NDVI during years 2000 to 2016. All maps were masked out above to 3500 m asl, representing the reflectance response of *Pinus hartwegii*, 0.50 Maximum NDVI was defined as appropriate threshold to detect areas without forest.

A high positive correlation between LAI and NDVI was found for both monthly values and trend analysis (r = 0.4 and 0.54, respectively); thus, positive trends in LAI would be concurrent with NDVI positive trends on forest sites. The main high browning trend (<-0.004 NDVI year^{-1}) located in the NW part of the Mountain suggest a loss of canopy vigor since a reduction in LAI (-0.015 m^2 m^2 per year) was observed, however, further investigation is needed to know the reasons of that. The positive trend in NDVI observed at the top of the Mountain matches with positive trends in both LAI (0.007 m^2 m^2), however, the values correspond to mountain grasslands rather than forest.

1.5.4. Climatic factors and forest growth

Autumn maximum temperature and winter precipitation from the previous year had a positive effect on forest growth at high-elevation forests (r = 0.32 to 0.56), this relationship

is stronger in NDVI than RWI, suggesting the direction between process, this is, starting with the photosynthesis process towards the carbon allocation in stems. However, the relationship with temperature becomes negative when the analysis is performed in the following months. Thus, maximum temperatures during March and April (end of the dormant period) are negatively associated to the NDVI (r= -0.56, Table 1.3) with no correlation with RWI. At lower altitudes, the linear relationship with RWI decreases showing the importance of other factors on growth rather than temperature, but not with NDVI where a similar effect through different elevations was detected. Regarding to aspect, South facing forest showed higher correlations than North-facing. It has been shown recently that over fine-scale at the high-elevation forest, degree-day sum or growing season length explain productivity better rather than classical temperature approach (Jochner *et al.*, 2017). Here, degree-days below to 0°C and number of frost-free days (NFFD) in May were correlated with forest growth (r = -0.27 and 0.28, respectively; in all cases: $p < 0.05$ and n = 114 years) as well as NFFD in June with NDVI (r = 0.62).

Table 1. 3 Climatic factors related to a ring-width chronology of *Pinus hartwegii* and NDVI according to bootstrapped response function at Tlaloc Mountain

Period	Variable	Pearson's correlation with RWI	Pearson's correlation with NDVI
Previous year's condition	T max Sep-Oct	**0.327***	**0.399***
	T avg Sep-Oct	**0.276***	**0.561***
	Precipitation Dec-Mar	0.101	**0.409***
	∑DD>5°C Sep-Dec	**0.221***	**0.589***
Current year's condition	T max Mar-Apr	-0.066	**-0.559***
	T min May	**0.295***	0.146
	T min Jun	0.155	**0.570***
	Precipitation Apr	0.140	**0.364***
	Precipitation May	**-0.224***	0.217

	∑DD>5°C Apr	-0.036	**-0.574***
	DD<0°C May	**-0.270***	0.056
	NFFD May	**0.284***	0.144
	NFFD Jun	0.139	**0.620***
DD <0 °C - Degree-days below to 0 °C		* p < 0.05	* p < 0.05
DD >5 °C - Degree-days sum above to 5 °C		n= 114 years	n=17 years

NFFF – Number of frost-free days

Combined months represents an average value for temperature and sum for precipitation and degree-days

1.5.5. Reconstruction of canopy vigor using tree-ring widths

Tree-ring widths were positively correlated ($p < 0.05$) to NDVI and LAI from winter (previous year) to spring season ($r = 0.52$ to 0.80, Figure 1. 7a, b). Consequently, a higher correlation with average NDVI from December to March ($r = 0.70$, $p < 0.05$), and November to April with LAI ($r = 0.72$, Figure 1. 7b) was detected. While temperature effect on forest growth decreases at lower altitudes, an analogous relationship with NDVI was not found. In fact, aspect seems to be a more important factor related to canopy vigor. For example, a higher correlation was found in NW sites ($r = 0.53$ to 0.64) than in SW sites ($r = 0.33$ to 0.41).

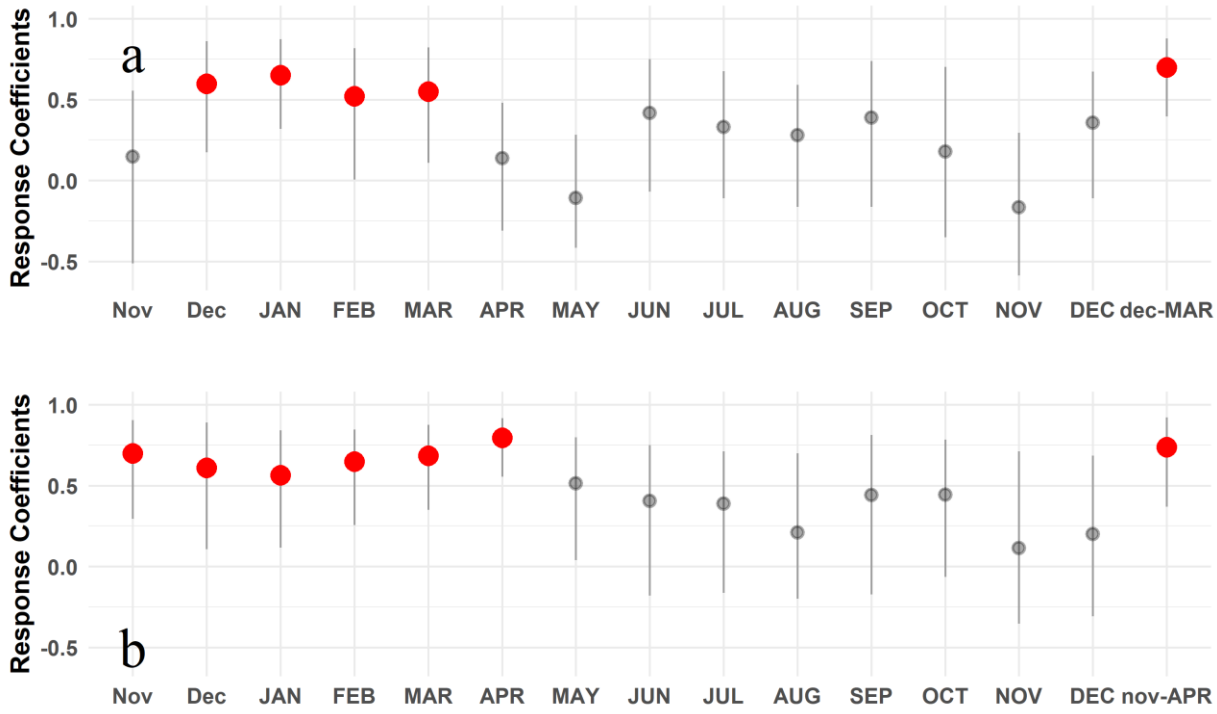

Figure 1. 7 Bootstrapped response function analysis between ring-width chronology of *Pinus hartwegii* and (a) monthly Normalized Difference Vegetation Index (NDVI), and (b) Leaf Area Index (LAI). Blue points are statistically significant ($p < 0.05$). Note that the months from the previous year are given in lowercase letters while current in uppercase letters and combined months represents the mean value for the corresponding period.

The reconstruction of NDVI from ring-width chronology is reliable as supported by the statistics of the regression that indicated the skills of the model to predict out of the observed range. About 300 pixels were enough to statistically explain the variation in canopy vigor along the studied mountain (Table 1.4 and Figure 1. 8). The correlation between variables (NDVI, and LAI) in the reconstruction equations ranged from 0.64 to 0.66 ($p < 0.05$), which denote that the regressions explain around the half of variability (up to 79% at pixel level). Despite the low number of years ($n = 17$), the equations for winter NDVI had positive statistics that denote the reliability in the reconstruction (RE = 0.30, and CE = 0.26). Thus, the reconstructions did better than the average over the calibration and validation period, respectively. The square root of the MSE was 0.03, an

indication of good accuracy in the reconstruction. Noticeably, the residuals are not correlated according to Durbin-Watson Test (p = 0.43), indicating the removal of time-dependence values. Similarly, the equation focused on LAI was reliable to perform a reconstruction since RE and CE were positive and showed a low RMSE (Table 1.4).

Table 1. 4 Canopy vigor reconstruction evaluated at a pixel-level using NDVI, and LAI as dependent variables and RWI as an independent variable, using a ring-width chronology of *Pinus hartwegii*. SE are standard errors.

Variable	Units	Number of pixels (n)	Mean equation	Pearson correlation coefficient (± SE)	Reduction of error (± SE)	Coefficient of efficiency (± SE)	Root Mean Square Error (± SE)	p-value	Durbin-Watson Test (± SE)
$NDVI_{dec-Mar}$	NA	310	y=0.5555 + 0.0689 RWI	0.64 ± 0.01	0.30 ± 0.01	0.26 ± 0.01	0.03 ± 0.001	<0.001	0.43 ± 0.02
$LAI_{nov-May}$	m^2 m^{-2}	78	y=0.7374 + 0.3173 RWI	0.66 ± 0.01	0.37 ± 0.01	0.27 ± 0.02	0.013 ± 0.003	<0.001	0.50 ± 0.03

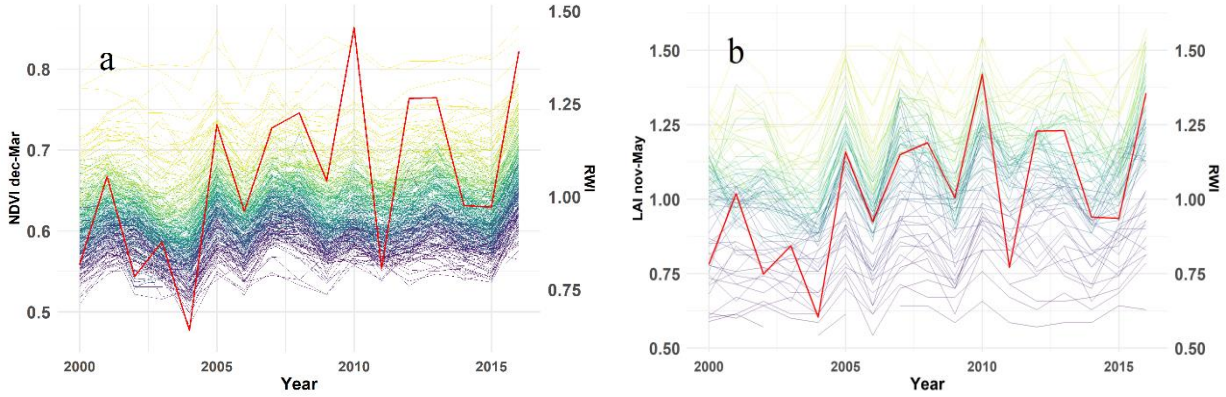

Figure 1. 8 Remotely-sensed time series at a pixel-level with the average ring-width index for Tlaloc Mountain (RWI, red line), (a) NDVI Dec-Mar, (b) LAI Nov-May. Note that the relationship is only showed for those equations with RE and CE > 0 and the number of pixels for LAI is less than NDVI for coarser spatial resolution. Color intensity from purple to yellow reflects the altitudinal pattern, where dark colors represents high-elevations and vice versa.

Spatially, a higher correlation was found between the ring-width chronology and winter-spring NDVI, than their respective maximum yearly values. For example, winter NDVI and RWI showed an average r of 0.50 ($p < 0.05$), and winter-spring LAI and RWI, $r = 0.55$ ($p < 0.05$) at a pixel level (Figure 1. 9). For NDVI, this connection was remarkably high in the middle-zone as well as in the northern part of the Tlaloc Mountain and conversely at the southern zone and the north-face top of the Mountain where low Maximum NDVI were detected. Although the lower resolution of LAI, a high spatial agreement was detected across the whole Mountain, except in those pixels with poor-information at the North of the Mountain. We did not find a better association between tree-growth and NDVI across either altitudinal level (3500 or 3700) or aspects since their means are statistically similar ($p = 0.34$ and $p = 0.73$, respectively). The last results suggest a robust relationship between NDVI and tree-ring data regardless of the topographic variation.

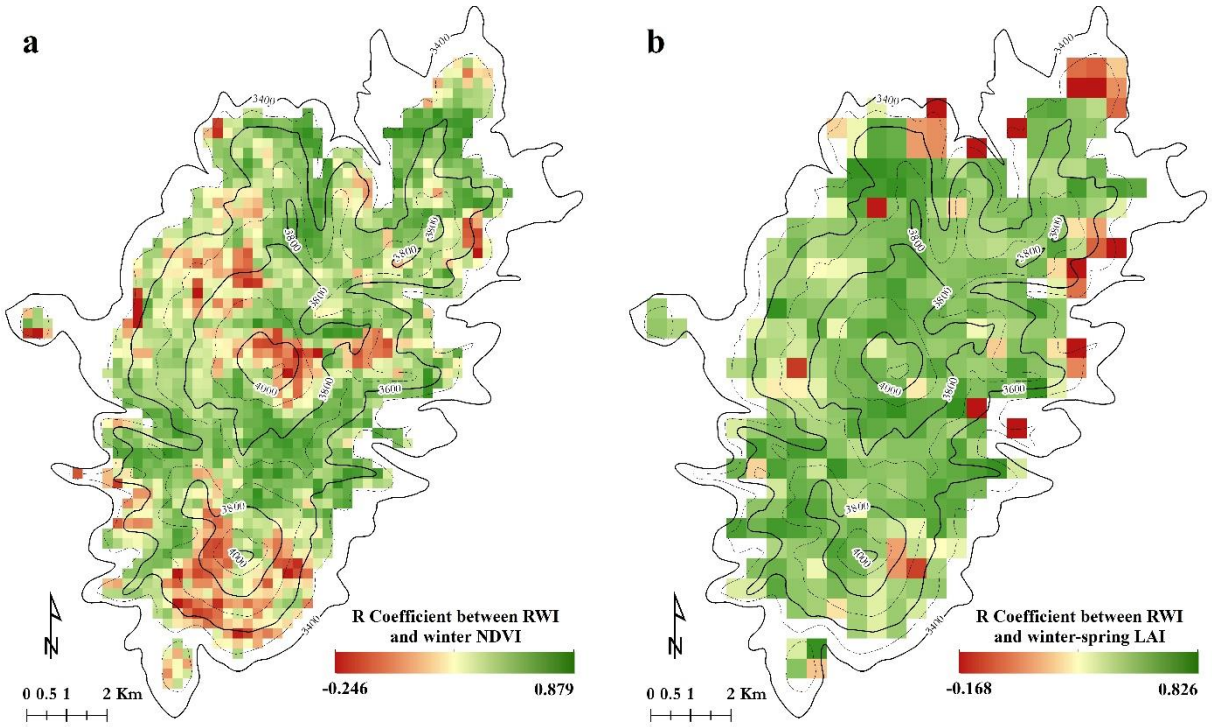

Figure 1. 9 Correlation coefficient according to linear regression (n = 17 years) between the average ring-width index for Tlaloc Mountain (RWI) and (a) winter NDVI (December from previous year to March from current year), and (b) winter-spring LAI (November from previous year to May from current year). Pixel resolution is (a) 250-meter, while (b) 500-meter.

The reconstructed remotely-sensed variables are integrative measures which could represent a state of vegetation condition in the past, involving photosynthetic activity and forest productivity. For example, periods with NDVI below to average (0.62 ± 0.001) were likely related to low growth and photosynthetic activity such as those occurred in 1869-1874, 1886-1889, 1956-1962, 1975-1980, and more recently in 2000-2004. Conversely, fewer frequent high growth events were observed in 1878-1884, 1892-1902, 1942-1951 (Figure 1. 10).

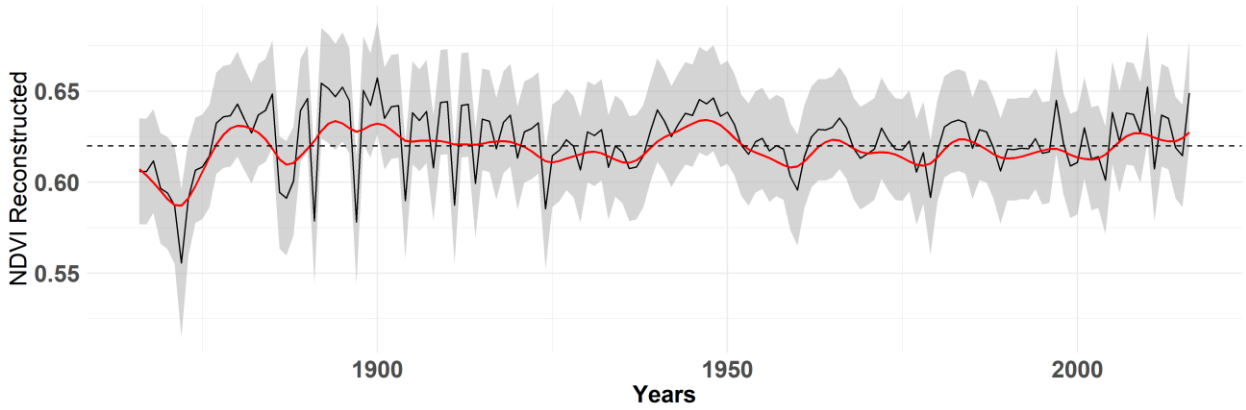

Figure 1. 10 Canopy vigor reconstruction using a ring-width chronology of *Pinus hartwegii* at Tlaloc Mountain. The black line represents the reconstructed variable (winter NDVI (Dec-Mar)); the red line is a 10-year spline to highlight the low-frequency events. The black dotted line is the overall mean of winter variable. Gray shaded area is the 95% prediction confidence interval.

1.5.6. Tree-growth and NDVI trend agreement

Our results revealed an agreement between values of Theil-Sen slopes measured at pixel-level (where the trees were sampled) and using a spatial window (3 x 3 pixels) for all variables (NDVI, and LAI), mainly explained by a high homogeneity in the forest stands. For example, the average coefficient of variation on NDVI was 0.045, this reveals a good similarity between a single pixel and those of surrounding forested areas. However, not all trends were statistically significant ($p < 0.01$) and those significant where located mainly at lower elevations. Considering their slope directions as a reference (positive, negative or no trend) of concordance, an agreement between ring-width indices and remotely-sensed information was detected at 3500-SW and 3500-NW (except NDVI). At the upper level, almost all slopes analyzed were consistent (no trend) except for 3900-SW (RWI), where we found a positive trend.

Table 1. 5 Theil-Sen slopes and trend concordance between Ring Width Index (RWI), NDVI and winter NDVI (wNDVI) anomalies from 2000 to 2016. NS indicates a no significant slope.

Site	Variable	Theil-Sen Slope	*p*-value	Trend	Theil-Sen Slope	*p*-value	Trend
		Single Pixel			Spatial Window		
3500-SW	RWI	0.0110	0.023*	Positive	0.0110	0.023*	Positive
	NVDI	0.0041	0.001*	Positive	0.0026	0.001*	Positive
	wNVDI	0.0035	0.001*	Positive	0.0047	0.001*	Positive
3500-NW	RWI	0.0109	0.132	NS	0.0109	0.132	NS
	NVDI	-0.0012	0.071**	Negative	-0.0006	0.031*	Negative
	wNDVI	0.0039	0.001*	Positive	0.0039	0.001*	Positive
3900-SW	RWI	0.0256	0.006*	Positive	0.0256	0.006*	Positive
	NVDI	0.0013	0.579	NS	0.0014	0.890	NS
	wNDVI	-0.0004	0.879	NS	-0.0006	0.963	NS
3900-NW	RWI	0.0117	0.306	NS	0.0117	0.306	NS
	NVDI	0.0007	0.517	NS	0.0002	0.890	NS
	wNDVI	0.0007	0.207	NS	0.0002	0.782	NS

* $p < 0.05$ and **$p < 0.1$

n=17 years

1.6. Discussion

1.6.1. Hypothesis testing summary

High-elevation forests are strongly temperature-limited, restraining photosynthesis, nutrient uptake, xylogenesis, etc. (Körner, 2012).The increases in temperature are expected to boost tree growth and vigor (greening effect) at high-elevation sites, especially these facing to the North, where temperature effect is more noticeable (H_i). Thus, temperature increases should be influencing not only tree-ring growth but also photosynthetic activity (NDVI), almost in the same way (H_{ii}) and if the relationship is robust and significant enough, the ring-width chronology could be used as a proxy to reconstruct past canopy vigor (H_{iii}). Evidently, we did not identify a direct temperature stimulation-

growth at the upper elevation, regardless tree age. Results were also supported by the NDVI analysis, which showed different patterns of greening or browning, with no observable altitude effect. Second, we found that climatic influence varies according to the spatial-position, but noticeable NDVI was more sensitive than RWI. Finally, the climatic variability (i.e. temperature) was harmoniously reflected in photosynthesis and carbon allocation (ring-width), allowing a canopy vigor reconstruction for the study site.

1.6.2. Forest growth at Tlaloc Mountain

The mean sensitivity of the ring-width series of *P. hartwegii* at Tlaloc Mountain is concurrent with those carried out along the Transmexican Volcanic Belt, confirming the reliability of dendrochronological procedures to relate the climate and tree growth in montane forests (Biondi, 2001; Villanueva-Díaz *et al.*, 2015; Astudillo-Sánchez *et al.*, 2017). Although our sampled procedure of trees was based on dominant trees, more than in water or nutrient stressed individuals as suggested in the dendroclimatology approach (Fritts, 1976), trees with position at the highest canopy level were effective to capture tree growth dynamics, as in others works (Berner *et al.*, 2013; Castruita-Esparza *et al.*, 2016).

Temperature is a determinant factor for tree growth at alpine and boreal forests, triggering the reactivation of cambial activity, xylem cell differentiation, and photosynthesis (Körner and Paulsen, 2004; Rossi *et al.*, 2007; Antonucci *et al.*, 2017; Li *et al.*, 2017). Thus, if we used the data by Wang *et al.* (2016) to reconstruct historical trends of temperature and precipitation in the study area for the last century, we would estimate average increases of 1.4°C and 150 mm, respectively (Figure 1. 2), this trend confirmed by Lobato-Sánchez and Altamirano-del-Carmen (2017) in Central Mexico, implies a better tree growth conditions in the present for high altitudes. But our results show that increases and decreases in tree growth are site dependent, indicating that climate change effects are more micro-site dependent. Thus, the universal ideal of better response of tree growth (also photosynthetic activity) in high-elevation forests as climate change occurs should be cautiously applied (Lapenis *et al.*, 2013; Silva *et al.*, 2016). For example, young trees showed increased (3500-NW), steady (3900-NW) or decreased growth (3900-SW and 3500-SW) (Figure 1. 3c). With higher temperature in the 3500-SW site, the young and old

trees seemed to be beneficed up the 1958, but afterward, BAI decreased. In site 3500-NW, old trees decreased in BAI after 1950, but young trees showed an increased BAI, suggesting a stimulation effect in recent decades. This fact is important because indicates that responses to climate change are not only micro-site dependent but also age-dependent. For example, Rossi *et al.* (2008) found lower cambial activity in old trees than young trees at high-elevation forests with reduced xylem differentiation and wood formation. The lack of growth stimulations at higher altitude (3900 m asl), might be related to a progressive water and nutrient limitation, because at high altitudes, the soil depth decrease and soil texture is coarser, making trees prone to water and nutrient stress (Marín *et al.*, 2002).

The decline in BAI for mature trees (Figure 1. 4), without signs of short-term recovery during mid-20th, is concurrent with some studies at high-latitudes forests (Berner *et al.*, 2013; Lapenis *et al.*, 2013). One explanation could be that the increased temperature around mid-20th caused higher water demand for evapotranspiration reducing water availability and forest productivity (Anderegg *et al.*, 2013). The reduction in BAI over time is an expected trend as trees ages, but no a unique response was seen with altitude and aspect variation. We do not have a response for the coincidence of the common breakpoint around the 1950's for young and mature trees, but we know that using as reference the period of 1950-1981, there is an unequivocal shit to higher temperatures in the present. The contrasting results in growth suggest that further investigation is needed to determine additional links between environmental changes and tree physiology (McCarroll and Loader, 2004).

1.6.3. Influence of climatic conditions on NDVI and RWI

Compared to RWI, NDVI correlates with climatic and topographic variables allowing a more comprehensive analysis of the forest growth over time and space. Thus, other factors like precipitation, temperature, elevation, and land-cover type are more consistently related to NDVI than tree-ring metrics (Wang *et al.*, 2014; Antonucci *et al.*, 2017; Bethany *et al.*, 2017; Mokria *et al.*, 2017; Qi *et al.*, 2017). Being a more general index, maximum seasonal NDVI showed to be more sensitive to climatic factors than

RWI, this could be explained by the strong correlation between NDVI and carbon uptake at geographical scales (GPP-photosynthesis) via light harvesting as a first step, while ring width is more related to carbon allocation or Net Primary Productivity (NPP) once the values are corrected by respiration (Šímová and Storch, 2017). Kaufmann *et al.* (2004), associated higher NDVI with lower summer temperatures, but higher temperature in previous winter which agree with our results (Table 1.3). Warmer winters could cause the next growing season to start early and reduce the frost damage in trees (Chen *et al.*, 2012; Astudillo-Sánchez *et al.*, 2017). The differential correlation of NDVI and RWI with climatic variables across site conditions, partially confirms our second hypothesis that climatic influence varies spatially. Also, our results support the use of downscaling techniques to generate site-level information in remote locations, improving the knowledge of ecosystem functioning (Wang *et al.*, 2016).

1.6.4. NDVI time series and relationship with RWI

The onset of vegetation green-up starts at some point between April-May and continues through September-October (Figure 1. 5a) when this species stop growing (Biondi *et al.*, 2005; Astudillo-Sánchez *et al.*, 2017). Similar growth patterns for the study species have been reported in other mountains, with an explanation based on changes in temperature (4-6 °C) (Biondi and Hartsough, 2010). This work showed that seasonal NDVI information could be related to the effective time for xylogenesis (Biondi *et al.*, 2005; Antonucci *et al.*, 2017), implying a potential for spatial analysis of wood formation. Remote sensing and dendrochronology techniques have been used recently to study physiological and growth dynamics in response to climatic change over long periods (Mokria *et al.*, 2017). During the last decade, some studies have used tree-ring information as a proxy to reconstruct the vegetation activity and to verify satellite-observed browning-greenness results, in North America (Kaufmann *et al.*, 2008) and Eurasia (He and Shao, 2006; Berner *et al.*, 2011; Chen *et al.*, 2012). Therefore, forest physiological variables such as canopy vigor evaluated from remote sensors can be combined with tree-ring information to better understand the carbon cycle and climate change (Coulthard *et al.*, 2017). This is possible because climatic conditions (temperature, moisture, and light) affect both photosynthesis and carbon uptake, generating environmental signals in time (tree-rings) and space

(NDVI). Additionally, our results are not influenced by the composition of the forest, since our study site is a monospecific stand, which avoid blurred effects in the spectral response of vegetation (Brehaut and Danby, 2018).

1.6.5. The “greening” and “browning” effect

Net Primary Productivity (NPP), Leaf Area Index (LAI) from remote sensing models are linked to the fraction of photosynthetically active radiation (fPAR) that in turns determines Gross Primary Production (GPP) (Šímová and Storch, 2017). Thus, our results of NDVI trend analysis are supported by that relationships. Spatially, at the high-elevation site facing to North the greening pattern is absent, except for scarce spots located on basalt and composed of *Juniperus monticola* shrubs rather than forest at the tree-line (Villanueva-Diaz *et al.*, 2016). Thus, the “greening effect” from NDVI data should be carefully interpreted, discriminating changes in the surface (fires, deforestation, etc.) and corroborating with additional information like LAI. For example, the negative NDVI trend facing to the South of Tlaloc Mountain (Figure 1. 6), could be related to lower rates of photosynthesis without changes in LAI, suggesting the location of water stressed stands. Low-intensity fires and particularly those ranked as high-intensity fires have a direct impact on the LAI affecting growth of the following years after the fire occurrence. Then, the NDVI values could be a good indicator of fire presence for particular years, however this has to be verified with fire records o derived from fire reconstructions available for some high-elevation peaks in central Mexico (Yocom *et al.*, 2012).

As noted Vicente-Serrano *et al.* (2016) and Bhuyan *et al.* (2017) different factors must be taken into account to successfully relate directly remotely-sensed data to direct growth: suitable spatial resolution and homogeneous forest stands, as well as maximizing the forest response using maximum composites (monthly or yearly). Nevertheless, a point of divergence between approaches, usually referred as trend inconsistency phenomenon (TIP) (Lapenis *et al.*, 2013), is also presented since fPAR passes from the atmosphere (assessed by sensor) through canopy (radiation use efficiency), and from canopy to cambium, combined with nutrient availability, and stand age (Berner *et al.*, 2011). This could be the reason for the high agreement between trends at low-altitudes, where a

better radiation use efficiency (youngest trees), better soil fertility and higher tree cover, keeps the same signal through components with a higher carbon allocation to stems, thus, the site with highest basal area increment showed the better agreement (Table 1.1 and Table 1.5).

1.6.6. Canopy vigor reconstruction

Some studies in high-latitude forests have reported positive correlation between summer NDVI and tree-ring width (Kaufmann *et al.*, 2004; Wang *et al.*, 2004; Lopatin *et al.*, 2006; Kaufmann *et al.*, 2008; Beck *et al.*, 2013). Other studies show variation in correlation according to forest type and climate conditions (Liang *et al.*, 2005; Vicente-Serrano *et al.*, 2016) and no correlation between NDVI and RWI has been also reported (Brehaut and Danby, 2018). Here, we found that winter NDVI had a positive correlation with the tree growth for the following year, in other words good canopy vigor in winter is an indication of better tree growth performance in the next growing season. Castruita-Esparza *et al.* (2016), have suggested that for Douglas-fir in Mexico, soil water storage in summer defines tree growth in the next year. Therefore, seasonal NDVI analysis is recommended to understand forest responses, besides that, further investigation is need to explore different vegetation index, such as Enhance Vegetation Index (EVI), which uses soil adjustment and atmospheric resistance factors that could be helpful in tree-line ecotones (Huete *et al.*, 2002). In the selected period, the greenness of the canopy (NDVI) and the foliage mass indirectly expressed as LAI in winter, are congruent to the carbon uptake variation imprinted in tree-ring width series. As in our work, Bethany *et al.* (2017) and Beck *et al.* (2013) noted that chronologies at lower-elevation exhibited better links with NDVI, but in addition to that, we have showed that the aspect is another important aspect to be considered.

Remotely-sensed proxies (i. e. NDVI) are powerful indicators of physiological status of plants (Kaufmann *et al.*, 2004) and given that long-term vegetation status records in forest are limited, the reconstructed values can be used to estimate the spatio-temporal canopy vigor in high-elevation forests (Andreu-Hayles *et al.*, 2011). *Pinus hartwegii* tree-ring series and documented records confirm drought episodes in central Mexico during 1886-

1889, 1952-1960, 1970-1979 and 2004 (Florescano, 1980; Metcalfe, 1987; Therrell *et al.*, 2002; Villanueva-Díaz *et al.*, 2015) and some of these periods match with our results. On the other hand, ring-width indices above the mean are detected during 1891-1893 and 1940-1951, enhancing photosynthetic capacity (Florescano, 1980; Villanueva-Díaz *et al.*, 2015).

1.7. Conclusions

Our results show that remote sensing and dendrochronology can be integrated to improve assessments of climate-induced ecosystem change. Both approaches indicated a general lack of growth stimulation at high-elevations. Basal area increment trends showed that young trees (<100 years) were more resilient for ongoing climate variability, with steady and even growth increases at lower altitudes. However, mature trees (100-200 years) were pushed to a common growth decrease around mid-20th with no clear explanation, opening a potential avenue for dendroecology studies using physiological responses of carbon assimilation and water loss. Locally downscaled climatic data provide new insights for the traditional dendroclimatology analysis, allowing a better understanding of climatic drivers in tree growth at areas with no climatic information. Additionally, seasonal normalized difference vegetation index (NDVI), instead of classical annual average, have showed a stronger relationship with tree-ring width, thus, further investigations are needed to identify local main patters in the growth response to NDVI.

1.8. References

Acosta Mireles, M., F. Carrillo Anzures, D. Delgado and E. Velasco Bautista. 2014. Permanent plot establishment to assess climate change impacts upon izta-popo national park. Revista Mexicana de Ciencias Forestales 5: 6-29.

Alfaro-Ramírez, F. U., J. T. Arredondo-Moreno, M. Pérez-Suárez and Á. R. Endara-Agramont. 2017. *Pinus hartwegii* lindl. Treeline ecotone: Structure and altitudinal limits at nevado de toluca, mexico. Revista Chapingo Serie Ciencias Forestales y del Ambiente XXIII: 261-273.

Anderegg, L. D. L., W. R. L. Anderegg and J. A. Berry. 2013. Not all droughts are created equal: Translating meteorological drought into woody plant mortality. Tree Physiology 33: 672-683.

Andreu-Hayles, L., R. D'Arrigo, K. J. Anchukaitis, P. S. A. Beck, D. Frank and S. Goetz. 2011. Varying boreal forest response to arctic environmental change at the firth river, alaska. Environmental Research Letters 6.

Antonucci, S., S. Rossi, A. Deslauriers, H. Morin, F. Lombardi, M. Marchetti and R. Tognetti. 2017. Large-scale estimation of xylem phenology in black spruce through remote sensing. Agricultural and Forest Meteorology 233: 92-100.

Astudillo-Sánchez, C. C., J. Villanueva-Díaz, A. R. Endara-Agramont, G. E. Nava-Bernal and M. A. Gómez-Albores. 2017. Climatic variability at the treeline of monte tlaloc, mexico: A dendrochronological approach. Trees 31: 441-453.

Babst, F., J. Esper and E. Parlow. 2010. Landsat tm/etm+ and tree-ring based assessment of spatiotemporal patterns of the autumnal moth (epirrita autumnata) in northernmost fennoscandia. Remote Sensing of Environment 114: 637-646.

Baird, R. A., D. Verbyla and T. N. Hollingsworth. 2012. Browning of the landscape of interior alaska based on 1986-2009 landsat sensor ndvi. Canadian Journal of Forest Research 42: 1371-1382.

Beck, P. S. A., L. Andreu-Hayles, R. D'Arrigo, K. J. Anchukaitis, C. J. Tucker, J. E. Pinzon and S. J. Goetz. 2013. A large-scale coherent signal of canopy status in maximum latewood density of tree rings at arctic treeline in north america. Global and Planetary Change 100: 109-118.

Beck, P. S. A. and S. J. Goetz. 2011. Satellite observations of high northern latitude vegetation productivity changes between 1982 and 2008: Ecological variability and regional differences. Environmental Research Letters 6: 049501.

Berner, L. T., P. S. A. Beck, A. G. Bunn and S. J. Goetz. 2013. Plant response to climate change along the forest-tundra ecotone in northeastern siberia. Global Change Biology 19: 3449-3462.

Berner, L. T., P. S. A. Beck, A. G. Bunn, A. H. Lloyd and S. J. Goetz. 2011. High-latitude tree growth and satellite vegetation indices: Correlations and trends in russia and canada (1982–2008). Journal of Geophysical Research: Biogeosciences 116: 1-13.

Bethany, L. C., T. Ramzi, J. A. Kevin, M. M. David and S. Fatih. 2017. Tree growth and vegetation activity at the ecosystem-scale in the eastern mediterranean. Environmental Research Letters 12: 084008.

Bhuyan, U., C. Zang, S. M. Vicente-Serrano and A. Menzel. 2017. Exploring relationships among tree-ring growth, climate variability, and seasonal leaf activity on varying timescales and spatial resolutions. Remote Sensing 9.

Biondi, F. 2001. A 400-year tree-ring chronology from the tropical treeline of north america. AMBIO: A Journal of the Human Environment 30: 162-166.

Biondi, F. and P. Hartsough. 2010. Using automated point dendrometers to analyze tropical treeline stem growth at nevado de colima, mexico. Sensors 10: 5827-5844.

Biondi, F., P. C. Hartsough and I. Galindo Estrada. 2005. Daily weather and tree growth at the tropical treeline of north america. Arctic, Antarctic, and Alpine Research 37: 16-24.

Biondi, F. and F. Qeadan. 2008a. Inequality in paleorecords. Ecology 89: 1056-1067.

Biondi, F. and F. Qeadan. 2008b. A theory-driven approach to tree-ring standardization: Defining the biological trend from expected basal area increment. Tree-Ring Research 64: 81-96.

Brehaut, L. and R. K. Danby. 2018. Inconsistent relationships between annual tree ring-widths and satellite-measured ndvi in a mountainous subarctic environment. Ecological Indicators 91: 698-711.

Bunn, A. G. 2008. A dendrochronology program library in r (dplr). Dendrochronologia 26: 115-124.

Bunn, A. G., M. K. Hughes, A. V. Kirdyanov, M. Losleben, V. V. Shishov, L. T. Berner, A. Oltchev and E. A. Vaganov. 2013. Comparing forest measurements from tree rings and a space-based index of vegetation activity in siberia. Environmental Research Letters 8.

Castruita-Esparza, L. U., A. Correa-Díaz, A. Gómez-Guerrero, J. Villanueva-Díaz, M. E. Ramírez-Guzmán, A. Velázquez-Martínez and G. Ángeles-Pérez. 2016. Basal area increment series of dominant trees of *pseudotsuga menziesii* (mirb.) franco show periodicity according to global climate patterns. Revista Chapingo Serie Horticultura XXII: 379-397.

Chen, Z. J., J. B. Li, K. Y. Fang, N. K. Davi, X. Y. He, M. X. Cui, X. L. Zhang and J. J. Peng. 2012. Seasonal dynamics of vegetation over the past 100 years inferred from tree rings and climate in hulunbei'er steppe, northern china. Journal of Arid Environments 83: 86-93.

Coulthard, B. L., R. Touchan, K. J. Anchukaitis, D. M. Meko and F. Sivrikaya. 2017. Tree growth and vegetation activity at the ecosystem-scale in the eastern mediterranean. Environmental Research Letters 12.

Council, N. R. 2006. Surface temperature reconstructions for the last 2,000 years. The National Academies Press. Washington, DC. 160 pp.

Eastman, J. 2016. Terrset manual. Clark University. 390 pp.

Eastman, J., F. Sangermano, E. Machado, J. Rogan and A. Anyamba. 2013. Global trends in seasonality of normalized difference vegetation index (ndvi), 1982–2011. Remote Sensing 5: 4799.

Florescano, E. 1980. Análisis histórico de las sequías en méxico. Secretaría de Agricultura y Recursos Hidráulicos, Comisión del Plan Nacional Hidráulico, Mexico.

Fritts, H. C. 1976. Tree rings and climate. Academic Press Inc, London. 567 pp.

García, E. 2004. Modificaciones al sistema de clasificación climática de koppen. 5th ed. Universidad Nacional Autónoma de México. México. 91 pp.

Goetz, S. J., A. G. Bunn, G. J. Fiske and R. A. Houghton. 2005. Satellite-observed photosynthetic trends across boreal north america associated with climate and fire disturbance. Proceedings of the National Academy of Sciences of the United States of America 102: 13521-13525.

Gómez-Guerrero, A., L. C. R. Silva, M. Barrera-Reyes, B. Kishchuk, A. Velazquez-Martinez, T. Martinez-Trinidad, F. O. Plascencia-Escalante and W. R. Horwath. 2013. Growth decline and divergent tree ring isotopic composition (δ^{13}c and δ^{18}o) contradict predictions of co_2 stimulation in high altitudinal forests. Global Change Biology 19: 1748-1758.

Hansen, M. C., P. V. Potapov, R. Moore, M. Hancher, S. A. Turubanova, A. Tyukavina, D. Thau, S. V. Stehman, S. J. Goetz, T. R. Loveland, A. Kommareddy, A. Egorov, L. Chini, C. O. Justice and J. R. G. Townshend. 2013. High-resolution global maps of 21st-century forest cover change. Science 342: 850-853.

Harris, I., P. D. Jones, T. J. Osborn and D. H. Lister. 2014. Updated high-resolution grids of monthly climatic observations – the cru ts3.10 dataset. International Journal of Climatology 34: 623-642.

He, J. and X. Shao. 2006. Relationships between tree-ring width index and ndvi of grassland in delingha. Chinese Science Bulletin 51: 1106-1114.

Holben, B. N. 1986. Characteristics of maximum-value composite images from temporal avhrr data. International Journal of Remote Sensing 7: 1417-1434.

Huete, A., K. Didan, T. Miura, E. P. Rodriguez, X. Gao and L. G. Ferreira. 2002. Overview of the radiometric and biophysical performance of the modis vegetation indices. Remote Sensing of Environment 83: 195-213.

Jenkerson, C., T. Maiersperger and G. Schmidt. 2010. Emodis: A user-friendly data source. U.S. Geological Survey Open-File Report 2010-1055: 10.

Jochner, M., H. Bugmann, M. Nötzli and C. Bigler. 2017. Tree growth responses to changing temperatures across space and time: A fine-scale analysis at the treeline in the swiss alps. Trees.

Karkauskaite, P., T. Tagesson and R. Fensholt. 2017. Evaluation of the plant phenology index (ppi), ndvi and evi for start-of-season trend analysis of the northern hemisphere boreal zone. Remote Sensing 9: 485.

Kaufmann, R. K., R. D. D'Arrigo, C. Laskowski, R. B. Myneni, L. Zhou and N. K. Davi. 2004. The effect of growing season and summer greenness on northern forests. Geophysical Research Letters 31: L09205 09201-09204.

Kaufmann, R. K., R. D. D'Arrigo, L. F. Paletta, H. Q. Tian, W. M. Jolly and R. B. Myneni. 2008. Identifying climatic controls on ring width: The timing of correlations between tree rings and ndvi. Earth Interactions 12: 1-14.

Kendall, M. G. 1975. Rank correlation methods. Charles Griffin. London. 272 pp.

Körner, C. 2012. Alpine treelines. Springer Basel. 220 pp.

Körner, C. 2017. A matter of tree longevity. Science 355: 130-131.

Körner, C. and J. Paulsen. 2004. A world-wide study of high altitude treeline temperatures. Journal of Biogeography 31: 713--732.

Krishnaswamy, J., R. John and S. Joseph. 2014. Consistent response of vegetation dynamics to recent climate change in tropical mountain regions. Global Change Biology 20: 203-215.

Lapenis, A. G., G. B. Lawrence, A. Heim, C. Y. Zheng and W. Shortle. 2013. Climate warming shifts carbon allocation from stemwood to roots in calcium-depleted spruce forests. Global Biogeochemical Cycles 27: 101-107.

Leavitt, S. W., T. N. Chase, B. Rajagopalan, E. G. Lee and P. J. Lawrence. 2008. Southwestern u.S. Tree-ring carbon isotope indices as a possible proxy for reconstruction of greenness of vegetation. Geophysical Research Letters 35.

Li, X., E. Liang, J. Gričar, S. Rossi, K. Čufar and A. M. Ellison. 2017. Critical minimum temperature limits xylogenesis and maintains treelines on the southeastern tibetan plateau. Science Bulletin 62: 804-812.

Liang, E., D. Eckstein and H. Liu. 2009. Assessing the recent grassland greening trend in a long-term context based on tree-ring analysis: A case study in north china. Ecological Indicators 9: 1280-1283.

Liang, E. Y., X. M. Shao and J. C. He. 2005. Relationships between tree growth and ndvi of grassland in the semi-arid grassland of north china. International Journal of Remote Sensing 26: 2901-2908.

Lobato-Sánchez, R. and M. A. Altamirano-del-Carmen. 2017. Detection of local temperature trends in mexico. Water Technology and Sciences (in Spanish) 8(6): 101-116.

Lopatin, E., T. Kolström and H. Spiecker. 2006. Determination of forest growth trends in komi republic (northwestern russia): Combination of tree-ring analysis and remote sensing data. Boreal Environment Research 11: 341-353.

Marín, L. E., O. Escolero-Fuentes and A. Trinidad-Santos. 2002. Physical geography, hydrogeology, and forest soils of the basin of mexico. *In*: Fenn M. E., de Bauer L. I. and Hernández-Tejeda T.s (eds.). Urban air pollution and forests: Resources at risk in the mexico city air basin. Springer New York. New York, NY. pp. 44-67.

Matías, L., J. C. Linares, Á. Sánchez-Miranda and A. S. Jump. 2017. Contrasting growth forecasts across the geographical range of scots pine due to altitudinal and latitudinal differences in climatic sensitivity. Global Change Biology: 1-11.

Maxwell, T. M., L. C. R. Silva and W. R. Horwath. 2018. Integrating effects of species composition and soil properties to predict shifts in montane forest carbon–water relations. Proceedings of the National Academy of Sciences.

McCarroll, D. and N. J. Loader. 2004. Stable isotopes in tree rings. Quaternary Science Reviews 23: 771-801.

Metcalfe, S. E. 1987. Historical data and climatic change in mexico: A review. The Geographical Journal 153: 211-222.

Miyeni, R. B., F. G. Hall, P. J. Sellers and A. L. Marshak. 1995. The interpretation of spectral vegetation indexes. IEEE Transactions on Geoscience and Remote Sensing 33: 481-486.

Mokria, M., M. Tolera, F. J. Sterck, A. Gebrekirstos, F. Bongers, M. Decuyper and U. Sass-Klaassen. 2017. The frankincense tree boswellia neglecta reveals high potential for restoration of woodlands in the horn of africa. Forest Ecology and Management 385: 16-24.

Muggeo, V. M. R. 2008. Segmented: An r package to fit regression models with broken-line relationships. R News 8: 20-25.

Myneni, R. Y. K. and T. Park. 2015. Mod15a2h modis/terra leaf area index/fpar 8-day l4 global 500m sin grid v006. Nasa eosdis land processes daac. Doi.Org/10.5067/modis/mod15a2h.006.

Neeti, N. and J. R. Eastman. 2011. A contextual mann-kendall approach for the assessment of trend significance in image time series. Transactions in GIS 15: 599-611.

ORNL DAAC. 2017. Modis collection 6 land products global subsetting and visualization tool. Ornl daac, oak ridge, tennessee, USA. Accessed january 30, 2018. Subset obtained for mod15a2h product at 19.4155n,98.7129w, time period: 2000-02-26 to 2016-12-26, and subset size: 24.5 x 24.5 km. Doi.Org/10.3334/ornldaac/1379.

Perry, J. P. 1991. The pines of mexico and central america. Timber Press. Portland, Oregon. 231 pp.

Qi, J., S. Niu, Y. Zhao, M. Liang, L. Ma and Y. Ding. 2017. Responses of vegetation growth to climatic factors in shule river basin in northwest china: A panel analysis. Sustainability 9: 368.

Ricker, M., G. Gutierrez-Garcia and D. C. Daly. 2007. Modeling long-term tree growth curves in response to warming climate: Test cases from a subtropical mountain forest and a tropical rainforest in mexico. Canadian Journal of Forest Research 37: 977-989.

Robinson, W. J. and R. Evans. 1980. A microcomputer-based tree-ring measuring system. Tree-Ring Bulletin 1980: 59-64.

Rossi, S., A. Deslauriers, T. Anfodillo and V. Carraro. 2007. Evidence of threshold temperatures for xylogenesis in conifers at high altitudes. Oecologia 152: 1-12.

Rossi, S., A. Deslauriers, T. Anfodillo and M. Carrer. 2008. Age-dependent xylogenesis in timberline conifers. New Phytol 177: 199-208.

Saenz-Romero, C., J. B. Lamy, E. Loya-Rebollar, A. Plaza-Aguilar, R. Burlett, P. Lobit and S. Delzon. 2013. Genetic variation of drought-induced cavitation resistance among *pinus hartwegii* populations from an altitudinal gradient. Acta Physiologiae Plantarum 35: 2905-2913.

Salzer, M. W., M. K. Hughes, A. G. Bunn and K. F. Kipfmueller. 2009. Recent unprecedented tree-ring growth in bristlecone pine at the highest elevations and possible causes. Proceedings of the National Academy of Sciences 106: 20348-20353.

Sen, P. K. 1968. Estimates of the regression coefficient based on kendall's tau. Journal of the American Statistical Association 63: 1379-1389.

Shunsuke, T. and S. Atsuko. 2018. Time lag and negative responses of forest greenness and tree growth to warming over circumboreal forests. Global Change Biology 0.

Silva, L. C. R. 2017. Carbon sequestration beyond tree longevity. Science 355: 1141-1141.

Silva, L. C. R. and M. Anand. 2013. Probing for the influence of atmospheric co_2 and climate change on forest ecosystems across biomes. Global Ecology and Biogeography 22: 83-92.

Silva, L. C. R., G. Sun, X. Zhu-Barker, Q. Liang, N. Wu and W. R. Horwath. 2016. Tree growth acceleration and expansion of alpine forests: The synergistic effect of atmospheric and edaphic change. Science Advances 2.

Šímová, I. and D. Storch. 2017. The enigma of terrestrial primary productivity: Measurements, models, scales and the diversity–productivity relationship. Ecography 40: 239-252.

Stokes, M. A. and T. L. Smiley. 1968. An introduction to tree-ring dating. University of Chicago Press. Chicago, IL. USA. 73 pp.

Therrell, M. D., D. W. Stahle, M. K. Cleaveland and J. Villanueva-Diaz. 2002. Warm season tree growth and precipitation over mexico. Journal of Geophysical Research Atmospheres 107: 6-1-6-8.

Vicente-Serrano, S. M., J. J. Camarero, J. M. Olano, N. Martin-Hernandez, M. Pena-Gallardo, M. Tomas-Burguera, A. Gazol, C. Azorin-Molina, U. Bhuyan and A. El-Kenawy. 2016. Diverse relationships between forest growth and the normalized difference vegetation index at a global scale. Remote Sensing of Environment 187: 14-29.

Villanueva-Díaz, J., J. Cerano Paredes, L. Vázquez Selem, D. W. Stahle, P. Z. Fulé, L. L. Yocom, O. Franco Ramos and J. Ariel Ruiz Corral. 2015. Red dendrocronológica del pino de altura (*pinus hartwegii* lindl.) para estudios dendroclimáticos en el noreste y centro de méxico. Investigaciones Geográficas, Boletín del Instituto de Geografía 2015: 5-14.

Villanueva-Diaz, J., L. Vazquez-Selem, A. Gomez-Guerrero, J. Cerano-Paredes, N. A. Aguirre-Gonzalez and O. Franco-Ramos. 2016. Dendrochronologic potential of *juniperus monticola* martinez in mountain tlaloc, mexico. Revista Fitotecnia Mexicana 39: 175-185.

Wang, H., F. Chen, R. Zhang and L. Qin. 2017. Seasonal dynamics of vegetation of the central loess plateau (china) based on tree rings and their relationship to climatic warming. Environment, Development and Sustainability 19: 2535-2546.

Wang, J., P. M. Rich, K. P. Price and W. D. Kettle. 2004. Relations between ndvi and tree productivity in the central great plains. International Journal of Remote Sensing 25: 3127-3138.

Wang, T., A. Hamann, D. Spittlehouse and C. Carroll. 2016. Locally downscaled and spatially customizable climate data for historical and future periods for north america. PLOS ONE 11: e0156720.

Wang, T., A. Hamann, D. L. Spittlehouse and T. Q. Murdock. 2012. Climatewna—high-resolution spatial climate data for western north america. Journal of Applied Meteorology and Climatology 51: 16-29.

Wang, Y., R. Lu, Y. Ma, H. Meng and S. Gao. 2014. Response to climate change of different tree species and ndvi variation since 1923 in the middle arid region of ningxia, china. Sciences in Cold and Arid Regions 6: 30-36.

Wigley, T. M. L., K. R. Briffa and P. D. Jones. 1984. On the average value of correlated time series, with applications in dendroclimatology and hydrometeorology. Journal of Climate and Applied Meteorology 23: 201-213.

Xu, C., Y. Li, J. Hu, X. Yang, S. Sheng and M. Liu. 2012. Evaluating the difference between the normalized difference vegetation index and net primary productivity as the indicators of vegetation vigor assessment at landscape scale. Environmental Monitoring and Assessment 184: 1275-1286.

Yocom, L. L., P. Z. Fulé and P. Brando. 2012. Human and climate influences on frequent fire in a high- elevation tropical forest. Journal of Applied Ecology 49: 1356-1364.

Zang, C. and F. Biondi. 2015. Treeclim: An r package for the numerical calibration of proxy-climate relationships. Ecography 38: 431-436.

CHAPTER II. FROM TREES TO ECOSYSTEMS: SPATIO-TEMPORAL SCALING OF CLIMATIC IMPACTS ON MONTANE REGIONS USING DENDROCHRONOLOGICAL, ISOTOPIC AND REMOTELY-SENSED DATA[2]

2.1. Resumen

Actualmente, la disponibilidad de información de sensores remotos en periodos de tiempo más amplios nos permite proponer enfoques multiproxi para entender el comportamiento fisiológico de los bosques ante cambio climático. En este capítulo, se trabajó en un enfoque múltiple incorporando series de anillos de crecimiento de árboles, firmas de isótopos estables de la madera, información de sensores remotos e información climática para desarrollar un análisis espacio-temporal de la fisiología de los árboles en un bosque de alta montaña (Tláloc- Estado de México). Para capturar una mayor variabilidad topográfica, se consideraron mediciones que incluyeron dos niveles de elevación y exposición contrastantes. Las principales preguntas fueron: ¿cómo el desempeño fisiológico de los árboles puede estar ligado a la información proveniente de sensores remotos? y ¿cómo la topografía modifica esta relación? Las firmas de isótopos estables de carbono y oxígeno ($\delta^{13}C$, $\delta^{18}O$), la discriminación de ^{13}C ($\Delta^{13}C$), y la eficiencia de uso de agua intrínseca (EUAi) para el periodo 2000- 2016, se transformaron mediante un análisis de componentes principales y después se correlacionaron con composiciones máximas de NDVI a cada 16 días. Además, los efectos de altitud, exposición y tiempo se probaron a través de modelos lineares mixtos. La información fisiológica y satelital mostró estar correlacionada, principalmente en el periodo de otoño-invierno del año previo y al principio de la estación de crecimiento. Las firmas del isótopo de carbono ($\delta^{13}C$) disminuyeron independientemente de su posición espacial, mientras que para oxígeno ($\delta^{18}O$) se encontró un efecto significativo de elevación y tiempo. A pesar de que $\Delta^{13}C$ no estuvo relacionada con elevación o exposición, se observó un incremento paralelo con EUAi pero destacando una reducción notable durante una sequía extrema. Los resultados permitieron desarrollar un protocolo multiproxi para el análisis espacio-temporal de los ecosistemas forestales y discutir relaciones particulares en el tiempo.

Palabras clave: *Pinus hartwegii*, dendroecología, NDVI, eficiencia de uso de agua

[2] Artículo en revisión en Global Biogeochemical Cycles 2019

2.2. Abstract

At present, the availability of remotely-sensed data in longer periods gives us the opportunity to propose multiproxy approaches for the understanding of forest physiology under ongoing climate change. In this chapter, we present a multiproxy approach incorporating tree-ring series, wood isotope signatures, remotely sensed variables and climatic information to perform a spatio-temporal analysis of tree physiology at a high-elevation forest (Tláloc – State of México). To capture more landscape variability, we consider direct measured information that includes two contrasting levels of elevation and aspect. The main questions addressed are how tree physiological performance can be linked to the satellite-derived information and how the landscape shape this relationship. Annually resolved carbon and oxygen isotopic ratios ($\delta^{13}C$, $\delta^{18}O$), carbon isotope discrimination ($\Delta^{13}C$), and intrinsic water use efficiency (iWUE), for the period 2000 to 2016, were transformed by principal component analysis and then correlated with NDVI 16-day composite time series. Furthermore, altitude, aspect and time effects were tested by linear mixed-effects models. The physiological variables and satellite information was shown to be correlated, mainly in the fall-winter season of the previous year and at the beginning of the growing season. The carbon isotope composition ($\delta^{13}C$) has decreased regardless of spatial position, while oxygen isotope composition ($\delta^{18}O$) showed an altitude and time effect. Although $\Delta^{13}C$ was not related to altitude or aspect, we observed a common increase in iWUE but with a notable concomitant reduction with a severe drought event. The results allowed us to develop a multiproxy protocol for the spatio-temporal analysis of forest ecosystems and discuss particular relationships over time.

Keywords: *Pinus hartwegii*, dendroecology, NDVI, intrinsic water use efficiency

2.3. Introduction

The change in tree physiology response in high-elevation forests, where tree growth is limited by temperature, need more research attention to address the effects of climate warming (Körner *et al.*, 2016; Jochner *et al.*, 2017). As atmospheric carbon dioxide (C_a) increases (410 ppm, at present) (Blunden and Arndt, 2018), trees are responding in different ways including responses with some homeostatic regulations that influence plant productivity, foliar mass production, and water use efficiency (Gedalof and Berg, 2010; Peñuelas *et al.*, 2011; Silva and Anand, 2013). However, traditional approaches have not or slightly considered a spatial component, which strongly limits the prediction of physiological performance at large scales based only in tree-ring records. Only a few studies have linked successfully isotopic compositions and remotely sensed data with a high potential to integrate with current dendroecology studies allowing elucidate the ecosystem processes spatially (Leavitt *et al.*, 2008; del Castillo *et al.*, 2015; Levesque *et al.*, 2019).

Tree responses to climate change are not expected to be universal (Gómez-Guerrero and Doane, 2018), and divergent tree species-behavior have been documented globally (Gómez-Guerrero *et al.*, 2013; Xu *et al.*, 2014; Granda *et al.*, 2017; Wang *et al.*, 2018). At local scales, micro-climatic and topographic conditions (i.e. altitude and aspect) indirectly influence the physiological responses, making tree growth predictions more complicate as climate change progresses (Treml *et al.*, 2012; Camarero *et al.*, 2015; Yi *et al.*, 2018).

To reconstruct plant physiological behavior under rising atmospheric CO_2 (C_a), tree-ring stable isotope ratios of carbon ($\delta^{13}C$) and oxygen ($\delta^{18}O$) (the dual-isotope approach) have served as a powerful tool that combines carbon assimilation and water relations across a range of spatial scales from tree to forest stands (Dawson *et al.*, 2002; McCarroll and Loader, 2004; Werner *et al.*, 2012). Carbon isotope ratios in tree-rings are related to the diffusion and biochemical process of substrate and products during photosynthesis (Farquhar *et al.*, 1982). Under limited water availability, trees avoid water loss through closing stomata, resulting in a reduction in stomatal conductance (g_s) and the ratio

between leaf intercellular (C_i) and C_a, causing lower discrimination against $^{13}CO_2$ and higher $\delta^{13}C$ (Farquhar *et al.*, 1989; McDowell *et al.*, 2008). The regulation of water loss from stomata imply a trade-off between carbon fixation and transpiration. Thus, the variation in water use efficiency (*iWUE*, the ratio between carbon acquired to water vapor loss via stomatal conductance) can influence forest productivity (Linares and Camarero, 2012; Sanders *et al.*, 2016). On the other hand, oxygen stable isotope signatures are coupled to the source of water and leaf evaporative enrichment, containing temperature and transpiration signals that help to distinguish effects of stomatal conductance (Barbour, 2007). Therefore, the dual-isotope approach can suggest how either photosynthesis (*A*) or g_s modulate the variation in *iWUE*, as a response to environmental change (Scheidegger *et al.*, 2000).

The response of forests to climate change has been intensively studied and understood from the tree-ring perspective that assesses productivity and indirectly health status and resilience capacity (Fritts, 1976; Lloret *et al.*, 2011). Multi-proxy approaches, that incorporates variables related to physiological process (i.e. stable isotope ratios in tree-rings) and anatomical wood properties (i.e. size of xylem conduits or maximum density) to customary dendrochronology techniques, has helped to provide additional insights into the physiological processes that modulate tree response to environmental change (McCarroll and Loader, 2004; Martínez-Vilalta, 2018). The addition of remotely-sensed information combined with standard proxies presents a new opportunity to assess and predict tree and forest response to climate variability and changes over spatio-temporal scales (del Castillo *et al.*, 2015; Maxwell *et al.*, 2018; Levesque *et al.*, 2019; Tei *et al.*, 2019).

The ecophysiological dynamics of an ecosystem can be derived and mapped from remotely-sensed data through a link between vegetation indices (i.e. Normalized Difference Vegetation Index NDVI) and tree-ring stable isotopes ratios (Guo and Xie, 2006; Leavitt *et al.*, 2008). Vegetation indices show a derivate of surface reflectance spectral profiles (chlorophyll absorption) with respect to wavelength, indicating physiological outcomes and photosynthetic capacity, across space and time (Miyeni *et*

al., 1995; Kaufmann *et al.*, 2008; del Castillo *et al.*, 2015; Vicente-Serrano *et al.*, 2016). For example, the use of NDVI can be a useful proxy of canopy photosynthetic activity related to tree-ring width measurements (Wang *et al.*, 2004; Bunn *et al.*, 2013; Brehaut and Danby, 2018; Correa-Díaz *et al.*, 2019).

In the multiproxy approach presented here, we incorporated tree-ring series, wood isotope signatures, remotely sensed data, and climatic information in a high-elevation forest in central Mexico, dominated by pure stands of Mexican Mountain Pine (*Pinus hartwegii* Lindl.) (Perry, 1991). To capture more variability in the landscape we consider two contrasting levels of altitude (3500 and 3900 m asl) and aspect (NW and SW). We present a specific protocol so that the readers can have a reference to handle information under a multiproxy approach. The questions addressed were: (i) how topographic factors like altitude and aspect have driven *P. hartwegii* physiological behavior over time, and (ii) how tree physiological performance can be spatially and temporally linked to a remotely-sensed variable such as NDVI. We also comment on the reliability of our approach by discussing the results in the framework of three possible leaf gas-exchange scenarios, constant C_i, C_i/C_a, and $C_a - C_i$ (Saurer *et al.*, 2004). Because tree growth and physiological performance are influenced by site conditions (Körner *et al.*, 1991; Maxwell *et al.*, 2018), we hypothesize that the combined site information from different altitudes and aspects with remotely sensed variables is an approach to gain a better spatio-temporal understanding of the physiological performance of forests. Additionally, based on the fact that previous winter NDVI is coupled with *P. hartwegii's* ring-width (Correa-Díaz *et al.*, 2019), we hypothesize that stable isotope ratios might be linked to a specific NDVI time period according to temperature restrictions on photosynthetic activity (Castillo *et al.*, 2015).

2.4. Materials and Methods

2.4.1. Study area

The study was conducted in a pure, uneven-aged *P. hartwegii* forest, along an altitude gradient (3500 and 3900 m asl) with two contrasting aspects (Northwest and Southwest) in a National Park (Iztaccíhuatl-Popocatépetl) in central Mexico, specifically at Tlaloc

Mountain with coordinates of 19.385° N and -98.738°O and a maximum elevation of 4, 125 m. Mean annual temperature ranges from 7 to 9°C and annual rainfall from 800 to 1,200 mm, so the climate is classified as C (w^2)(w) according to Köppen climate classification as modified by García (2004) for Mexico regions (Figure 2. 1). The climate is characterized by abundant precipitation during summer (June to September, 70 % of total) and a dry period through winter-spring transition. Recently, a temperature increase (≈1.4°C) has been detected for the last decades at the study site (Harris *et al.*, 2014; Lobato-Sánchez and Altamirano-del-Carmen, 2017) as well at nearby high-altitude forests dominated by *P. hartwegii* (Biondi *et al.*, 2009).

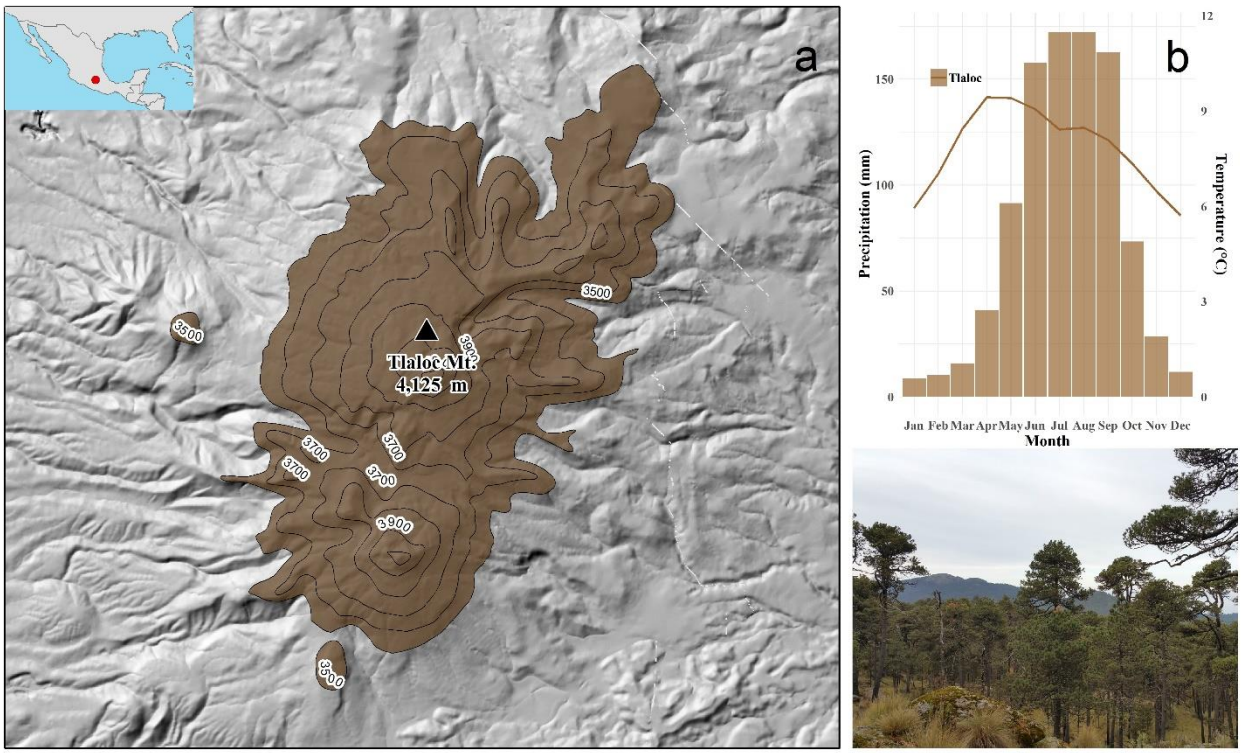

Figure 2. 1 (a) Localization of the study area (Tlaloc-TLA), (b) Climograph of the mean monthly temperature and precipitation values according to climatic data extracted using ClimateNA (Wang et al., 2016), and (c) General view of Mexican high-elevation forest.

2.4.2. Sampling and dendrochronological procedure

In 2016, a total of 70 healthy mature trees were sampled across four sites with different combinations in altitude and aspect (3500-NW, 3500-SW, 3900-NW and 3900-SW). In each site of the four sites, at least 15 trees were sampled to capture the common site-

signal of the study area (Fritts, 1976). For each tree, a single increment core bark to bark was sampled, at breast height (1.3 m) using a 12 mm diameter Haglöf increment borer. Increment cores were air-dried and mounted on wood pieces and polished using sandpaper until tree-ring boundaries were clear.

A Velmex measuring system was used to obtain the ring-width to a precision of 0.001 mm. Then, standard dendrochronology techniques were followed to process the increment cores (Stokes and Smiley, 1968). The quality control of dating and basal area increment (BAI) chronologies by site were done using the Dendrochronology Program Library in R (‘*dplR*’) (Biondi and Qeadan, 2008; Bunn, 2008). To compare the forest growth trends with the physiological performance of *P. hartwegii*, we focused on the period 2000 to 2016 for BAI chronologies but the complete time series can be found in Correa-Díaz *et al.* (2019).

2.4.3. Isotopic analysis of tree-rings

We used the best four correlated trees with the master chronology per site, to obtain the physiological response to elevated *Ca* during the last 17 years. Increment cores were dissected under a microscope by scalpel into annual growth rings from 2000 to 2016, then every single tree-ring sample was finely grounded by a handheld rotary tool (MDC Dental III ®) to homogenize the sample and gather enough material for isotopic analysis (carbon and oxygen) (Leavitt, 2010). We use bulk wood instead of determining α-cellulose since it has been shown that bulk wood is also related to climate parameters and physiological information (Gori *et al.*, 2013; Mischel *et al.*, 2015; Rossella *et al.*, 2017). For carbon, 1.2 mg was packed into tin capsules and introduced into a PDZ Europa ANCA-GSL elemental analyzer for combustion at 1,000 °C. Then, the reduced gas was transferred to PDZ Europa 20-20 isotope ratio mass spectrometer. For oxygen samples, 0.5 mg of bulk wood were prepared in silver capsules and analyzed using an elementary Pyro-Cube coupled to an Isoprime VisION mass spectrometer. All samples were processed in the Stable Isotope Facility at the University of California, Davis.

Stable isotope ratios ($^{13}C/^{12}C$ and $^{18}O/^{16}O$) are expressed according to the Vienna Pee Dee Belemnite (VPDB) standard for $\delta^{13}C$ and Vienna Standard Mean Ocean Water for $\delta^{18}O$, both in delta notation (δ) in parts per thousand (‰) (1).

$$\delta^{y}X = [(R_{sample} / R_{standard})-1] \times 1000 \quad (1)$$

where X is the atom of interest (either carbon or oxygen), *y* is the atomic mass of the heavy isotope, R_{sample} and $R_{standard}$ are the measured ratios in the sample and the standard, respectively. The analytical error (standard deviation) of the isotope measurements reported by the laboratory was < 0.09 ‰.

To calculate the carbon isotopic discrimination relative to the source (atmospheric CO_2), this is accounting for the depletion effect for fossil fuel burning, we used the equation (2).

$$\Delta^{13}C = (\delta^{13}C_{air} - \delta^{13}C_{plant}) / (1 + \delta^{13}C_{plant}/1000) \quad (2)$$

where subscripts refer to carbon isotope composition in the atmosphere and the plant, respectively (Farquhar *et al.*, 1989). To reconstruct the physiological parameter of intrinsic water use efficiency (iWUE), the ratio of photosynthetic uptake of CO_2 by water loss, carbon isotopic discrimination was converted to the ratio of leaf intercellular (C_i) and atmospheric CO_2 (C_a), using the next equation (3).

$$\Delta^{13}C = a + (b-a) (C_i/C_a) \quad (3)$$

where *a* is the diffusional fractionation of $^{13}CO_2$ through the stomata (≈4.4 ‰) and *b* is the biochemical fractionation by Rubisco (≈27 ‰). Then, iWUE was calculated using C_i, C_a and the difference in diffusivity of CO_2 and water in the air (0.625 $g_{H2O} = g_{CO2}$) according to Fick's Law (Farquhar *et al.*, 1989).

$$iWUE = A/g_s = C_a \times [1- (C_i/C_a)] * 0.625 \quad (4)$$

where *A* is the rate of CO_2 assimilation by the leaves and g_s is the leaf stomatal conductance. Consequently, yearly iWUE can be compared to different climatic factors to indicate physiological responses to water availability or changing growing conditions. Notably, all our measurements were done in trees older than 50 years (121 ± 11 years) so the juvenile effect in isotopic measurements is negligible (McCarroll and Loader, 2004). Theoretical scenarios for changes in iWUE were evaluated using the framework proposed by Saurer *et al.* (2004). Here, we used simple standard deviation between theoretical scenarios and calculated iWUE by site as a first approximation of the gas-exchange response of *P. hartwegii* to climate variations.

We used the few available monthly $\delta^{18}O$ values from the Global Network of Isotopes in Precipitation (GNIP) from a nearby station dominated by *P. hartwegii* (Desierto de los Leones, Mexico), located in the same regional isohyet, to assess the magnitude of changes in source water over the study period.

2.4.4. Altitude, aspect and time effects on the physiological adjustment of Mexican mountain pine

We analyzed altitude, aspect and time effects in $\delta^{13}C$, $\delta^{18}O$, $\Delta^{13}C$, C_i, iWUE, and BAI via linear mixed-effects models for repeated measured data using the '*nlme'* package in R (Pinheiro *et al.*, 2018). These models rely on the assumption that a tree's pattern of response depends on observed and unobserved characteristics, which can be included in the model as random effects (Everitt, 2005). Either random intercept or intercept/slope models were tested; including altitude, aspect, and calendar year as fixed factors while tree and year were included as random factors. The correlational structure of the repeated measurement by year of the data was included by an autoregressive process of order 1 (AR1). Differences between sites (altitude x aspect) were tested by post hoc Bonferroni's test using *emmeans* library in R (Hochberg, 1988).

2.4.5. A combined index of physiological variables and correlation with satellite-derived photosynthesis

First, to represent every physiological variable ($\delta^{13}C$, $\delta^{18}O$, $\Delta^{13}C$, or iWUE) on a new common temporal variable at region level, we ran a principal component analysis and selected the corresponding first principal score (PC1) for each variable (Andreu *et al.*, 2007; Jenkerson *et al.*, 2010). Then, we correlated an NDVI 16-day composite time series (250-meter spatial resolution), produced by U.S. Geological Survey's (USGS), with the PC1 of each physiological variable according to a pixel-wise Kendall's tau correlation (τ) (Figure 2. 2). Kendall's tau correlation is a rank-based measure of association, that is highly recommended when the data do not come from a bivariate normal distribution (Hollander *et al.*, 2013). Afterward, we masked out all none statistically significant correlated pixels by map according to their p-values. Finally, a total of 21 correlation maps (November from the previous year until September of the current year) by each physiological variable were analyzed, using the number of pixels and the highest correlation as an indicator of maximum association between photosynthetic and physiological activity.

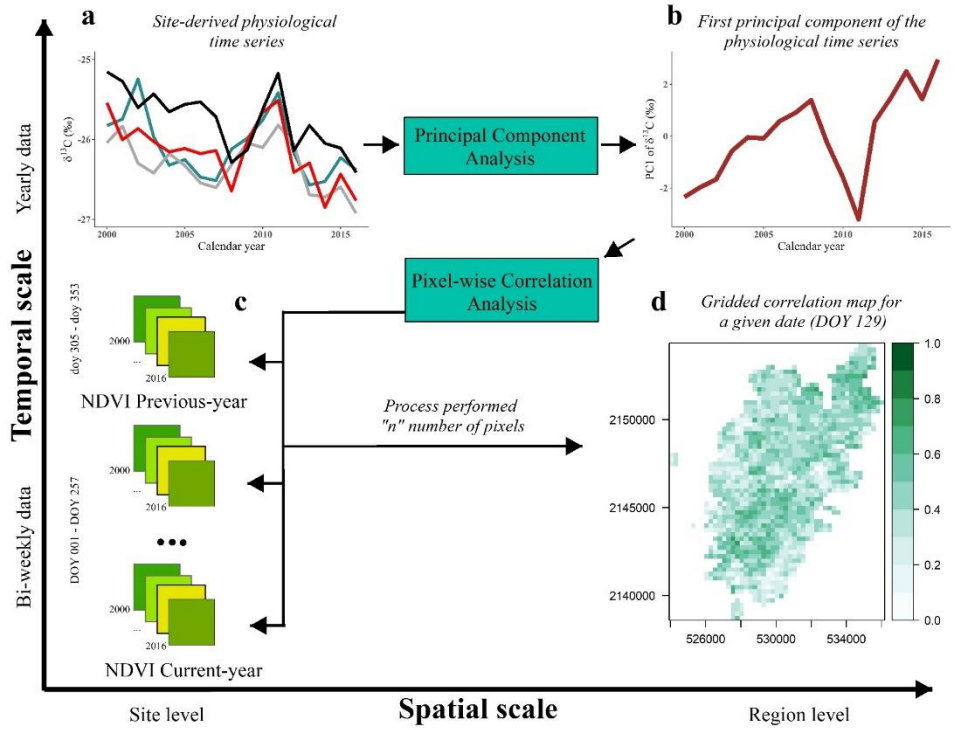

Figure 2. 2 Overview of the process to link physiological to remotely sensed information across space and time. (a) Physiological information is displayed according to a combination of topographic conditions (altitude and aspect), in this case representing stable isotope ratios of carbon ($\delta^{13}C$). (b) This information is turned into a new variable according to Principal Component Analysis (PCA). (c) The new variable is correlated with bi-weekly NDVI at a pixel level, starting from previous November to current September. (d) Once non-significant pixels are masked out, the spatio-temporal association of the forest ecosystem process is integrated.

2.4.6. Climatic variables and their influence on the physiological performance

Because of the lack of long term climatological data, we used the downscaled time series (according to 250-m digital elevation model) generated by software package ClimateNA v550 (Wang *et al.*, 2012; Wang *et al.*, 2016), which is based on the Climate Research Unit database (CRU ts 4.01) produced by the University of East Anglia (Harris *et al.*, 2014). The climate data included monthly temperature (maximum, average and minimum), precipitation, degree-days above 5°C (DD > 5°C), degree-days below 18°C

(DD < 18°C), evaporation reference (mm), climatic moisture deficit (mm) and relative humidity (%) from 2000 to 2016. Furthermore, leaf-to-air vapor pressure deficit (VPD) was calculated using the temperature and relative humidity according to Allen *et al.* (1998) equations. The VPD is the difference between the vapor pressure inside the stomata (e_s) and actual vapor pressure (e_a). Finally, a bootstrapped Pearson's correlation was used between climatic data and physiological chronologies ($\delta^{13}C$, $\delta^{18}O$, $\Delta^{13}C$, and iWUE) using *'treeclim'* in R (Zang and Biondi, 2015).

2.5. Results

2.5.1. The altitudinal/aspect effect in *P. hartwegii* physiology

The carbon isotope composition ($\delta^{13}C$) *P. hartwegii* has decreased regardless of altitude or aspect over the last 17 years ($p < 0.001$) (Table 2.1). We did not find a significant difference among sites ($p > 0.05$); nevertheless, compared to low-elevation, the high-elevation sites had a larger rate of dilution (0.074 and 0.033 ‰ per year, respectively). The carbon isotope discrimination ($\Delta^{13}C$) did not show time, altitude or aspect effect, except for a marginal relationship for altitude x aspect interaction (Table 2.1). As with $\delta^{13}C$, there were no significant differences among sites in $\Delta^{13}C$ ($p > 0.05$), but a marginal effect was detected at the 3500-SW site ($p = 0.09$). The oxygen isotope composition ($\delta^{18}O$) showed both an altitude ($p = 0.02$) and time effect ($p < 0.001$). The largest difference among sites was for the 3500-SW site and both high-elevation sites (3900-SW and 3900-NW) (Figure 2. 3b), which led to a larger rate of decrease in $\delta^{18}O$ for 3500-SW (-0.102 ‰ per year). Relevant the fact that the highest $\delta^{13}C$, lowest discrimination, and high-peak for $\delta^{18}O$ were in 2011, which is synchronous with the warmest and lowest relative humidity year for the period analyzed (notorious drought event).

Table 2. 1 Results of the linear mixed-effects models (random intercept model) fitted to the physiological variables of *Pinus hartwegii* from 2000 to 2016. In the analysis, tree and year were tested as random factors. DF, degrees of freedom. Significance levels $^{\dagger}p < 0.1$, $^{*}p < 0.05$, $^{**}p < 0.01$ and $^{***}p < 0.001$.

Variable	Fixed Effect	Estimated regression coefficient	Std. error	DF	p-value
$\delta^{13}C$	Year	-0.050	0.008	231	<0.0001***
	Aspect	-0.040	0.436	12	0.928
	Altitude	-0.198	0.436	12	0.659
	Altitude x Aspect	0.636	0.617	12	0.323
$\Delta^{13}C$	Year	0.006	0.008	231	0.415
	Aspect	0.038	0.488	12	0.939
	Altitude	0.813	0.488	12	0.121
	Altitude x Aspect	-1.234	0.690	12	0.098†
$\delta^{18}O$	Year	-0.073	0.014	223	<0.0001***
	Aspect	-0.410	0.556	12	0.475
	Altitude	1.404	0.554	12	0.026*
	Altitude x Aspect	-1.717	0.786	12	0.049*
C_i	Year	1.340	0.133	231	<0.0001***
	Aspect	0.723	8.325	12	0.932
	Altitude	13.962	8.324	12	0.119
	Altitude x Aspect	-21.112	11.774	12	0.098†
C_i/C_a	Year	0.001	0.001	231	0.415
	Aspect	0.002	0.022	12	0.939
	Altitude	0.036	0.022	12	0.121
	Altitude x Aspect	-0.055	0.030	12	0.099†
Ca-Ci	Year	0.789	0.130	231	<0.0001***
	Aspect	-0.717	8.316	12	0.933
	Altitude	-13.961	8.316	12	0.119
	Altitude x Aspect	21.137	11.763	12	0.098†

iWUE	Year	0.493	0.081	231	<0.0001***
	Aspect	-0.448	5.198	12	0.933
	Altitude	-8.726	5.198	12	0.119
	Altitude x Aspect	13.210	7.352	12	0.098†

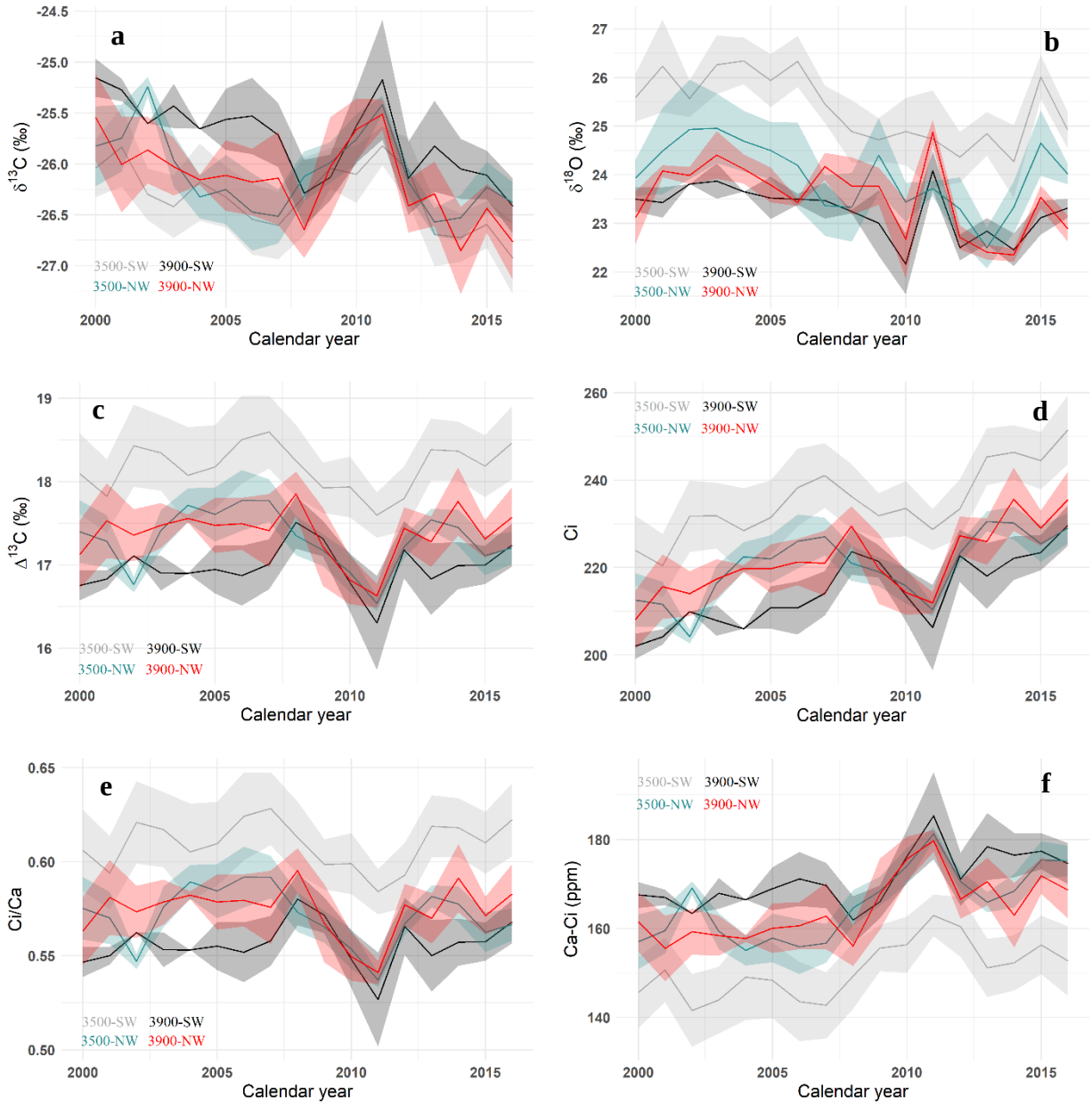

Figure 2. 3 (a) The carbon isotope ($\delta^{13}C$), (b) oxygen isotope ($\delta^{18}O$), and (c) carbon isotope discrimination ($\Delta^{13}C$), (d) leaf intercellular CO_2 concentration (C_i), (e) leaf–atmosphere CO_2 ratio (C_i/C_a), and (f) atmosphere-leaf CO_2 difference (C_a - C_i)

chronologies for *P. hartwegii* from 2000 to 2016. Red, black, blue and grey lines represent 3900-NW, 3900-SW, 3500-NW, and 3500-SW sites, respectively. Shaded areas are standard errors.

The leaf intercellular CO_2 concentration (C_i) and its difference with atmospheric CO_2 (C_a) changed over time but neither altitude nor aspect effect was significant ($p > 0.05$). The smaller rate of increase of C_i was found at 3500-NW (0.97 ppm per year ≈ + 7.75 % respect to the year 2000) with a parallel increase for the other sites (≈ 1.62 ppm per year). Conversely, the largest difference between CO_2 concentrations (atmosphere and leaves, $C_a - C_i$) was for 3500-NW (1.07 ppm per year ≈ + 11.58 % respect to 2000's value). The 3500-SW, 3900-NW and 3900-SW sites had similar values (≈ 0.42 ppm per year). The temporal trend in C_i/C_a did not change over time across all combinations of altitude and aspect ($p = 0.415$). However, a notable physiological adjustment was noticed in 2011, coinciding with a change in both C_i and C_i/C_a, and a larger difference between CO_2 concentrations.

A significant positive correlation between $\delta^{18}O$ and $\delta^{13}C$ was found at high-elevation sites (3900-NW and 3900-SW); however, no significant relationship was detected for low-elevation sites, particularly at 3500-SW ($r = 0.05$) (Figure 2. 4a). The oxygen isotope composition ($\delta^{18}O$) from the 3500-SW site was only significantly positively correlated with $\delta^{18}O$ summer rainfall ($r = 0.76$, $p = 0.03$), from May to September. The rest of the conditions, mainly at high-elevation, showed a poor correlation with $\delta^{18}O$ summer rainfall.

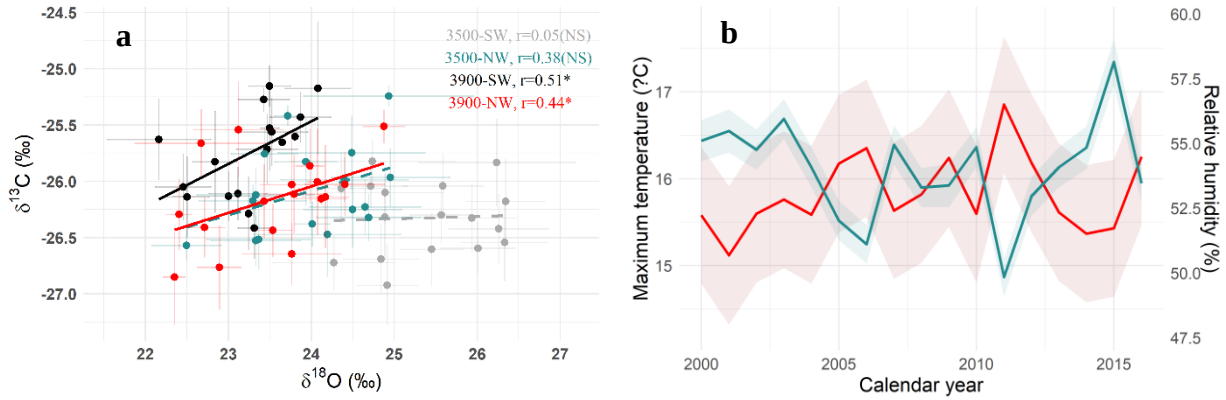

Figure 2. 4 (a) Scatterplot between $\delta^{18}O$ and $\delta^{13}C$ by sites. Significant and no significant linear regressions are represented by the solid and dashed line, respectively. * denotes a significant correlation, and (b) Average maximum temperature (red line) and relative humidity (blue line) (%) at the study site. Shaded areas represent standard deviations.

2.5.2. iWUE and leaf gas-exchange scenarios

The temporal trends in iWUE showed a significant increase in the last 17 years ($p < 0.001$), regardless of altitude or aspect, but there was no significant difference among sites (Figure 2. 4). The iWUE increases by year were larger at 3500-NW (0.66 µmol mol^{-1} per year ≈ + 11.6 % respect to the year 2000) than the other sites (0.26 µmol mol^{-1} per year). According to the standard deviation between theoretical scenarios and calculated iWUE, *P. hartwegii* reflected a different adjustment strategy among years and sites. For example, all sites follow the C_a - C_i constant scenario during the first nine years (until 2008), however, in 2011 (the warmest year of the period), the largest increase in iWUE perfectly matches with the C_i constant scenario regardless of altitude or aspect (Figure 2. 5). Afterward, almost all sites followed the C_i/C_a constant scenario with few exceptions.

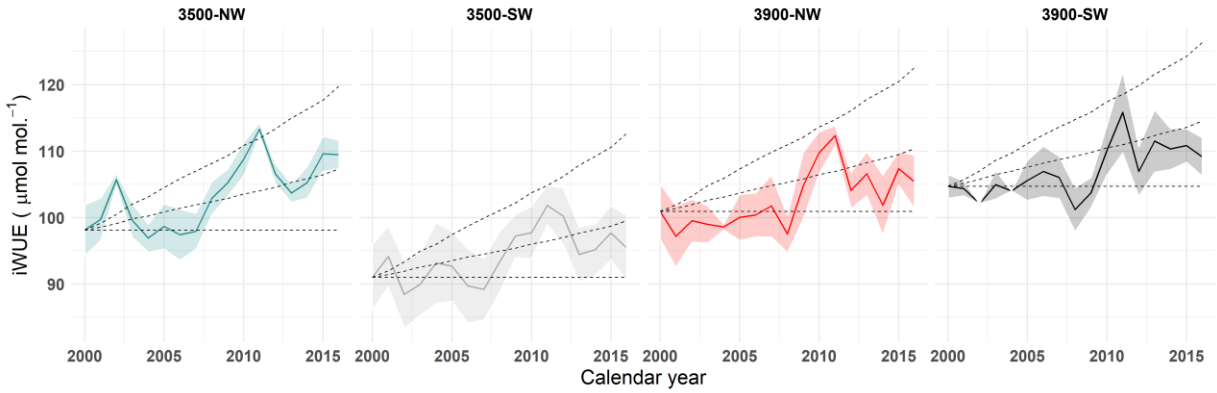

Figure 2. 5 The observed changes iWUE for *P. hartwegii* from 2000 to 2016 by site condition. Shaded areas are standard errors, and theoretical scenarios are represented by dashed lines. The three theoretical scenarios are from the top to bottom: C_i constant, C_i/C_a constant and C_a - C_i constant.

2.5.3. Linking photosynthetic activity and physiological performance

The first principal component (PC1) of each physiological variable was significant, representing about 75% of their respective variability, and enough to capture a regional signal and be compared with NDVI data. Spatio-temporal analysis revealed that previous winter NDVI had a strong influence in both $\delta^{13}C$ and $\delta^{18}O$ PC1 chronologies since a significant negative correlation was detected over different dates during this period. Thus, based on two decision factors (area and highest average correlation), the most important dates included the second half of November (day of the year 321) for $\delta^{13}C$ (τ = -0.48, 54 % of total area), and the second half of December (day 353) and first-half of February (day 033) (τ = -0.46 and 58 % of total area) for $\delta^{18}O$ (Figure 2. 6a and 2. 6b). Although we found a higher density of significant pixels at lower elevations (3500-3700 m asl), located mainly on North-facing aspects for both isotopes, their average correlation was statistically similar to other elevation/aspects combinations (Kruskal-Wallis test, p = 0.37, and p = 0.41, respectively). For the spring season, mid-May (day 129) was also significantly negatively related to $\delta^{13}C$ (τ = -0.47, 65 % of total area) but not statistically related with $\delta^{18}O$. Indeed, this was the highest association with a physiological variable considering both area and average correlation (Figure 2. 6a).

In the same way to $\delta^{13}C$, the second half of previous November and mid-May were correlated to carbon isotope discrimination ($\Delta^{13}C$) but with an opposite sign and less surface area. Thus, higher carbon isotope discrimination ($\Delta^{13}C$) was coupled with higher NDVI values during the second half of November (day 321 and τ = 0.46) and mid-May (day 129, and τ = 0.41). A weak relationship was shown with iWUE during this time series. The most important dates were first-half of February (day 033) (τ = 0.42, 19 % of total area) and first-half of September (day 241) (τ = 0.44, 22 % of total area).

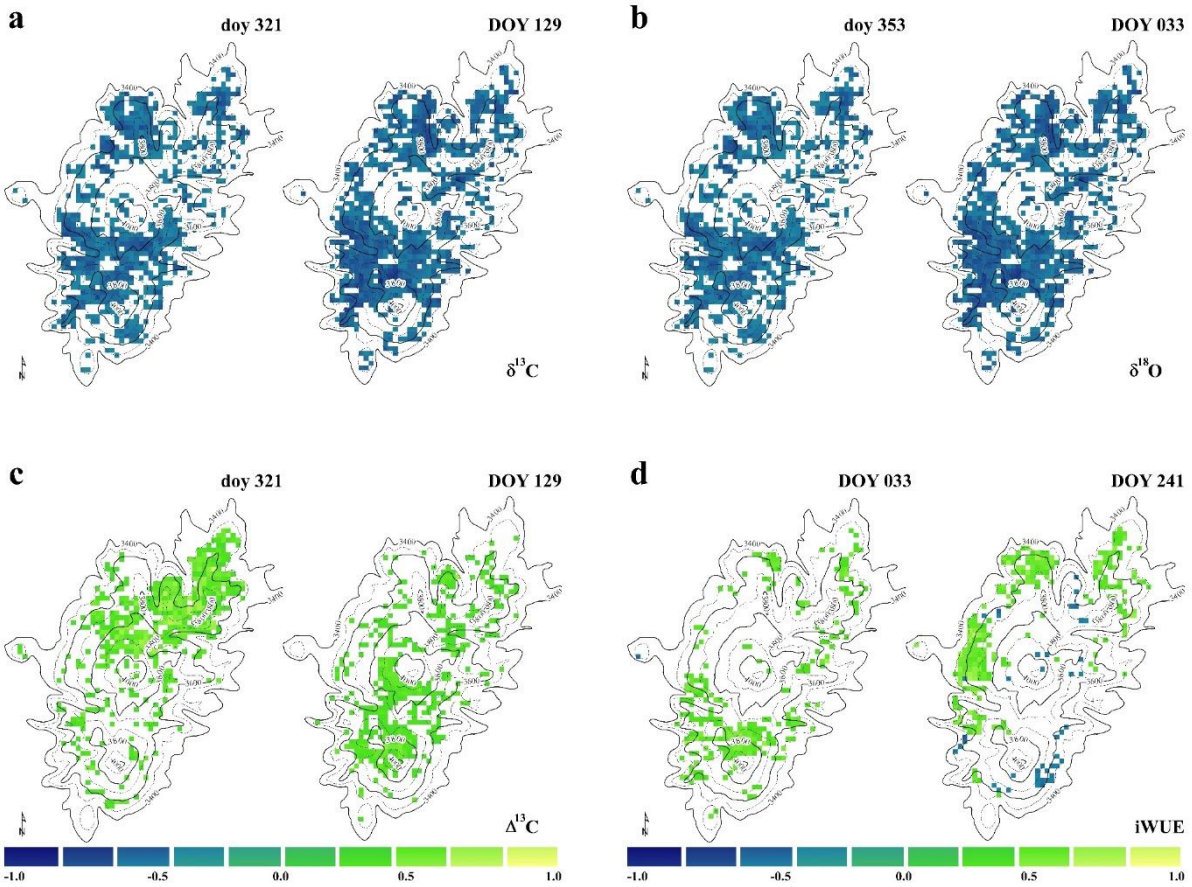

Figure 2. 6 Largest spatio-temporal association, expressed as Kendall's correlation coefficient (τ), between the first principal component (PC1) of (a) carbon isotope chronology ($\delta^{13}C$), (b) oxygen isotope chronology ($\delta^{18}O$), (c) carbon isotope discrimination ($\Delta^{13}C$), (d) intrinsic water use efficiency chronology (iWUE) with NDVI 16-day maximum composition. Note that day of the year (day) in lowercase is referred to previous-year while current-year is in uppercase.

2.5.4. Climatic influences on physiological variables

The period from May to June showed a strong link between $\delta^{13}C$ and maximum temperature, precipitation, vapor pressure deficit, and evaporation reference. While average maximum temperature ($r = 0.58$, $p < 0.05$), vapor pressure deficit ($r = 0.64$, $p < 0.05$) and evaporation reference ($r = 0.63$, $p < 0.05$) were positively correlated with $\delta^{13}C$; they were negatively correlated between precipitation ($r = -0.66$, $p < 0.05$) and relative humidity ($r = -0.62$, $p < 0.05$) (Table 2. 2). The correlations between the climatic data and $\delta^{13}C$ site-chronologies showed significant differences, compared to the 3900-SW site that was less sensitive to climatic variables. On the other hand, $\delta^{18}O$ site-chronologies were significantly correlated with multiple climatic variables in December from the previous year compared to summer conditions. For instance, average temperature ($r = -0.68$, $p < 0.05$) and degree-day sum above 5°C (DD > 5°C) ($r = -0.68$, $p < 0.05$) were negatively correlated across all conditions analyzed. Moreover, a positive association was detected with degree-day sum below 18°C (DD < 18°C) across all sites ($r = 0.67$, $p < 0.05$), which could suggest a physiological threshold for stomatal activity. Fisher's exact test showed that the 3500-SW site had the lowest association with climatic variables for $\delta^{18}O$.

The association between $\Delta^{13}C$ site-chronologies and the climatic variables was not as large as $\delta^{13}C$ since there were zero variables correlated from the previous year's condition (Table 2. 2). However, because of inverse relationship with $\delta^{13}C$, maximum temperature, precipitation, and evaporation reference during the summer season (May to June) were significantly correlated to $\Delta^{13}C$, as well as the climatic moisture deficit from April to October ($r = -0.57$, $p < 0.05$). Remarkably, accumulated climatic moisture deficit (mm) from April to October negatively influenced $\Delta^{13}C$ at low-altitude sites ($r = -0.55$, $p < 0.05$) but no relationship was found at high-altitude sites ($r = -0.13$, $p > 0.05$). No clear association between climatic variables and iWUE was observed, except for minimum temperature in January. The 3500-NW site was more sensitive to climatic variables, mainly for previous December conditions. North-facing sites (3500-NW and 3900-NW) were negatively associated with evaporation reference in December from previous-year to February ($r = -0.46$, $p < 0.05$).

Table 2. 2 Climatic variables correlated to regional carbon isotope ($\delta^{13}C$), oxygen isotope ($\delta^{18}O$), carbon isotope discrimination ($\Delta^{13}C$), and intrinsic water use efficiency (iWUE) chronologies from 2000 to 2016. $^{*}p < 0.05$

Period	Variable	Pearson's correlation with $\delta^{13}C$	Pearson's correlation with $\delta^{18}O$	Pearson's correlation with $\Delta^{13}C$	Pearson's correlation with iWUE
Previous year's condition	Precipitation Nov	-0.463*	NS	NS	NS
	Average Temperature Dec	-0.583*	-0.683*	NS	NS
	DD >5°C Dec	NS	-0.676*	NS	NS
	DD <18°C Dec	NS	0.677*	NS	NS
	Evaporation reference Dec	NS	-0.541*	NS	NS
	Vapor pressure deficit Dec	NS	-0.549*	NS	NS
Current year's condition	Minimum temperature Jan	NS	NS	NS	0.444*
	Maximum temperature May-Jun	0.577*	NS	-0.441*	NS
	Precipitation May-Jun	-0.664*	NS	0.495*	NS
	Evaporation reference May-Jun	0.629*	NS	-0.453*	NS
	CMD May	0.457*	NS	NS	NS
	∑CMD Apr-Oct	NS	NS	-0.570*	NS
	Relative humidity May-Jun	-0.617*	NS	NS	NS
	Vapor pressure deficit May-Jun	0.640*	NS	NS	NS

DD >5 °C - Degree-days sum above 5 °C

DD <18 °C - Degree-days sum below 18 °C

CMD – Climatic moisture deficit

Combined months represents an average value for temperature and sum for precipitation and degree-days

n=17 years

2.5.5. Tree growth trends from 2000 to 2016

As a general overview across the entire chronology (1866-2016), low-elevation sites (3500-NW and 3500-SW) showed a higher basal area increment (BAI), up to four times more basal productivity, than high-elevation sites (3900-NW and 3900-SW) (See Figure 2. 7 and Correa-Díaz *et al.* (2019) for further information). However, a progressive downward trend observed since the mid- 20th century changed notably this trend. Indeed, during the last decades, the 3500-SW site had average productivity close to the 3900-NW site (≈14 cm^2 $year^{-1}$) despite that younger trees were located at low-altitude sites (95.50 ± 6.1 years at 3500-SW and 145.52 ± 19.9 years at 3900-NW). For the 2000-2016 period, the highest average productivity was observed at 3500-NW (28.90 cm^2 $year^{-1}$) and the lowest at 3900-SW (5.80 cm^2 $year^{-1}$). Forest growth differences among sites were confirmed by Bonferroni's test ($p < 0.05$), excluding 3500-SW and 3900-NW, as described above (Figure 2. 7a).

There was no change in forest growth among sites ($p < 0.05$) except for low increases at the 3500-NW site (Table 2.3). This might reflect relative stability in the average productivity despite rising iWUE. However, year-to-year growth variations showed a common decrease in certain years; for example, a reduction was measured for high-elevation sites in 2003, 2004 and 2011, and an increase was observed in 2005 and 2010.

Table 2. 3 Basal area increment (log BAI) modeled by linear mixed-effects (random intercept model) from 2000 to 2016. Significance levels $^{\dagger}p < 0.1$, $^{*}p < 0.05$, $^{**}p < 0.01$ and $^{***}p < 0.001$

Site	Coefficients	Estimated coefficient	Standard error	p-value	Mean basal area increment (cm^2 $year^{-1}$)
3500-SW	Intercept	18.819	12.134	0.122	14.942
	Year	-0.008	0.006	0.180	
3500-NW	Intercept	-30.644	11.301	0.007**	28.895
	Year	0.017	0.006	0.003**	
3900-SW	Intercept	-10.901	20.07	0.587	5.810
	Year	0.006	0.009	0.535	
3900-NW	Intercept	25.441	14.464	0.079†	13.920
	Year	-0.011	0.007	0.110	

We did not detect a significant correlation between average BAI and any physiological variables ($\delta^{13}C$, $\delta^{18}O$, $\Delta^{13}C$, and iWUE) across all years. The highest correlation was found for $\delta^{18}O$ (r = -0.40, 3900-SW) and iWUE (r = 0.34, 3500-NW), but neither were significant. For iWUE, a positive correlation was found on North-facing sites and a negative for South-facing sites; stronger correlations (positive and negative) were found for low-altitude sites (Figure 2. 7b).

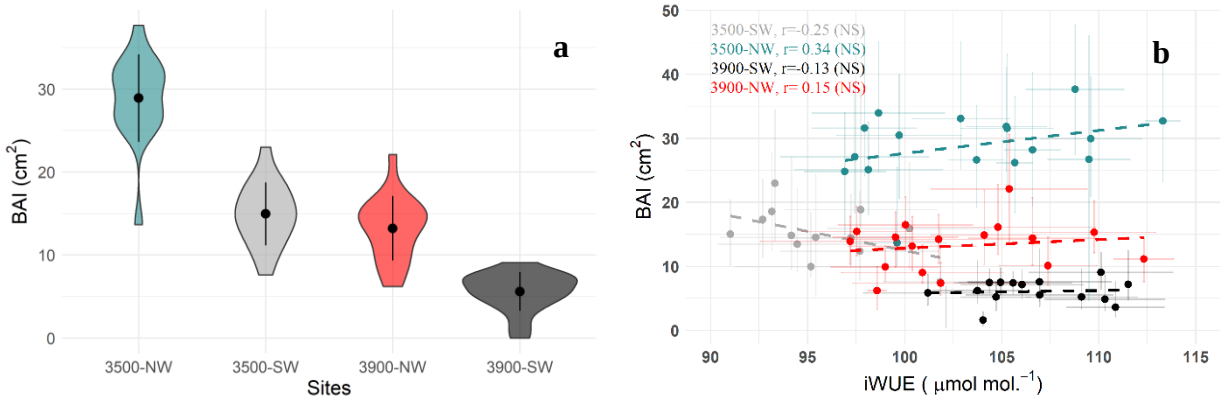

Figure 2. 7 (a) Violin plot of basal area increment (BAI) of *Pinus hartwegii* from 2000 to 2016. Lines are standard errors and red, black, blue and grey lines represent 3900-NW, 3900-SW, 3500-NW, and 3500-SW sites, respectively. (b) Relationship between basal area increment (BAI) and intrinsic water use efficiency (iWUE) by site. Dashed

lines represent no significant linear regression and NS denotes a no significant correlation.

2.6. Discussion

2.6.1. Changes in $\delta^{13}C$ and $\delta^{18}O$ overtime

Stable isotope signatures in tree-rings provide information of physiological performance over the growing season (Farquhar *et al.*, 1989; Battipaglia *et al.*, 2013) reflecting the atmospheric conditions of the period when wood was formed from 2000 to 2016. Tree $\delta^{13}C$ ratios in our study were slightly lower than those reported for *P. hartwegii* in nearby forests (Gómez-Guerrero *et al.*, 2013; Silva *et al.*, 2015). However, these values consistently reflect a dilution effect (^{13}C-Suess effect) of CO_2 due to the release of depleted $^{13}CO_2$ from combusted fossil C fuels into the atmosphere (Figure 2. 3a) (Keeling *et al.*, 2017; Beramendi-Orosco *et al.*, 2018). Results indicate that even with short-time periods of tree-ring measurements such as 17 years, it was possible to capture high-frequency events related to year-to-year variations, as well as with low-frequency events like declining $\delta^{13}C$ values. Tree $\delta^{18}O$ ratios for *P. hartwegii* match with a progressive lighter oxygen composition trend observed during last decades in central Mexico (Gómez-Guerrero *et al.*, 2013), but notably, the 3500-SW site had a heavy composition not commonly reported for this forest species, with values from 24 to 26 ‰ (Figure 2. 3b). Nevertheless, the estimated $\delta^{18}O$ reduction from low to high altitude sites was about -6 ‰ per altitude (km), a value higher than that previously estimated for *P. hartwegii* forests (-2‰ per altitude (km)) (Hartsough *et al.*, 2008).

2.6.2. Elevation-aspect physiological adjustment of *P. hartwegii*

Although previous studies have reported altitude as a significant component of the variation in $\delta^{13}C$ and $\Delta^{13}C$ in trees (an increase for $\delta^{13}C$ and a decrease for $\Delta^{13}C$) (Körner *et al.*, 1988; Körner *et al.*, 1991; Marshall and Zhang, 1994; Hultine and Marshall, 2000; Warren *et al.*, 2001; Zhu *et al.*, 2010), we did not find an altitude effect for $\delta^{13}C$ ($p = 0.659$) or $\Delta^{13}C$ ($p = 0.121$) (Table 2.1). For example, Wu *et al.* (2015) reported a significant difference in $\delta^{13}C$, C_i and iWUE at a lower range elevation than ours (250 vs 400 m). A rise in altitude translates into a decrease in air temperature and partial pressures (CO_2

and O_2 molecules move faster in thin air) and results in a variation in leaf anatomical traits (i.e. stomatal density, leaf conductance and leaf mass per area) (Hultine and Marshall, 2000; Warren *et al.*, 2001) through adjusting for changes in gas exchange (more efficient C fixation at high elevations) (Körner *et al.*, 1991). Indeed, leaf thickness and leaf nitrogen content increase with altitude, explaining the higher photosynthetic capacity per unit leaf area at high-elevations (Körner, 2012). Nevertheless, altitude itself is not biologically relevant, rather it is an indirect driver of climatic and edaphic and site factors affecting tree specific response (Hultine and Marshall, 2000; Zhu *et al.*, 2010; Maxwell *et al.*, 2018). Körner (2012) pointed out that $\delta^{13}C$ becomes less negative at wet sites, but under dry conditions, this effect may be hidden and no specific trend found. On average, cellulose $\delta^{13}C$ increased ≈ 0.8 ‰ per 1,000 m of elevation for above-mentioned temperature and partial pressure effects (Körner *et al.*, 1988; Körner *et al.*, 1991) but here the effect was only found on south-facing sites compared to north-facing sites. This difference was most clear when values were expressed as $\Delta^{13}C$ (Figure 2. 3c) where lower discrimination is expected at high-elevations (Marshall and Zhang, 1994). The 3500-NW site was expected to discriminate more but the values were similar to the high elevation sites, probably as a result of better water status.

A direct altitude effect for $\delta^{18}O$ is not as clear as with $\delta^{13}C$ since several factors determine $\delta^{18}O$ such as soil water, leaf water enrichment, and biochemical fractionation (Saurer *et al.*, 1997; Scheidegger *et al.*, 2000; McCarroll and Loader, 2004). Despite that precipitation and transpiration become more depleted in ^{18}O as temperature decreases with altitude (Barbour, 2007), it has been shown that tree-ring $\delta^{18}O$ at tree-line strongly mirrored variations in soil water $\delta^{18}O$ which lead to similar values observed across an altitudinal gradient (Treydte *et al.*, 2014). High-elevation forests highly depend on the water of the soil surface as they are often shallow with limited water storage capacity. Hartsough *et al.* (2008) suggest that our study species, *P. hartwegii,* mainly uses shallow soil water reservoirs rather than deeper moisture reserves. Other water sources like fog or snow are unlikely as the area is not exposed to sea moisture or long periods of snow. The fact that the 3500-SW site showed the only significant correlation with summer $\delta^{18}O$

precipitation reinforces the idea that high-productive sites demand higher amounts of soil water.

Carbon isotope discrimination ($\Delta^{13}C$) has remained relatively stable for the last 17 years in the study sites (Figure 2. 2c), although a decreasing long-term trend was reported for *P. hartwegii* at the Transmexican Volcanic Belt (Gómez-Guerrero *et al.*, 2013; Silva *et al.*, 2015). In the same way, a relatively stable ratio between intercelullar and ambient CO_2 concentrations (C_i/C_a) supports not only the idea of an active plant mechanism (Table 2.1) (Leonardi *et al.*, 2012) but also suggests increased demand for intercellular CO_2 over time. A recent metanalysis suggests that the overall response of plants to rising C_a is an adaptative feedback response to maintain the ratio C_i/C_a at a relatively constant ratio, achieved through adjustments in stomatal anatomy and chloroplast biochemistry (Franks *et al.*, 2013).

2.6.3. NDVI activity and physiological performance of trees

At this moment, the multiproxy approaches are limited by the availability of satellite information and products (i. e. temporal and spectral resolution) (Wang *et al.*, 2010; Levesque *et al.*, 2019), however, in the near future these approaches will be an effective way to monitor forest ecosystems function. Although the inference and prediction at large scales based on tree-ring records (scaling process) are sometimes complicated and skewed at the landscape (Babst *et al.*, 2018), the integral information complemented by remotely-sensed variables like canopy vigor (i.e. photosynthetic activity in NDVI) and tree-ring isotope ratios have proven to be related to wood formation processes (when climatic signals are printed in wood tissue). However, it is clear that exists a time lag between factors affecting photosynthesis and wood formation which can introduce discrepancies (trend inconsistency phenomenon) (Lapenis *et al.*, 2013; Cuny *et al.*, 2014). To partially overcome these uncertainties in our approach, we limited the analysis to elevations above 3500 m asl to assure pure stands of *P. hartwegii* to avoid a potential blurred effect due to a mixture of species on reflectance data. Second, the shared variance held by the first principal component (PC1) across contrasting altitudes and aspects helps us to capture an overall response for *P. hartwegii* at a regional scale. This multivariate technique could

be changed for another statistic approach or sampling design according to specific goals but keeping a complete overview of spatial variability. Finally, to detect the lag effect between processes, the correlation analysis was performed through a window of time sufficiently wide (from previous November to current September) and with a lower temporal resolution (bi-weekly), which can narrow time periods of photosynthetic activity related to wood isotopic composition.

Despite the above-mentioned challenges, previous studies have already found links between isotopic compositions and remotely sensed data. For example, Guo and Xie (2006) found that August-September NDVI has the same trend as $\delta^{13}C$ of C_3 plant leaves from the Tibet Plateau. Leavitt *et al.* (2008), in the Southwestern of USA, found a positive relationship between isotope indices of pinyon pine (*P. edulis* and *P. monophylla*) and summer NDVI, revealing a potential for long-term assessment of carbon cycling. In the same way, del Castillo *et al.* (2015) detected a positive association between $\Delta^{13}C$ and either mean annual NDVI (r = 0.65) or summer NDVI (r = 0.69) in Spain, which agrees with our study. This means that high greenness or photosynthetic activity during these months are coupled with lower $\delta^{13}C$ (more negative) or higher discrimination, explained by an open stomata strategy. Finally, Levesque *et al.* (2019) found a strong negative relationship between $\delta^{18}O$ and satellite-derived net primary productivity (NPP) across the eastern United States, opening a potential avenue for new studies testing not only carbon and oxygen but also other isotope ratios (i.e nitrogen ratio) as remotely sensed data products improve.

For *P. hartwegii*, the growing season goes from the end of April to October (≈ 7 months) (Biondi *et al.*, 2005; Astudillo-Sánchez *et al.*, 2017) but the most notably green-up according to NDVI starts in May, which agrees with our results that show a maximum association with $\delta^{13}C$ and $\Delta^{13}C$. Correa-Díaz *et al.* (2019) found that several climatic variables in May (minimum temperature, number of frost-free days, and precipitation) were significantly associated with tree-ring width. Besides that, the previous winter season was also important for both variables, thus, higher NDVI with warmer temperatures could generate photosynthetic reserves, which upon allocation to structural

woody components undergo further isotope fractionation steps. The tree-ring $\delta^{13}C$ and $\delta^{18}O$ depend on two factors: (i) the isotopic composition of the source (i.e. atmospheric CO_2 and soil water) and (ii) the isotope fractionation processes associated with transport, diffusion, enzyme reactions and tissue construction in the plant (McCarroll and Loader, 2004).

2.6.4. Drivers of iWUE and 2011, a drought year

Consistent with previous literature, we found an enhancement in iWUE regardless of spatial position (Peñuelas *et al.*, 2011; Wu *et al.*, 2015; Reed *et al.*, 2018), where our rates of increase are within average responses seen for the same species (0.26 - 0.37 µmol mol^{-1} per year) (Gómez-Guerrero *et al.*, 2013), but one site (3500-NW) contrasts and exhibited an increasing rate close to tropical rainforest responses (≈ 0.7 µmol mol^{-1} per year) (Loader *et al.*, 2011).

A relevant finding in our study is that intrinsic water use efficiency showed alternated responses under different gas-exchange regulation scenarios (Saurer *et al.*, 2004). From one year to another, the scenarios of constant C_i, C_i/C_a, and C_i/C_a seems to relate to the dryness of the year. For example, during the first nine years (2000-2008) trees followed the $C_a - C_i$ constant scenario, which suggests a weak stomatal response as iWUE remains stable (Figure 2. 5). In 2011, the warmest year according to climatic information, a universal response for all sites was seen with higher iWUE (the C_i constant scenario) (Figure 2. 5), which support the hypothesis of a link among physiological variables along with other proxies and suggest a specific spatio-temporal landscape outcome. Afterward, most of the trees followed the C_i/C_a constant scenario, representing a proportional adjustment for A and g_s. These shifts between leaf gas-exchange strategies among years, highlight the concept of “optimal stomatal behavior” in woody plants which implies a dynamic adjustment in g_s while reducing exposure to drought stress, with a hypothetical saturation of the photosynthesis at higher CO_2 concentrations (Voelker *et al.*, 2016; Giguère-Croteau *et al.*, 2019).

According to the Mexican Drought Monitor (based on North America Drought Monitor) (SMN, 2019), the summer of 2011 was exceptionally dry at our study area. This drought certainly affected the physiological performance of *P. hartwegii,* mainly through stomatal restriction to avoid water loss, leading to a $\delta^{13}C$ signature less negative with a concomitant effect on iWUE (Figure 2. 3 and 2. 5). The positive correlation between $\delta^{18}O$ and $\delta^{13}C$ implies a strong stomatal reaction of gas exchange, whereas *A* is relatively unaffected; thus, at high-elevation sites (Figure 2. 4a), stomata operate over a wide range because there is no need to reduce water loss, a situation expected when water is not limiting (Scheidegger *et al.*, 2000; Barnard *et al.*, 2012). Indeed, the slopes of the correlation analysis are site-dependent based on different moisture conditions; therefore, the lowest correlation between isotopes was in 3500-SW (different $\delta^{18}O$ signature). At this site, the higher changes on $\delta^{18}O$ and little effect on $\delta^{13}C$ could indicate that g_s and *A* are simultaneously affected while trees are subjected to different environmental influences.

2.6.5. Previous winter and summer season as drivers of isotopic composition

As in related studies, we found that wood $\delta^{13}C$ is dominated by a positive relationship with temperature, mainly for spring-summer season (xylogenesis formation period), and negatively associated to summer precipitation (Table 2.2) (Ferrio and Voltas, 2005; Gagen *et al.*, 2006; Wu *et al.*, 2015; Lavergne *et al.*, 2018). This shows that dry summers (higher temperature and VPD) cause water stress in trees, leading to stomatal regulation strategy (i.e. g_s and C_i reduced) and ^{13}C-rich cellulose (less negative) to avoid water loss (McCarroll and Loader, 2004). This situation was accentuated during summer 2011 when trees were more sensitive to VPD and soil water availability. Furthermore, we found that enhanced previous winter conditions (i.e. higher precipitation and warmer temperatures) can also affect the isotopic signature, mainly through the NDVI activity (Correa-Díaz *et al.*, 2019). Regarding spatial position, we found that $\delta^{13}C$ is less sensitive to climate at high elevations (South aspect) than middle elevation range or lower forest limit which agrees with Wu *et al.* (2015) analysis.

For wood $\delta^{18}O$, the climatic association is less clear because of a more complicated enrichment-process; however, our results highlight that the previous December is an important period affecting the $\delta^{18}O$ signature compared to summer temperature and precipitation. Furthermore, our observed correlations for $\Delta^{13}C$ are consistent with results reported by Wieser *et al.* (2016) and Voltas *et al.* (2013), where weather conditions (temperature and precipitation) prevailing during April through June were related to tree-ring $\Delta^{13}C$.

2.6.6. Tree growth trends and relationship with iWUE

Higher temperature and or atmospheric CO_2 have been not consistently associated with increased tree growth even with iWUE rises (Peñuelas *et al.*, 2011; Linares and Camarero, 2012; Gómez-Guerrero *et al.*, 2013; Wu *et al.*, 2015; Granda *et al.*, 2017; Reed *et al.*, 2018). Here, a particular combination of altitude and aspect indicates a CO_2 fertilization effect that occurred in the last decades. This means that *P. hartwegii's* trees close to their altitudinal distribution range have not benefited from recent atmospheric changes. The growth increases at North-facing sites might reflect better site moistures and lower radiation; however, BAI chronologies also captured the effect of environmental conditions such as those dry years in 2004, 2011 and wet years in 2005 and 2010. These particular years are concurrent with previous reports in Central Mexico using a dendrochronological network of *P. hartwegii* (Villanueva-Díaz *et al.*, 2015) and reports for the North American Drought Monitor (SMN, 2019). These results indicate that the main factors affecting the physiological response of trees in our study were micro-site, as suggested by other authors (Lyu, et al., 2019). Future analysis should include different age-classes over longer time periods, separating the unique and common effects of CO_2 and climatic variables on forest growth to disentangle their synergetic effects (Ray-Mukherjee *et al.*, 2014).

2.7. Conclusions

An integrating multiproxy approach to assess the physiological response of forest has been developed combining tree-ring series, wood isotope ratios, remotely sensed variables and climatic information. As expected, when maximizing the regional response

of the forest considering contrasting site conditions but homogeneous forest species, the Normalized Difference Vegetation Index (NDVI) is related to carbon and oxygen tree-ring stable isotope ratios in different time periods, mainly at winter and beginning of the growing season. Although the limited time span of remotely-sensed data this approach can help to gain a better understanding of physiological adaptation to rising CO_2 levels through define photosynthetic activity periods related to carbon and water cycling. Furthermore, the results highlight the importance of topographic conditions (i.e. altitude and aspect) in the physiological response of the *P. hartwegii,* where carbon isotope composition ($\delta^{13}C$) does not show an expected altitude effect due to different water status. Finally, we observed that iWUE reflects extreme climatic events (i.e. droughts) but with a rising trend which was not necessarily translated to forest growth increase at tree-line ecotone.

2.8. References

Allen, R. G., L. S. Pereira, D. Raes and M. Smith. 1998. Crop evapotranspiration - guidelines for computing crop water requirements. FAO Irrigation and drainage paper 56. Rome, Italy. FAO - Food and Agriculture Organization of the United Nations

Andreu, L., E. Gutiérrez, M. Macias, M. Ribas, O. Bosch and J. J. Camarero. 2007. Climate increases regional tree-growth variability in iberian pine forests. Global Change Biology 13: 804-815.

Astudillo-Sánchez, C. C., J. Villanueva-Díaz, A. R. Endara-Agramont, G. E. Nava-Bernal and M. A. Gómez-Albores. 2017. Climatic variability at the treeline of monte tlaloc, mexico: A dendrochronological approach. Trees 31: 441-453.

Babst, F., P. Bodesheim, N. Charney, A. D. Friend, M. P. Girardin, S. Klesse, D. J. P. Moore, K. Seftigen, J. Björklund, O. Bouriaud, A. Dawson, R. J. DeRose, M. C. Dietze, A. H. Eckes, B. Enquist, D. C. Frank, M. D. Mahecha, B. Poulter, S. Record, V. Trouet, R. H. Turton, Z. Zhang and M. E. K. Evans. 2018. When tree rings go global: Challenges and opportunities for retro- and prospective insight. Quaternary Science Reviews 197: 1-20.

Barbour, M. M. 2007. Stable oxygen isotope composition of plant tissue: A review. Functional Plant Biology 34: 83-94.

Barnard, H. R., J. R. Brooks and B. J. Bond. 2012. Applying the dual-isotope conceptual model to interpret physiological trends under uncontrolled conditions. Tree Physiology 32: 1183-1198.

Battipaglia, G., M. Saurer, P. Cherubini, C. Calfapietra, H. R. McCarthy, R. J. Norby and M. Francesca Cotrufo. 2013. Elevated co_2 increases tree-level intrinsic water use efficiency: Insights from carbon and oxygen isotope analyses in tree rings across three forest face sites. New Phytologist 197: 544-554.

Beramendi-Orosco, L. E., G. González-Hernández, A. Martínez-Reyes, O. Morton-Bermea, F. J. Santos-Arévalo, I. Gómez-Martínez and J. Villanueva-Díaz. 2018. Changes in co_2 emission sources in mexico city metropolitan area deduced from radiocarbon concentrations in tree rings. Radiocarbon 60: 21-34.

Biondi, F., P. Hartsough and I. G. G. Estrada. 2009. Recent warming at the tropical treeline of north america. Frontiers in Ecology and the Environment 7: 463-464.

Biondi, F., P. C. Hartsough and I. Galindo Estrada. 2005. Daily weather and tree growth at the tropical treeline of north america. Arctic, Antarctic, and Alpine Research 37: 16-24.

Biondi, F. and F. Qeadan. 2008. A theory-driven approach to tree-ring standardization: Defining the biological trend from expected basal area increment. Tree-Ring Research 64: 81-96.

Blunden, J. and D. S. Arndt. 2018. State of the climate in 2017. Bulletin American Meteorology Society 99: 332.

Brehaut, L. and R. K. Danby. 2018. Inconsistent relationships between annual tree ring-widths and satellite-measured ndvi in a mountainous subarctic environment. Ecological Indicators 91: 698-711.

Bunn, A. G. 2008. A dendrochronology program library in r (dplr). Dendrochronologia 26: 115-124.

Bunn, A. G., M. K. Hughes, A. V. Kirdyanov, M. Losleben, V. V. Shishov, L. T. Berner, A. Oltchev and E. A. Vaganov. 2013. Comparing forest measurements from tree rings and a space-based index of vegetation activity in siberia. Environmental Research Letters 8.

Camarero, J. J., A. Gazol, J. D. Galván, G. Sangüesa-Barreda and E. Gutiérrez. 2015. Disparate effects of global-change drivers on mountain conifer forests: Warming-induced growth enhancement in young trees vs. Co_2 fertilization in old trees from wet sites. Global Change Biology 21: 738-749.

Castillo, J. d., J. Voltas and J. P. Ferrio. 2015. Carbon isotope discrimination, radial growth, and ndvi share spatiotemporal responses to precipitation in aleppo pine. Trees: Structure and Function 29: 223-233.

Correa-Díaz, A., L. C. R. Silva, W. R. Horwath, A. Gómez-Guerrero, J. Vargas-Hernández, J. Villanueva-Díaz, A. Velázquez-Martínez and J. Suárez-Espinoza.

2019. Linking remote sensing and dendrochronology to quantify climate-induced shifts in high-elevation forests over space and time. Journal of Geophysical Research: Biogeosciences 124: 166-183.

Cuny, H. E., C. B. K. Rathgeber, D. Frank, P. Fonti and M. Fournier. 2014. Kinetics of tracheid development explain conifer tree- ring structure. New Phytologist 203: 1231-1241.

Dawson, T. E., S. Mambelli, A. H. Plamboeck, P. H. Templer and K. P. Tu. 2002. Stable isotopes in plant ecology. Annual Review of Ecology and Systematics 33: 507-559.

del Castillo, J., J. Voltas and J. P. Ferrio. 2015. Carbon isotope discrimination, radial growth, and ndvi share spatiotemporal responses to precipitation in aleppo pine. Trees 29: 223-233.

Everitt, B. S. 2005. Analysis of repeated measures data. An r and s-plus® companion to multivariate analysis. Springer London. London. pp. 171-199.

Farquhar, G. D., J. R. Ehleringer and K. T. Hubick. 1989. Carbon isotope discrimination and photosynthesis. Annual Review of Plant Physiology and Plant Molecular Biology 40: 503-537.

Farquhar, G. D., M. H. O´Leary and J. A. Berry. 1982. On the relationship between carbon isotope discrimination and intercellular carbon dioxide concentration in leaves. Australian Jounal of Plant Physiology 9: 121-137.

Ferrio, J. P. and J. Voltas. 2005. Carbon and oxygen isotope ratios in wood constituents of *pinus halepensis* as indicators of precipitation, temperature and vapour pressure deficit. Tellus B 57: 164-173.

Franks, P. J., M. A. Adams, J. S. Amthor, M. M. Barbour, J. A. Berry, D. S. Ellsworth, G. D. Farquhar, O. Ghannoum, J. Lloyd, N. McDowell, R. J. Norby, D. T. Tissue and S. Caemmerer. 2013. Sensitivity of plants to changing atmospheric co_2 concentration: From the geological past to the next century. New Phytologist 197: 1077-1094.

Fritts, H. C. 1976. Tree rings and climate. Academic Press Inc, London. 567 pp.

Gagen, M., D. McCarroll and J.-L. Edouard. 2006. Combining ring width, density and stable carbon isotope proxies to enhance the climate signal in tree-rings: An example from the southern french alps. Climatic Change 78: 363-379.

García, E. 2004. Modificaciones al sistema de clasificación climática de koppen. 5th ed. Universidad Nacional Autónoma de México. México. 91 pp.

Gedalof, Z. e. and A. A. Berg. 2010. Tree ring evidence for limited direct co_2 fertilization of forests over the 20th century. Global Biogeochemical Cycles 24.

Giguère-Croteau, C., É. Boucher, Y. Bergeron, M. P. Girardin, I. Drobyshev, L. C. R. Silva, J.-F. Hélie and M. Garneau. 2019. North america's oldest boreal trees are more efficient water users due to increased co_2, but do not grow faster. Proceedings of the National Academy of Sciences: 201816686.

Gómez-Guerrero, A. and T. Doane. 2018. Chapter seven - the response of forest ecosystems to climate change. *In*: Horwath W. R. and Kuzyakov Y.s (eds.). Developments in soil science. Elsevier. pp. 185-206.

Gómez-Guerrero, A., L. C. R. Silva, M. Barrera-Reyes, B. Kishchuk, A. Velazquez-Martinez, T. Martinez-Trinidad, F. O. Plascencia-Escalante and W. R. Horwath. 2013. Growth decline and divergent tree ring isotopic composition ($\delta^{13}c$ and $\delta^{18}o$) contradict predictions of co_2 stimulation in high altitudinal forests. Global Change Biology 19: 1748-1758.

Gori, Y., R. Wehrens, M. Greule, F. Keppler, L. Ziller, N. La Porta and F. Camin. 2013. Carbon, hydrogen and oxygen stable isotope ratios of whole wood, cellulose and lignin methoxyl groups of *picea abies* as climate proxies. Rapid Communications in Mass Spectrometry 27: 265-275.

Granda, E., J. J. Camarero, J. D. Galván, G. Sangüesa-Barreda, A. Q. Alla, E. Gutierrez, I. Dorado-Liñán, L. Andreu-Hayles, I. Labuhn, H. Grudd and J. Voltas. 2017. Aged but withstanding: Maintenance of growth rates in old pines is not related to enhanced water-use efficiency. Agricultural and Forest Meteorology 243: 43-54.

Guo, G. and G. Xie. 2006. The relationship between plant stable carbon isotope composition, precipitation and satellite data, tibet plateau, china. Quaternary International 144: 68-71.

Harris, I., P. D. Jones, T. J. Osborn and D. H. Lister. 2014. Updated high-resolution grids of monthly climatic observations – the cru ts3.10 dataset. International Journal of Climatology 34: 623-642.

Hartsough, P., S. R. Poulson, F. Biondi and I. G. Estrada. 2008. Stable isotope characterization of the ecohydrological cycle at a tropical treeline site. Arctic, Antarctic, and Alpine Research 40: 343-354.

Hochberg, Y. 1988. A sharper bonferroni procedure for multiple tests of significance. Biometrika 75: 800-802.

Hollander, M., D. A. Wolfe and E. Chicken. 2013. Nonparametric statistical methods. Third Edition ed. John Wiley & Sons. New York, USA. 848 pp.

Hultine, K. R. and J. D. Marshall. 2000. Altitude trends in conifer leaf morphology and stable carbon isotope composition. Oecologia 123: 32-40.

Jenkerson, C., T. Maiersperger and G. Schmidt. 2010. Emodis: A user-friendly data source. U.S. Geological Survey Open-File Report 2010-1055: 10.

Jochner, M., H. Bugmann, M. Nötzli and C. Bigler. 2017. Tree growth responses to changing temperatures across space and time: A fine-scale analysis at the treeline in the swiss alps. Trees.

Kaufmann, R. K., R. D. D'Arrigo, L. F. Paletta, H. Q. Tian, W. M. Jolly and R. B. Myneni. 2008. Identifying climatic controls on ring width: The timing of correlations between tree rings and ndvi. Earth Interactions 12: 1-14.

Keeling, R. F., H. D. Graven, L. R. Welp, L. Resplandy, J. Bi, S. C. Piper, Y. Sun, A. Bollenbacher and H. A. J. Meijer. 2017. Atmospheric evidence for a global secular increase in carbon isotopic discrimination of land photosynthesis. Proceedings of the National Academy of Sciences 114: 10361-10366.

Körner, C. 2012. Alpine treelines. Springer Basel. 220 pp.

Körner, C., D. Basler, G. Hoch, C. Kollas, A. Lenz, C. F. Randin, Y. Vitasse and N. E. Zimmermann. 2016. Where, why and how? Explaining the low-temperature range limits of temperate tree species. Journal of Ecology 104: 1076-1088.

Körner, C., G. D. Farquhar and Z. Roksandic. 1988. A global survey of carbon isotope discrimination in plants from high altitude. Oecologia 74: 623-632.

Körner, C., G. D. Farquhar and S. C. Wong. 1991. Carbon isotope discrimination by plants follows latitudinal and altitudinal trends. Oecologia 88: 30-40.

Lapenis, A. G., G. B. Lawrence, A. Heim, C. Y. Zheng and W. Shortle. 2013. Climate warming shifts carbon allocation from stemwood to roots in calcium-depleted spruce forests. Global Biogeochemical Cycles 27: 101-107.

Lavergne, A., V. Daux, M. Pierre, M. Stievenard, A. M. Srur and R. Villalba. 2018. Past summer temperatures inferred from dendrochronological records of *fitzroya cupressoides* on the eastern slope of the northern patagonian andes. Journal of Geophysical Research: Biogeosciences 123: 32-45.

Leavitt, S. W. 2010. Tree-ring c–h–o isotope variability and sampling. Science of The Total Environment 408: 5244-5253.

Leavitt, S. W., T. N. Chase, B. Rajagopalan, E. G. Lee and P. J. Lawrence. 2008. Southwestern u.S. Tree-ring carbon isotope indices as a possible proxy for reconstruction of greenness of vegetation. Geophysical Research Letters 35.

Leonardi, S., T. Gentilesca, R. Guerrieri, F. Ripullone, F. Magnani, M. Mencuccini, T. V. Noije and M. Borghetti. 2012. Assessing the effects of nitrogen deposition and climate on carbon isotope discrimination and intrinsic water-use efficiency of angiosperm and conifer trees under rising co_2 conditions. Global Change Biology 18: 2925-2944.

Levesque, M., L. Andreu-Hayles, W. K. Smith, A. P. Williams, M. L. Hobi, B. W. Allred and N. Pederson. 2019. Tree-ring isotopes capture interannual vegetation productivity dynamics at the biome scale. Nature Communications 10: 742.

Linares, J. C. and J. J. Camarero. 2012. From pattern to process: Linking intrinsic water-use efficiency to drought-induced forest decline. Global Change Biology 18: 1000-1015.

Lloret, F., E. G. Keeling and A. Sala. 2011. Components of tree resilience: Effects of successive low-growth episodes in old ponderosa pine forests. Oikos 120: 1909-1920.

Loader, N. J., R. P. D. Walsh, I. Robertson, K. Bidin, R. C. Ong, G. Reynolds, D. McCarroll, M. Gagen and G. H. F. Young. 2011. Recent trends in the intrinsic water-use efficiency of ringless rainforest trees in borneo. Philosophical Transactions of the Royal Society B: Biological Sciences 366: 3330-3339.

Lobato-Sánchez, R. and M. A. Altamirano-del-Carmen. 2017. Detection of local temperature trends in mexico. Water Technology and Sciences (in Spanish) 8(6): 101-116.

Marshall, J. D. and J. Zhang. 1994. Carbon isotope discrimination and water-use efficiency in native plants of the north-central rockies. Ecology 75: 1887-1895.

Martínez-Vilalta, J. 2018. The rear window: Structural and functional plasticity in tree responses to climate change inferred from growth rings. Tree Physiology.

Maxwell, T. M., L. C. R. Silva and W. R. Horwath. 2018. Integrating effects of species composition and soil properties to predict shifts in montane forest carbon–water relations. Proceedings of the National Academy of Sciences.

McCarroll, D. and N. J. Loader. 2004. Stable isotopes in tree rings. Quaternary Science Reviews 23: 771-801.

McDowell, N., W. T. Pockman, C. D. Allen, D. D. Breshears, N. Cobb, T. Kolb, J. Plaut, J. Sperry, A. West, D. G. Williams and E. A. Yepez. 2008. Mechanisms of plant survival and mortality during drought: Why do some plants survive while others succumb to drought? New Phytologist 178: 719-739.

Mischel, M., J. Esper, F. Keppler, M. Greule and W. Werner. 2015. Δ^2h, δ^{13}c and δ^{18}o from whole wood, α-cellulose and lignin methoxyl groups in *pinus sylvestris*: A multi-parameter approach. Isotopes in Environmental and Health Studies 51: 553-568.

Miyeni, R. B., F. G. Hall, P. J. Sellers and A. L. Marshak. 1995. The interpretation of spectral vegetation indexes. IEEE Transactions on Geoscience and Remote Sensing 33: 481-486.

Peñuelas, J., J. G. Canadell and R. Ogaya. 2011. Increased water-use efficiency during the 20th century did not translate into enhanced tree growth. Global Ecology and Biogeography 20: 597-608.

Perry, J. P. 1991. The pines of mexico and central america. Timber Press. Portland, Oregon. 231 pp.

Pinheiro, J., D. Bates, S. DebRoy, D. Sarkar and R. C. Team. 2018. Nlme: Linear and nonlinear mixed effects models. R package version 3.1131.1.

Ray-Mukherjee, J., K. Nimon, S. Mukherjee, D. W. Morris, R. Slotow and M. Hamer. 2014. Using commonality analysis in multiple regressions: A tool to decompose regression effects in the face of multicollinearity. Methods in Ecology and Evolution 5: 320-328.

Reed, C. C., A. P. Ballantyne, L. A. Cooper and A. Sala. 2018. Limited evidence for co_2-related growth enhancement in northern rocky mountain lodgepole pine populations across climate gradients. Global Change Biology 24: 3922-3937.

Rossella, G., J. Katie, B. Soumaya, A. Heidi and O. Scott. 2017. Evaluating climate signal recorded in tree-ring $\delta^{13}c$ and $\delta^{18}o$ values from bulk wood and α-cellulose for six species across four sites in the northeastern us. Rapid Communications in Mass Spectrometry 31: 2081-2091.

Sanders, T. G. M., I. Heinrich, B. Günther and W. Beck. 2016. Increasing water use efficiency comes at a cost for norway spruce. Forests 7: 296.

Saurer, M., K. Aellen and R. Siegwolf. 1997. Correlating $\delta^{13}c$ and $\delta^{18}o$ in cellulose of trees. Plant, Cell & Environment 20: 1543-1550.

Saurer, M., R. T. W. Siegwolf and F. H. Schweingruber. 2004. Carbon isotope discrimination indicates improving water- use efficiency of trees in northern eurasia over the last 100 years. Global Change Biology 10: 2109-2120.

Scheidegger, Y., M. Saurer, M. Bahn and R. Siegwolf. 2000. Linking stable oxygen and carbon isotopes with stomatal conductance and photosynthetic capacity: A conceptual model. Oecologia 125: 350-357.

Silva, L. C. R. and M. Anand. 2013. Probing for the influence of atmospheric co_2 and climate change on forest ecosystems across biomes. Global Ecology and Biogeography 22: 83-92.

Silva, L. C. R., A. Gómez- Guerrero, T. A. Doane and W. R. Horwath. 2015. Isotopic and nutritional evidence for species- and site-specific responses to n deposition and elevated co_2 in temperate forests. Journal of Geophysical Research: Biogeosciences 120: 1110-1123.

SMN. 2019. Mexico drought monitor (msm). Servicio Meteorológico Nacional de México (SMN) "Published on the Internet:" https://smn.cna.gob.mx/es/climatologia/monitor-de-sequia/monitor-de-sequia-en-mexico.

Stokes, M. A. and T. L. Smiley. 1968. An introduction to tree-ring dating. University of Chicago Press. Chicago, IL. USA. 73 pp.

Tei, S., A. Sugimoto, A. Kotani, T. Ohta, T. Morozumi, S. Saito, S. Hashiguchi and T. Maximov. 2019. Strong and stable relationships between tree-ring parameters and forest-level carbon fluxes in a siberian larch forest. Polar Science.

Treml, V., T. Ponocná and U. Büntgen. 2012. Growth trends and temperature responses of treeline norway spruce in the czech-polish sudetes mountains. Climate Research 55: 91-103.

Treydte, K., S. Boda, E. Graf Pannatier, P. Fonti, D. Frank, B. Ullrich, M. Saurer, R. Siegwolf, G. Battipaglia, W. Werner and A. Gessler. 2014. Seasonal transfer of oxygen isotopes from precipitation and soil to the tree ring: Source water versus needle water enrichment. New Phytologist 202: 772-783.

Vicente-Serrano, S. M., J. J. Camarero, J. M. Olano, N. Martin-Hernandez, M. Pena-Gallardo, M. Tomas-Burguera, A. Gazol, C. Azorin-Molina, U. Bhuyan and A. El-Kenawy. 2016. Diverse relationships between forest growth and the normalized difference vegetation index at a global scale. Remote Sensing of Environment 187: 14-29.

Villanueva-Díaz, J., J. Cerano Paredes, L. Vázquez Selem, D. W. Stahle, P. Z. Fulé, L. L. Yocom, O. Franco Ramos and J. Ariel Ruiz Corral. 2015. Red dendrocronológica del pino de altura (*pinus hartwegii* lindl.) para estudios dendroclimáticos en el noreste y centro de méxico. Investigaciones Geográficas, Boletín del Instituto de Geografía 2015: 5-14.

Voelker, S. L., J. R. Brooks, F. C. Meinzer, R. Anderson, M. K.-F. Bader, G. Battipaglia, K. M. Becklin, D. Beerling, D. Bert, J. L. Betancourt, T. E. Dawson, J.-C. Domec, R. P. Guyette, C. Körner, S. W. Leavitt, S. Linder, J. D. Marshall, M. Mildner, J. Ogée, I. Panyushkina, H. J. Plumpton, K. S. Pregitzer, M. Saurer, A. R. Smith, R. T. W. Siegwolf, M. C. Stambaugh, A. F. Talhelm, J. C. Tardif, P. K. Van de Water, J. K. Ward and L. Wingate. 2016. A dynamic leaf gas-exchange strategy is conserved in woody plants under changing ambient co_2: Evidence from carbon isotope discrimination in paleo and co_2 enrichment studies. Global Change Biology 22: 889-902.

Voltas, J., J. J. Camarero, D. Carulla, M. Aguilera, A. Ortiz and J. P. Ferrio. 2013. A retrospective, dual-isotope approach reveals individual predispositions to winter-drought induced tree dieback in the southernmost distribution limit of scots pine. Plant, Cell & Environment 36: 1435-1448.

Wang, J., P. M. Rich, K. P. Price and W. D. Kettle. 2004. Relations between ndvi and tree productivity in the central great plains. International Journal of Remote Sensing 25: 3127-3138.

Wang, L., G. S. Okin and S. A. MacKo. 2010. Remote sensing of nitrogen and carbon isotope compositions in terrestrial ecosystems. Isoscapes: Understanding movement, pattern, and process on earth through isotope mapping. pp. 51-70.

Wang, T., A. Hamann, D. Spittlehouse and C. Carroll. 2016. Locally downscaled and spatially customizable climate data for historical and future periods for north america. PLOS ONE 11: e0156720.

Wang, T., A. Hamann, D. L. Spittlehouse and T. Q. Murdock. 2012. Climatewna—high-resolution spatial climate data for western north america. Journal of Applied Meteorology and Climatology 51: 16-29.

Wang, Y., Y. Zhang, O. Fang and X. Shao. 2018. Long-term changes in the tree radial growth and intrinsic water-use efficiency of chuanxi spruce (*picea likiangensis* var. Balfouriana) in southwestern china. Journal of Geographical Sciences 28: 833-844.

Warren, C. R., J. F. McGrath and M. A. Adams. 2001. Water availability and carbon isotope discrimination in conifers. Oecologia 127: 476-486.

Werner, C., H. Schnyder, M. Cuntz, C. Keitel, M. J. Zeeman, T. E. Dawson, F. W. Badeck, E. Brugnoli, J. Ghashghaie, T. E. E. Grams, Z. E. Kayler, M. Lakatos, X. Lee, C. Máguas, J. Ogée, K. G. Rascher, R. T. W. Siegwolf, S. Unger, J. Welker, L. Wingate and A. Gessler. 2012. Progress and challenges in using stable isotopes to trace plant carbon and water relations across scales. Biogeosciences 9: 3083-3111.

Wieser, G., W. Oberhuber, A. Gruber, M. Leo, R. Matyssek and T. E. E. Grams. 2016. Stable water use efficiency under climate change of three sympatric conifer species at the alpine treeline. Frontiers in Plant Science 7.

Wu, G., X. Liu, T. Chen, G. Xu, W. Wang, X. Zeng and X. Zhang. 2015. Elevation-dependent variations of tree growth and intrinsic water-use efficiency in schrenk spruce (*picea schrenkiana*) in the western tianshan mountains, china. Frontiers in Plant Science 6.

Xu, Y., W. Li, X. Shao, Z. Xu and P. Nugroho. 2014. Long-term trends in intrinsic water-use efficiency and growth of subtropical *pinus tabulaeformis* carr. And *pinus taiwanensis* hayata in central china. Journal of Soils and Sediments 14: 917-927.

Yi, K., J. T. Maxwell, M. K. Wenzel, D. T. Roman, P. E. Sauer, R. P. Phillips and K. A. Novick. 2018. Linking variation in intrinsic water-use efficiency to isohydricity: A comparison at multiple spatiotemporal scales. New Phytologist 0.

Zang, C. and F. Biondi. 2015. Treeclim: An r package for the numerical calibration of proxy-climate relationships. Ecography 38: 431-436.

Zhu, Y., R. T. Siegwolf, W. Durka and C. Korner. 2010. Phylogenetically balanced evidence for structural and carbon isotope responses in plants along elevational gradients. Oecologia 162: 853-863.

CHAPTER III. TREE-RING WOOD DENSITY ADJUSTMENTS IN ALPINE FORESTS AT CENTRAL MEXICO MIRRORS THE NORMALIZED DIFFERENCE VEGETATION INDEX (NDVI)[3]

3.1. Resumen

La actual variación climática afecta notablemente a los bosques de alta montaña, influyendo el proceso de formación de la madera (xilogénesis). Sin embargo, estudios previos han carecido de establecer vínculos de la xilogénesis con componentes espaciales del dosel, como la actividad fotosintética. Por tanto, en este estudio se exploraron tendencias (i.e. usando modelos lineares mixtos) y relaciones entre densidad de la madera con variables derivadas de sensores remotos (MODIS) en dos bosques de alta montaña en México (Monte Tláloc-TLA y Jocotitlán-JOC). Los resultados mostraron que la elevación y la edad cambial explicaron los valores de densidad mientras que la exposición no tuvo relación. A pesar de los valores medios de densidad (densidad mínima de madera temprana-MID y densidad máxima de madera tardía-MXD) fueron estadísticamente similares entre montañas, TLA presentó un incremento en MID. Entonces, anillos más densos fueron más frecuentes después de 1950 para MID en TLA y marginalmente en JOC, pero un comportamiento diferente fue observado para MXD. TLA presentó una mejor correlación con variables de sensores remotos, principalmente con el índice de vegetación de diferencia normalizada-NDVI, que en JOC. Correlaciones positivas fueron calculadas para MXD, negativas para MID y un patrón divergente para la densidad media-AVE. Finalmente, relaciones con variables climáticas sugieren que MID estuvo fuertemente influenciado por la temperatura, mientras que MXD por la humedad de suelo, pero solo a bajas elevaciones.

Palabras clave: *Pinus hartwegii*, dendroecología, bosques de alta montaña

[3] Artículo por enviar a Atmosphere 2019

3.2. Abstract

Ongoing climate variability strongly affects high-elevation forests, influencing the wood formation process (e.g. xylogenesis). Nevertheless, previous studies often lack to establish links with spatial components of canopy performance such as photosynthesis. Thus, we explore temporal trends (e.g. using linear mixed-effects models) and the connection of wood density to remotely sensed variables (MODIS-derived) in two high-elevation forests in Mexico (Tlaloc-TLA and Jocotitlán-JOC Mountain). Our results showed that altitude and the cambial age effect explained wood density behavior while aspect was a negligible factor. Although average wood density profiles (minimum earlywood-MID and maximum latewood density-MXD) were statistically similar between mountains, TLA exhibited an increase in MID. Thus, denser rings were frequent after 1950 for MID in TLA and marginally in JOC, but a different pattern was seen for MXD. TLA exhibited strongest correlations to remotely sensed variables, mainly with Normalized Difference Vegetation Index-NDVI, than JOC. Positive correlations were seen for MXD, negative for MID and a divergent pattern for average density-AVE. Finally, climatic connections suggest that MID was strongly influenced by temperature, whereas MXD to soil moisture but only at low-elevation sites.

Keywords: *Pinus hartwegii*, dendroecology, high-elevation forests

3.3. Introduction

Wood density is highly recognized for its relationship to the water and nutrient conduction systems from roots to leaves (McDowell and Allen, 2015). However, wood components arrangement is also important for plant mechanical support and for long-term carbon storing function (Chave *et al.*, 2009). Besides that, the retrospective analysis of tree-ring density is useful to capture the historical plant responses to climate variations (Granda *et al.*, 2017). Tree-ring density is a key variable to assess the ability of trees to store carbon under the ongoing climate variability (Babst *et al.*, 2014). Wood density is a reflection of components like cell wall thickness and lumen area in a wood volume; which provides information on hydraulic properties (Hacke *et al.*, 2001), carbon fixation (Chave *et al.*, 2009), water economy (Martinez-Meier *et al.*, 2015; Granda *et al.*, 2017), and paleoclimate records (i.e. temperature) (Briffa *et al.*, 2004; Chen *et al.*, 2012a; Cerrato *et al.*, 2019). For example, maximum latewood density (MXD) is useful to reconstruct past growing season temperatures while minimum earlywood density (MID) helps to understand water transport efficiency (Wang *et al.*, 2002; Wu *et al.*, 2008; Camarero *et al.*, 2014; Camarero and Gutiérrez, 2017).

Climate change is occurring with parallel effects of rising atmospheric CO_2, elevated temperatures, altered precipitation patterns, and extreme weather events (IPCC, 2013; Blunden and Arndt, 2018). In this context, high-elevation forests that are particularly sensitive ecosystems (Holtmeier, 2009; Körner, 2012), are suitable to test climate change effects since temperature variation is lower than that observed at low-land ecosystems (Körner, 2007). Under this climatic outlook, we expect that trees growing at the tree-line zone adjust their tree-ring density to secure an efficient water transport system and provide adequate support, balancing the trade-offs of transpiration and photosynthesis. For example, recent human-induced warming conditions in the French Alps are associated with adjustments of latewood and earlywood density, which may be also related to tree dieback resulted from droughts (Rozenberg, 2019).

While many studies have addressed long-term trends in wood density from forests in the Northern Hemisphere, there is a need for more studies at temperate ecosystems such as

Mexican forests (González-Cásares *et al.*, 2016; Pompa-García and Venegas-González, 2016; Morgado-González *et al.*, 2019). Retrospective wood density studies are essential to understand past climate variability effects on forest ecosystems over long temporal and large-spatial scales. In Mexico, high-elevation forests are dominated by the Mexican Mountain Pine (*Pinus hartwegii* Lindl.), a forest species sensitive to climate as documented by dendrochronological studies (Yocom *et al.*, 2012; Villanueva-Díaz *et al.*, 2015; Cerano-Paredes *et al.*, 2016; Astudillo-Sánchez *et al.*, 2017) and threatened by habitat reduction (Gómez-Mendoza and Arriaga, 2007; Ricker *et al.*, 2007; Rehfeldt *et al.*, 2012). Recently, Correa-Díaz *et al.* (2019) found a declining radial growth trend in mature *P. hartwegii* trees starting around the middle twentieth century. It is therefore worthy to investigate if this forest, among others closely located, shows a significant variation in tree-ring density as an early signal of potential diebacks. Indeed, it has been shown that reduced growth in along with higher minimum wood density and wood chemical composition may serve as early-warning signals of drought-triggered forest dieback (Hevia *et al.*, 2019).

At present, new research is focused to link dendrochronology (e.g. tree-ring widths, wood isotopic compositions, etc.) to remotely sensed information, with a potential to evaluate xylogenesis process spatially (Kaufmann *et al.*, 2008; Berner *et al.*, 2011; Bunn *et al.*, 2013; Vicente-Serrano *et al.*, 2016; Correa-Díaz *et al.*, 2019). However, tree-ring density and remotely sensed data have not been fully studied (D'Arrigo *et al.*, 2000; Andreu-Hayles *et al.*, 2011; Beck *et al.*, 2013). Thus, recognized knowledge gaps exist in how other tree-ring wood density variables such as Minimum Earlywood Density (MID), Average Wood Density (AVE) or even Maximum Latewood Density (MXD) are linked to Normalized Difference Vegetation Index (NDVI) across different forests ecosystems and if others remotely-sensed variables (i.e. Enhanced Vegetation Index-EVI and Leaf Area Index-LAI) can capture a more comprehensive footprint of xylogenesis than traditional NDVI.

Here, we present the temporal variation in tree-ring wood density for two high-elevation forests in central Mexico and the spatio-temporal links with remotely sensed variables.

To assure topographic variation, we selected two mountains with contrasting geomorphology and at each of them, we included contrasting sites with different elevation and aspect. The objectives were: (i) evaluate the topographic effect (altitude and aspect) in tree-ring wood density profiles, (ii) correlate climatic variables with wood density components, (iii) assess temporal trends and stability in long-term tree-ring densities and (iv) estimate links between wood density and remotely-sensed variables using a well-known source of remote-sensing data based on Moderate Resolution Imaging Spectro-radiometer (MODIS). We hypothesized that wood density vary with topographic conditions and that this variation is associated to remotely-sensed variables. Furthermore, since a declining radial growth trend has been observed in *P. hartwegii* forests, we expect a physiological adjustment reflected in a temporal variation in tree-ring wood density (Correa-Díaz *et al.*, 2019).

3.4. Materials and Methods

3.4.1. Study sites

Two high-elevation mountain ranges across the Trans-Mexican volcanic belt were studied, known as Tlaloc Mountain (TLA) (19.39° N, -98.74°O and 4,125 m asl) and Jocotitlán (JOC) (19.72° N, -99.76°O and 3,910 m asl) located in Central Mexico (Figure 3. 1). At present, there is no commercial logging in the study sites since both places are located within conservation polygons (National and State Park for TLA and JOC, respectively). The dominant tree species is *Pinus hartwegii* Lindl, occupying the upper altitudinal range as pure, uneven-aged stands (Perry, 1991). In this study, we sampled *P. hartwegii* trees using altitudinal transects (3500-3900 and 3700-3800 m asl for TLA and JOC, respectively) and contrasting aspects (Northwest and Southwest) to test climate change responses across its altitudinal distribution range. Although temperature variables are quite similar between mountain ranges (7.7 ± 0.3 °C, 17.48 ± 0.7 °C, and -2.29 ± 0.5 °C for binned average, maximum, and minimum temperatures by mountains during the 1902-2016 period, respectively) according to software ClimateNA v6.11 (Wang *et al.*, 2016), TLA received around 130 mm more of annual rainfall than JOC (Figure 1b and 1c). Nevertheless, both sites are classified as temperate subhumid (*C(w^2)*) according to Köppen climate classification as modified by García (2004) for Mexico conditions. The

type of soil in both sites is classified as an Andosol, which is a typical soil of the volcanic highlands with both, high water-holding, and carbon storage capacities (Dubroeucq *et al.*, 2002).

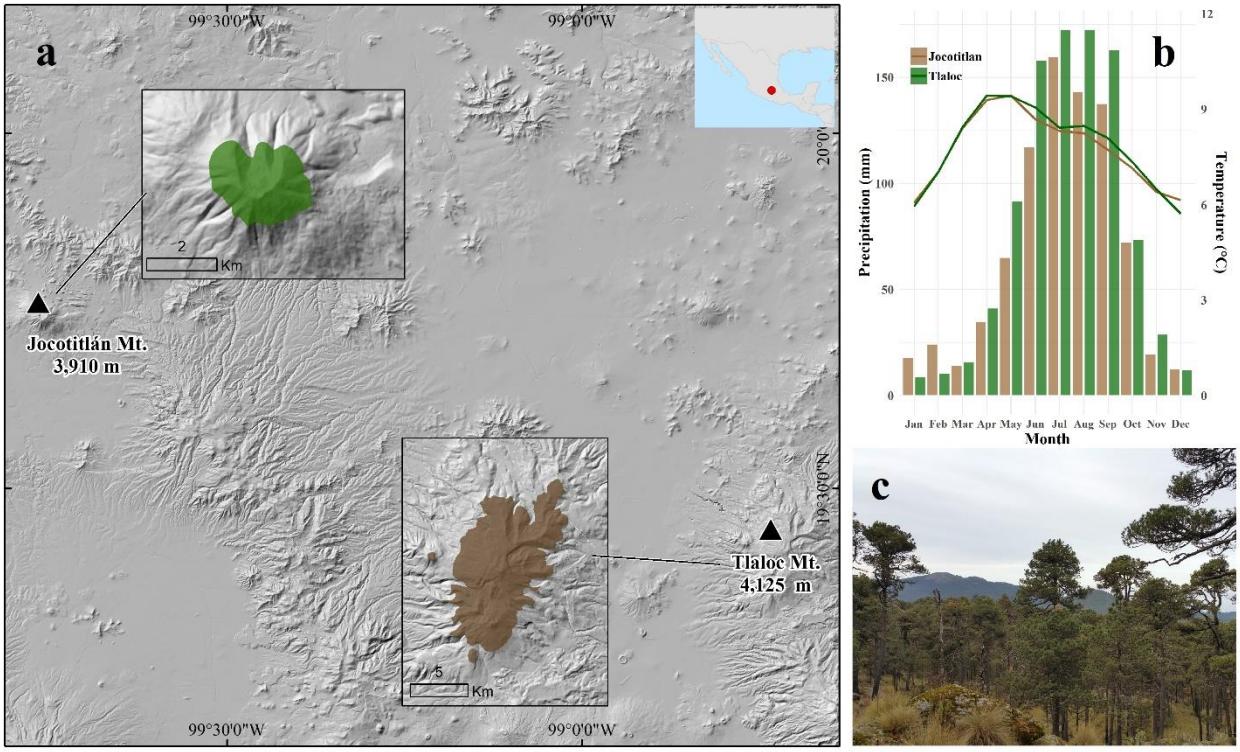

Figure 3. 1 (a) Localization of the study area (Tlaloc-TLA and Jocotitlán-JOC), (b) Climograph of the mean monthly temperature and precipitation values according to climatic data extracted using ClimateNA (Wang et al., 2016), and (c) General view of Mexican high-elevation forest.

3.4.2. Sample collection and density measurements

At both mountains (TLA and JOC), we collected 80 increment-core samples at breast-height, using a six-mm diameter Pressler borer. The average tree samples per topographic condition (altitude x aspect) was 10. Dominant and healthy mature trees were sampled. Once the increment cores were oven-dried, they were sawn using a twin blade to obtain 1.5 mm thick cross-sections and then, resin-extracted with a pentane bath. In order to obtain X-ray data, each core was exposed about 25 minutes to X-ray densitometry (Polge, 1978; Mothe *et al.*, 1998). Then, the X-ray microfilms were scanned with a resolution at 4000 dpi using WinDendro (Regent Instruments Inc., Canada).

WinDendro software converts the gray levels of the X-ray microfilms to density values by comparing them to a standard of known physical and optical density through a calibration curve (Schweingruber, 1996). Some trees were discarded in this process because of blurred information by micro rings (≈ 20% of total). Finally, we calculated for each annual ring; MID, AVE, and MXD. All samples were prepared and processed at INRA Val de Loire Centre, Orleáns France.

3.4.3. Mountain and topographic gradient effect on density profiles

The variations in tree-ring density variables (MID, AVE, and MXD) were tested by non-linear mixed-effects models for repeated measured data using R (‘*nlme’* package) (Franceschini *et al.*, 2012; Pinheiro *et al.*, 2018). First, we tested significant differences for the average wood density profiles between mountain ranges, using trees and cambial age as random factors. The correlational structure of the repeated measurement by year was included by an autoregressive process of order 1 (AR1). Since we found no significant differences between mountain profiles, we decided to combine them into a regional database to test the elevation, aspect, and cambial age effects. Differences between topographic conditions (estimated marginal means) were tested by pairwise comparison using the post hoc Bonferroni’s adjustment using *emmeans* library in R (Hochberg, 1988).

3.4.4. Unbiased trends of density profiles and temporal stability

In order to obtain MID, AVE, and MXD unbiased data by the cambial age effect, we adjusted the density measurements with a linearly non-parametric method (Rozenberg, 2019). This method uses the sum of the non-adjusted time series plus the mean of the cambial age effect minus cambial age effect at each cambial age. The use of the subtraction operator instead of the ratio allows producing time series in the original density scale (g cm $^{-3}$). Afterward, we tested the calendar year effect by linear mixed-effects models for repeated measured data as described above, using the slope and significance as indicators of long-term trends.

Empirical cumulative distribution functions (CDF) were calculated for adjusted MID, AVE, and MXD time series to probe the stability of the tree-ring density using a breaking point in 1950. Then, we used the nonparametric Kolmogorov-Smirnov (KS) test to prove that the distribution function of the period < 1950 is equal to the following (> 1950), similar to the approach used by Andreu-Hayles *et al.* (2011).

3.4.5. Climatic influence on tree-ring wood density profiles

We correlated monthly temperature (maximum and minimum), precipitation and soil moisture to adjusted average density profiles by altitude level (i.e. 3500, 3700, 3800, 3900 m asl) using the bootstrapped Pearson's correlation using '*treeclim*' in R (Zang and Biondi, 2015). All climatic variables, excluding soil moisture, were obtained using a downscaled time series (according to 250-m digital elevation model) generated by software package ClimateNA v550 (Wang *et al.*, 2012; Wang *et al.*, 2016), based on the Climate Research Unit database (CRU ts 4.01). Soil moisture was retrieved using the data from the project Climate Change Initiative (CCI) from the European Space Agency (ESA). This spatial database consists of three surface soil moisture daily-data sets from 1978 to 2016, where we used the combined product (volumetric units $m^3\ m^{-3}$) with a spatial resolution of 0.25°.

3.4.6. Linking remotely sensed variables from MODIS to wood density profiles

We compared the Normalized Difference Vegetation Index (NDVI) and Enhanced Vegetation Index (EVI) 16-day composite time series (250-meter spatial resolution) (Didan, 2015), and Leaf Area Index (LAI) 8-day composite time series (500-meter spatial resolution) (Myneni *et al.*, 2015), extracted by the application for extracting and exploring analysis ready samples (AppEEARS) (AppEEARS, 2019) with the adjusted tree-ring density values (using non-parametric and dendrochronological approaches) from 2000 to 2016. Preprocessing analysis included pixel quality analysis (avoiding snow- and cloud-contaminated pixels), harmonic interpolation (when pixel gaps were presented) and maximum value composite for LAI data (16-day composite) (Jenkerson *et al.*, 2010; Eastman, 2016).

A Pearson product-moment correlation coefficient was used to explore the link between temporal and spatial variables as described by Correa-Diaz et al., 2019, where the yearly measurements (i.e. MXD chronology) are spatially correlated with remotely-sensed maps from November of the previous year until September of the current year. Once the correlation maps are calculated, not statistically significant pixels are masked out according to their p-values. This procedure allows for detecting the highest spatio-temporal association between yearly and weekly data.

3.5. Results

3.5.1. Tree-ring density statistics and the cambial age effect

Maximum latewood density (MXD) ranged from 0.35 to 0.97 g cm $^{-3}$, with no statistical difference for the mean value (0.68 g cm $^{-3}$ for TLA and JOC) (Bonferroni's adjustment, p = 0.53). We also did not find a statistical difference for the mean earlywood profile (0.38 g cm $^{-3}$, p = 0.32) (Figure 3. 2a). The minimum earlywood density (MID) ranged from 0.16 to 0.72 g cm $^{-3}$at both mountains. Average density (AVE) for both mountains was statistically similar (0.48 g cm $^{-3}$, p=0.40) (Figure 3. 2b). Tree-ring wood density series at TLA spanned from 1793 to 2016, with a maximum cambial age of 196 y, whereas the maximum cambial age for JOC was 134 y (1880 to 2016).

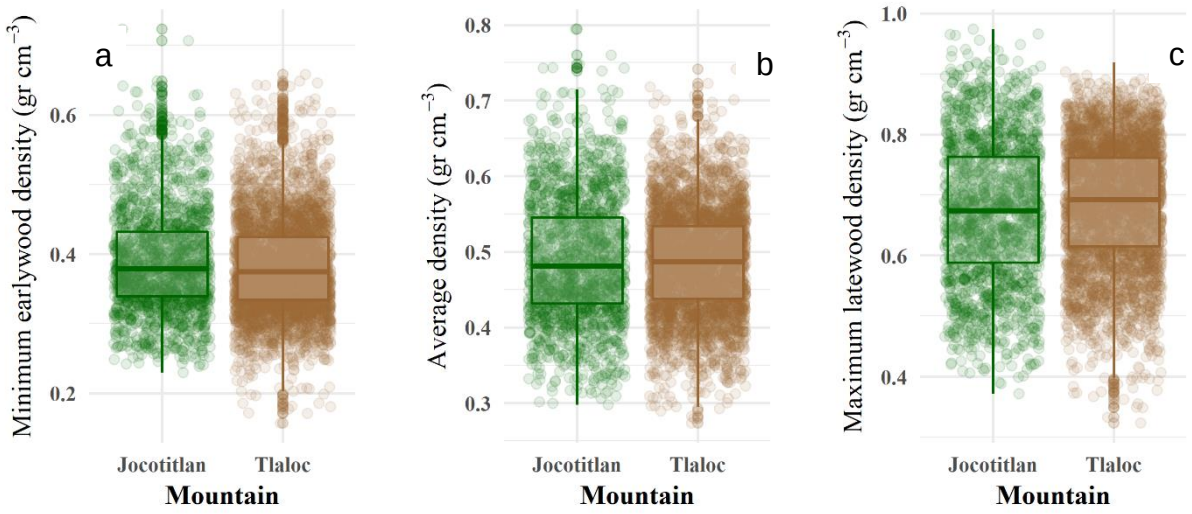

Figure 3. 2 Tree-ring wood density at two high-elevation forests in central Mexico (a) minimum earlywood, (b) average and (c) maximum latewood density. Note that for all cases the mean values were statistically similar.

Raw tree-ring widths were negatively associated to MID and AVE for TLA (r = -0.50 and r = -0.33) and JOC (r = -0.45 and r = -0.39), and positively related to MXD only at TLA (r = 0.29). The cambial age effect showed a sharp increase in the tree-ring wood density near to the pith (in the juvenile stage), with an inflection point around a cambial age of 40 years. Conversely to the expected plateau in wood density for mature trees (> 100 years), we found a constantly increasing trend in MID and AVE for TLA but an evident reduction in MXD for JOC (Figure 3. 3).

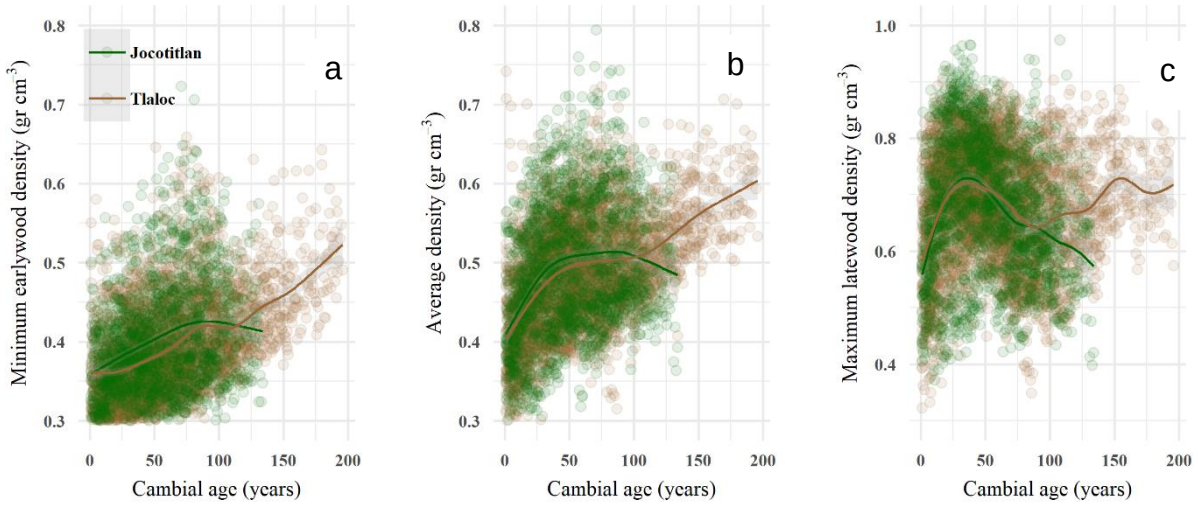

Figure 3. 3 Cambial age effect for (a) minimum earlywood density (MID), (b) average density (AVE) and (c) maximum latewood density (MXD). The solid line represents a generalized additive model fit by Mountain.

3.5.2. Elevation and aspect variations for tree-ring wood density

We found that all tree-ring wood density variables showed an altitude ($p < 0.01$) and cambial age effect ($p < 0.01$) with no differences between mountains ($p = 0.81$). The aspect was not statistically significant for MID ($p = 0.52$), AVE ($p = 0.58$), or MXD ($p = 0.46$), however the interaction altitude x aspect was significant for MXD ($p = 0.04$), and marginally significant for MID ($p = 0.08$) (Table 3.1).

Table 3. 1 Results of the analysis of variance on linear mixed-effects models fitted to the tree-ring wood variables of *Pinus hartwegii*. In the analysis, tree and cambial age were tested as random factors. DF, degrees of freedom. Significance levels †p < 0.1, *p < 0.05, **p < 0.01 and ***p < 0.001

Variable	Fixed Effect	DF	F-value	p-value
MID	Altitude	55	5.152	0.003**
	Aspect	55	0.420	0.520
	Altitude x Aspect	55	2.378	0.080†
	Cambial age	5508	52.079	<0.001***
AVE	Altitude	55	7.622	<0.001***

	Aspect	55	0.309	0.581
	Altitude x Aspect	55	1.609	0.198
	Cambial age	5508	0.580	<0.001***
MXD	Altitude	55	6.450	<0.001***
	Aspect	55	0.549	0.462
	Altitude x Aspect	55	3.054	0.036*
	Cambial age	5508	67.623	<0.001***

Significantly higher MID and AVE were seen at 3700 m asl, regardless site aspect. Thus, statistical differences (using Bonferroni's adjustment for multiple comparisons) for MID were between the 3700-NW site (altitude-aspect) and 3500-NW, 3800-SW, and 3900-NW sites ($p < 0.05$) (Figure 3. 4a). For AVE, differences were between the 3700-SW site and 3800-SW, and 3900-NW ($p < 0.05$), and marginally for 3500-NW and 3900-SW sites ($p < 0.10$) (Figure 3. 4b). Finally, differences for MXD were found between the 3700-SW site and 3800-NW, 3900-NW, 3800-SW and 3900-SW sites ($p < 0.05$) (Figure 3. 4c).

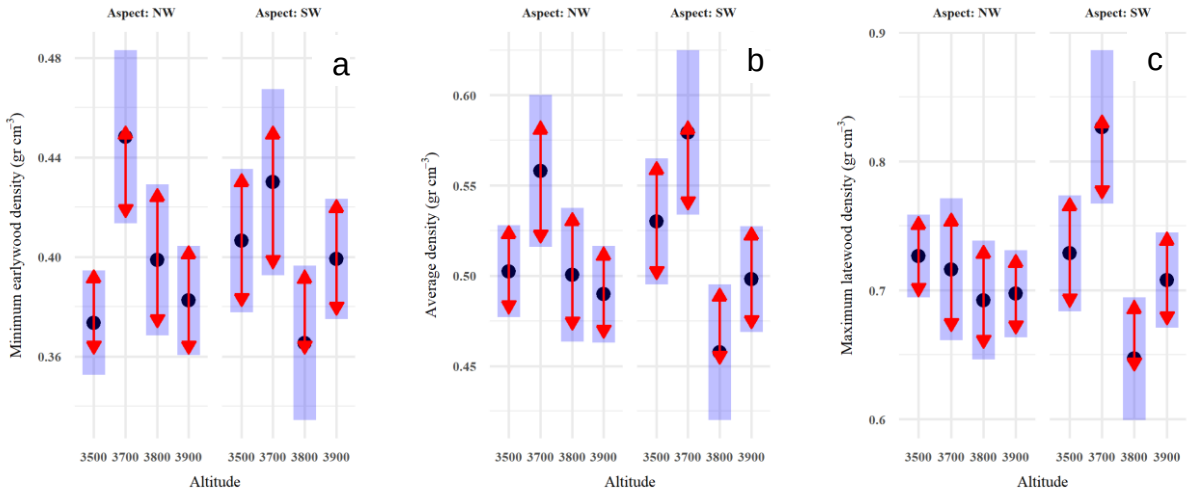

Figure 3. 4 Graphical comparison for topographic condition (altitude and aspect) in tree-ring wood density variables. Blue bars represent confidence intervals for estimated marginal means, and red arrows are comparisons among them. Thus, if the arrows overlap, the difference is not significant.

3.5.3. Trends and stability in adjusted tree-ring wood density profiles

Results showed that in TLA site, MID statistically increase over time (p = 0.001) (calendar year) and no significant change was seen at JOC site (Figure 3. 5a). The slightly average increment in MID for TLA is equivalent to 0.003 g cm $^{-3}$ decade^{-1}. However, a carefully analysis revealed that the high-elevation sites (3900-NW and 3900-SW) had significant increases (p = 0.001) while no trend exists for low-elevation sites (p = 0.20). On the other hand, AVE and MXD did not show a year effect at any mountain (p > 0.10) (Figure 3. 5b and 3. 5c). Nevertheless, an elevation belt analysis showed a slight increase for MXD (0.006 g cm $^{-3}$ decade^{-1}, p < 0.10) in JOC at 3800 m asl. The range in tree-ring wood density (i.e. the difference between MXD and MID) revealed the same pattern that MID, where a calendar year effect was significant in TLA (p = 0.03) but not in JOC (p = 0.66). Thus, a lower range or a negative trend was observed in the high-elevation sites over the last decades (p = 0.04) for TLA, mainly related to higher MID.

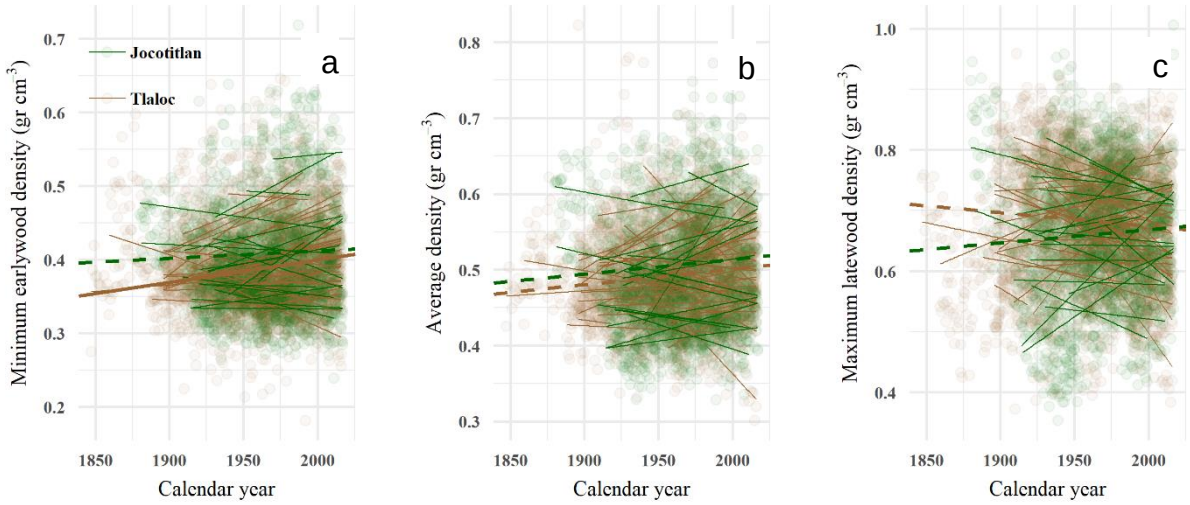

Figure 3. 5 Linear mixed effect predictions for minimum earlywood density (MID), average density (AVE) and maximum latewood density (MXD) grouped by tree level. The solid line represents a long-term linear trend when the calendar year was significant while the opposite with the dotted.

The empirical Cumulative Distribution Functions (CDF) and the Kolmogorov-Smirnov test confirmed that all tree-ring wood density distributions were significantly different between the two periods, < 1950 and > 1950 (Table 3.2). Remarkably, we saw the same pattern between mountains for MID and AVE, showing a shift to denser rings after the second

half of the 20th century. However, for MXD a different conclusion arose at each mountain, whereas a larger CDF after 1950 ($p < 0.001$) was found in TLA (less denser rings), and a smaller CDF was found for JOC (denser rings > 1950) ($p < 0.001$).

Table 3. 2 Comparison of empirical cumulative distribution functions (CDF) between two periods (< 1950 and > 1950) for tree-ring wood density variables according to Kolmogorov-Smirnov tests.

Tree-ring wood density variable	Tlaloc < 1950 vs >1950		Jocotitlán < 1950 vs >1950	
Minimum earlywood density	Null hypothesis	p-value	Null hypothesis	p-value
Equal[1]	Rejected	<0.001	Rejected	0.005
Larger[2]	Not rejected	0.11	Not rejected	0.07
Smaller[3]	Rejected	<0.001	Rejected	0.002
Average density				
Equal[1]	Rejected	<0.001	Rejected	0.01
Larger[2]	Not rejected	0.71	Not rejected	0.81
Smaller[3]	Rejected	<0.001	Rejected	0.006
Maximum latewood density				
Equal[1]	Rejected	<0.001	Rejected	<0.001
Larger[2]	Rejected	<0.001	Not rejected	0.22
Smaller[3]	Not rejected	0.24	Rejected	<0.001

[1] Ho: The CDF's come from the same distribution

[2] Ho: The CDF of <1950 is not less than CDF of >1950. <1950 is a larger CDF ≈ Less dense rings

[3] Ho: The CDF of <1950 is not greater than CDF of >1950. Smaller CDF ≈ Denser rings

3.5.4. Responses of wood density to climate

MID responded positively to the temperature (maximum and minimum) during almost the complete year, regardless of their altitude. Remarkably both mountains followed the same pattern, with the maximum correlations in April for minimum temperature ($r = 0.55$, $p < 0.01$) and during the summer season for maximum temperature ($r = 0.54$, $p < 0.01$) (Figure 3. 6a). In contrast, precipitation and soil moisture were not significantly related to MID except for few months at 3500 and 3700 m asl levels (Figure 3. 6a). A divergent response was seen for maximum temperature correlated to MXD since the lowest elevation belt (i.e. 3500 m asl) showed negative correlations mainly in April ($r = -0.40$, $p < 0.01$) while positive for the highest elevation site in JOC ($r = 0.22$, $p < 0.01$). In the same way, we found negative (3500 m asl), and positive (3800 m asl) correlations with minimum temperature. Finally, MXD showed a negative relationship with soil moisture during the summer at the lowest elevation belt (3500 m asl) (Figure 3. 6b).

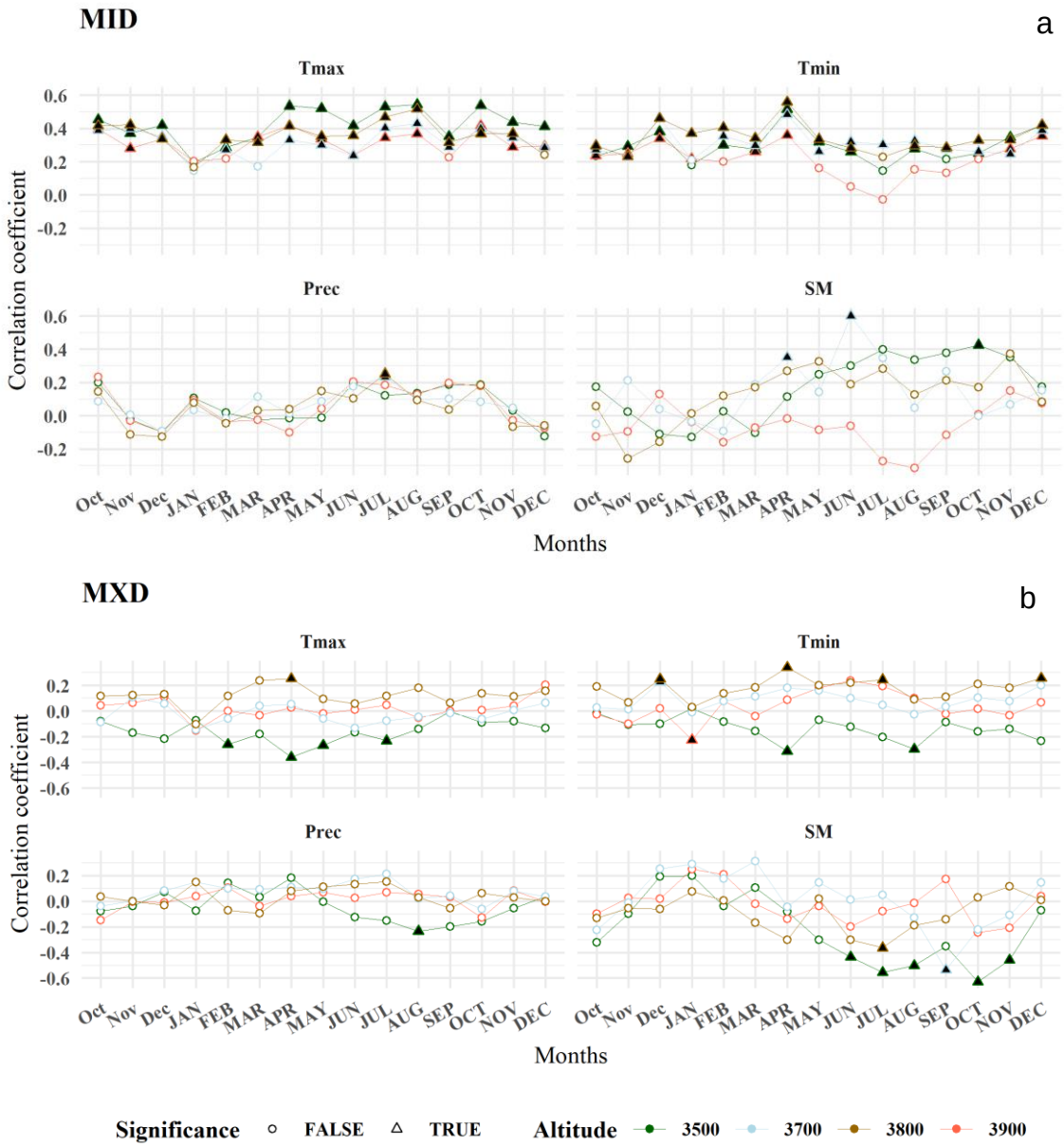

Figure 3. 6 Correlations between adjusted minimum earlywood density (MID) and maximum latewood density (MXD) and monthly climatic variables (Tmax- maximum temperature (°C), Tmin- minimum temperature (°C), Prec- precipitation (mm) and SM- Soil moisture (m^3 m^{-3}) at two high elevation forests (3500 - 3900 for Tlaloc, and 3700 – 3800 for Jocotitlán). Significant correlations are indicated by triangles at the 0.01 significance level. Months of the previous year are indicated by lowercase letters while current in uppercase letters.

3.5.5. The connection between remotely sensed information and wood density traits

Significant correlations were detected between remotely sensed information and tree-ring wood density variables; however, the better associations (referred to the total surface with high correlations) were in TLA for MXD. Figure 3. 7 summarizes the Pearson correlation with the total area for both mountains. Overall, positive correlations were for MXD, negative for MID and a divergent pattern for AVE.

The MXD correlated strongest with the NDVI for TLA from previous winter to spring with a maximum association in early-March (day of the year 065, r = 0.59, and 56% total area), and with LAI in late August (doy 241, r = 0.58, 37% total area). However, these associations were not similar for the JOC site (Figure 3. 7). The MID was negatively correlated with NDVI from previous winter to spring with a maximum association in middle-January for TLA (doy 017, r = -0.60, 44% total area), and with EVI from previous-December (previous doy 337, r = -0.54, 35% total area). Finally, AVE was negatively correlated with EVI in early-April for JOC (doy 097, r = -0.55, 55% total area). Spatially, we did not find an altitudinal or aspect effect, thus, significant pixels were located across different topographic conditions. For TLA, the northernmost part was more suitable to establish significant links between tree-ring wood density variables and remotely sensed data (Figure 3. 8a). Thus, the MXD was able to mirror the photosynthetic activity from the spring season, reflecting low peaks in 2003, 2011 and 2013 (Figure 3. 8b).

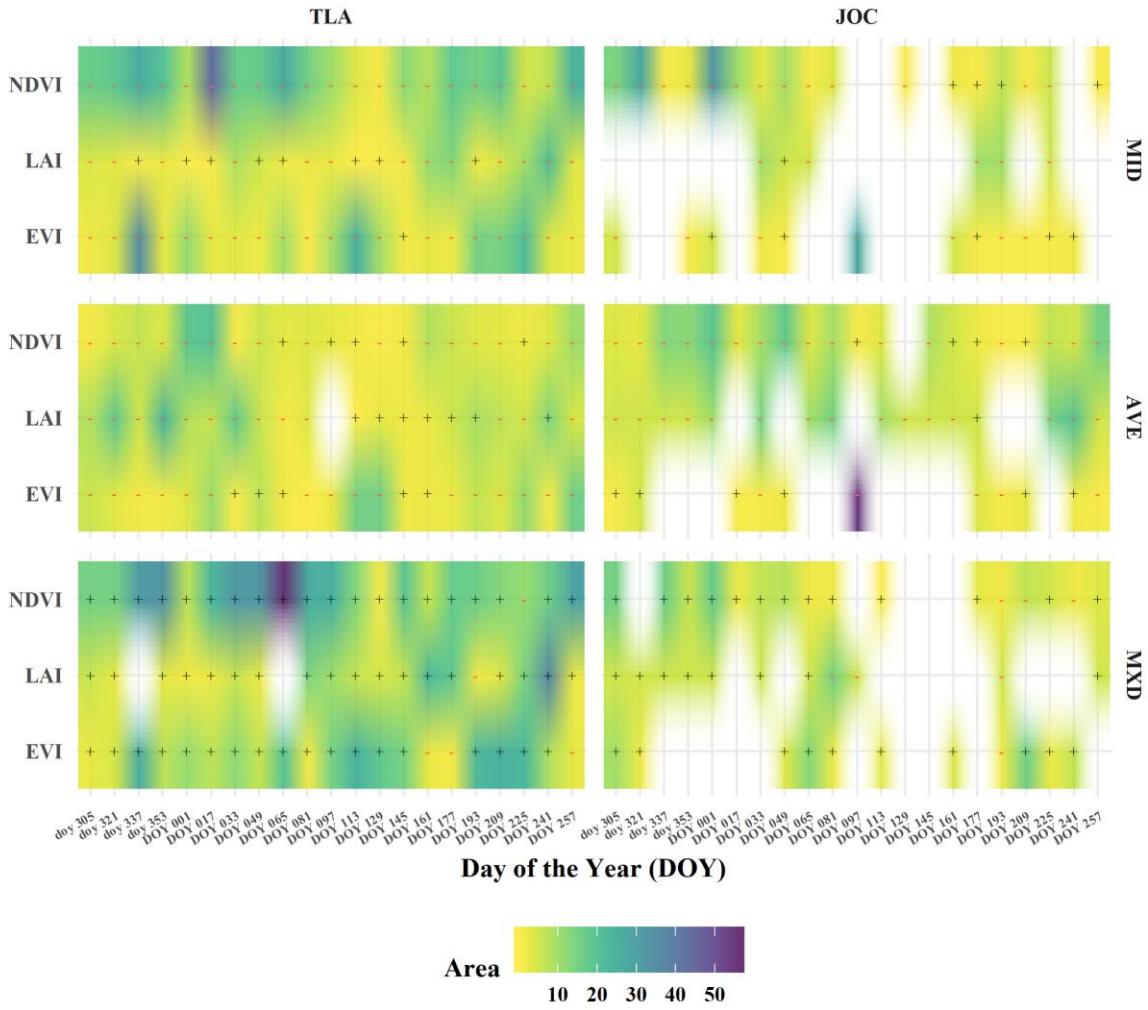

Figure 3. 7 Temporal associations between density chronologies (Minimum earlywood density-MID, average density-AVE, and maximum latewood density-MXD) with remotely sensed variables derived from MODIS (Normalized Difference Vegetation Index-NDVI, Leaf Area Index-LAI, and Enhanced Vegetation Index- EVI) in two high-elevation forests in central Mexico (Tlaloc-TLA and Jocotitlán -JOC). The color ramp represents the area covered by a significant correlation while the symbols (negative in red and positive in black) describe the slope of the correlation. Note that day of the year (day) in lowercase is referred to previous-year while current-year is in uppercase.

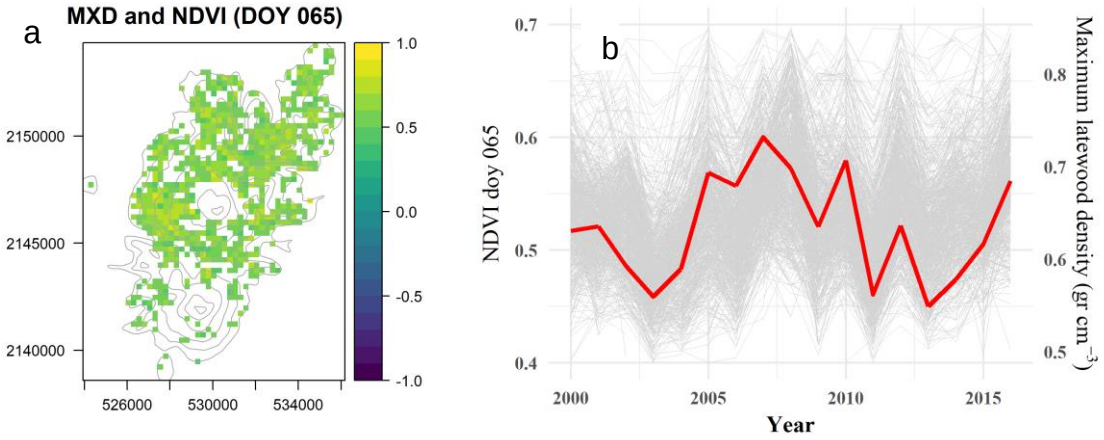

Figure 3. 8 (a) Example of the highest spatial correlation between the maximum latewood density time series (MXD) and the Normalized Difference Vegetation Index (NDVI) on the day of the year 065 at Tlaloc (TLA). Gray lines are contour-lines at 100-m intervals starting at 3500 m asl. (b) Temporal profile of significant NDVI pixels for the left panel (grey lines) with MXD (red line).

3.6. Discussion

3.6.1. Hypothesis testing summary

Tree-ring width analysis is not the only important source of retrospective information about how forests are facing climate variability (Bradley, 2015). Our results highlighted that temporal wood density analysis can provide insights into how temperate high-elevation forests adjust their wood formation process (i.e. xylogenesis) to cope with climate variation. First, we showed that although both mountains (TLA and JOC) had the same forest species and average wood density, different wood density trends were observed with a notable MID increase at TLA, which support our hypothesis of an active adjustment to climate variability. Second, as we expected, no temporal stability in wood density was seen at any condition; indeed, denser rings were observed after the second half of the 20th century for MID and AVE regardless of the location. Conversely to the well-known idea that MXD is highly correlated to summer temperatures, we found a poor association and even MID showed a better agreement with temperature. Finally, although we compared three different spatial variables (NDVI, LAI, and EVI), the NDVI was the most important related to MXD at TLA but no concurrent at JOC.

3.6.2. Average wood density profiles of *Pinus hartwegii*

Pinus hartwegii wood density has been previously reported (Zobel, 1965; Rojas Garcia and Villers Ruiz, 2005; Rojas-Garcia and Villers-Ruiz, 2008; Morgado-González *et al.*, 2019). While average wood density values reported by Zobel (1965) and Morgado-González *et al.* (2019) are lower and higher than density found here, results from Rojas Garcia and Villers Ruiz (2005) agree with this study (0.48 g cm $^{-3}$) (Figure 3. 2). Nevertheless, this is the first study providing long-term micro density records for *Pinus hartwegii* (e.g minimum earlywood and maximum latewood).

We found average MXD values lower than *Pinus cooperi* Blanco from Northern Mexico (0.77 g cm $^{-3}$) (Pompa-García and Venegas-González, 2016) but higher than *Pinus cembra* L from the European Alps (0.56 g cm $^{-3}$) (Cerrato *et al.*, 2019), and *Pinus uncinata* Ramon ex DC in the Spanish Pyrenees (0.60 g cm $^{-3}$) (Granda *et al.*, 2017) (Figure 3. 2c). Conversely, we found higher average MID values compared with *Abies alba* Mill and *Pinus uncinata* in the Spanish Pyrenees (0.31 and 0.34 g cm $^{-3}$, respectively) (Camarero and Gutiérrez, 2017; Granda *et al.*, 2017) but lower than *Juniperus thurifera* L also in Spain (Camarero *et al.*, 2014) (Figure 3. 2a).

3.6.3. Tree-ring wood density across mountains, elevations, and aspects

As shown in Figure 3. 3, temporal variations in wood density are strongly influenced by the cambial age and tree-ring width (Rossi *et al.*, 2008; Zubizarreta-Gerendiain *et al.*, 2012; Ivković *et al.*, 2013). The negative correlation found between raw tree-ring width and density (MID and AVE) implied that any increase in radial growth resulted in lower wood density until it reaches a plateau. Lower density and wider cell lumen improves hydraulic conductivity but with a higher risk for cavitation (Camarero *et al.*, 2014). On the other hand, the positive relationship with MXD for TLA suggests the densification of woody tissues (higher carbon investment) at wider rings but only until a threshold is reached, where the relation remains stable (≈ 3 mm ring width) (Granda *et al.*, 2017).

Altitude was an important predictor explaining *P. hartwegii* wood density response whereas aspect was a poor predictor (Table 3.1). Morgado-González *et al.* (2019) found

similar results at TLA; however, they found that altitude x aspect interaction was statistically significant for AVE, while in our study was significant for MID and MXD ($p < 0.10$) but no for AVE ($p = 0.20$). Possible discrepancies could be attributed to the acquisition method since Morgado-González *et al.* (2019) tested X-ray computed tomography rather than X-ray densitometer. Many studies focused on understanding wood density response with altitude have not found a clear pattern across regions. For example, an increase (Kiaei, 2012), a decrease (Govorčin *et al.*, 2003) or even no change with altitude have been reported (Fajardo, 2018). Thus, the increase in wood density at intermediate altitudes (e.g. 3700 m asl) with a decrease at extreme altitudes (e.g. 3500 and 3900 m asl) (Figure 3. 4) is a pattern previously reported by Topaloğlu *et al.* (2016) for *Fagus orientalis* Lipsky.

3.6.4. The increase of minimum earlywood density in TLA and denser rings after 1950

The MID increase and the reduction of wood density range (i.e. MXD – MID) in TLA, highlight that trees, at high-elevation sites, are adjusting their wood formation process to climate (Figure 3. 5a). They are reducing the water transport with a lower risk of cavitation, despite that high-elevation sites had warmer and better water status conditions than low-elevation sites (Sáenz-Romero *et al.*, 2013). Nevertheless, it is interesting to point out that no all trees followed the same trend which denotes high phenotypic plasticity of *P. hartwegii* (Viveros-Viveros *et al.*, 2009) (Figure 3. 5).

Conversely to other studies showing a decrease in either average or latewood density during the second half of the twentieth century in Northern ecosystems (Briffa *et al.*, 1998; Franceschini *et al.*, 2010; Franceschini *et al.*, 2012), MID was the main wood density variable adjusted to climate variability and thus essential to understand Mexican high-elevation forests responses. The rising MID observed in TLA is concurrent with the CDF analysis since we saw a shift to denser rings after 1950 (Table 3. 2) but conversely to linear mixed models' approach, this pattern was also observed in AVE (Table 3. 2). This implies that when the individual variability of trees is not accounted (i.e. CDF analysis), MID and AVED are indistinctly increasing. In fact, although not all long-term trends in

Figure 3. 5 are statistically significant ($p < 0.05$), they matched with slope direction as Kolmogorov-Smirnov test results. For example, a less dense MXD trend found in TLA after 1950 agrees with a negative slope observed in Figure 3. 5c, in the same way, the denser MXD trend detected in JOC agreed with positive slope (Figure 3. 5c). Andreu-Hayles *et al.* (2011) reported the same wood density adjustment with a shift to denser rings after 1950 for *Picea glauca* in Alaska.

3.6.5. Climate – wood density responses

The maximum latewood density (MXD) is a well-known proxy for summer temperatures in northern forests (D'Arrigo *et al.*, 1992; Briffa *et al.*, 2004; Chen *et al.*, 2012b; Camarero and Gutiérrez, 2017; Cerrato *et al.*, 2019). Overall, MXD increases in response to higher temperatures during the growing season, allowing the production and deposition of more cell wall compounds than during shorter growing seasons (Cerrato *et al.*, 2019). However, in Mexican temperate forests an inverse relationship has been reported, Pompa-García and Venegas-González (2016) found a negative correlation with maximum temperature during the spring season. In our study, we did not find a noticeable influence of temperature but rather soil moisture was important during late growing season (Figure 3. 6b). MXD is related to cell differentiation processes (thickening or lignification) in latewood tracheids at the end of the summer season (Rossi *et al.*, 2007). The negative response found between MXD and soil moisture suggests that the growth of *P. hartwegii* is controlled by soil moisture at the lowest elevation belt (3500 m asl) which drive the thickening of cell walls and the production of tracheid lumens (Bouriaud *et al.*, 2005; Camarero *et al.*, 2014). The soil water content affects lumen size by influencing the turgor pressure during tracheid's differentiation process (von Wilpert, 1991; Liang *et al.*, 2016).

On the other hand, the positive correlations between MID and temperature (maximum and minimum) suggest that the higher values in MID are accelerated by high temperatures with an exception at the highest elevation belt (3900 m asl). Positive relationships between MID and temperature have been observed in areas subjected to seasonal droughts such as the Mediterranean region (Camarero *et al.*, 2014).

3.6.6. Mountain dependent associations between wood density and MODIS variables

During the last decades, a major effort has been made to evaluate the dynamics of wood formation (xylogenesis) at a tracheid level, assessing the rates of differentiation (cell enlarging and wall thickening), however, these studies are rare and spatially restricted (Cuny *et al.*, 2014; Cuny *et al.*, 2019). Thus, to assess xylogenesis at larger spatio-temporal scales, studies have explored relations between remotely sensed variables and the carbon allocation process. For example, several studies have correlated tree-ring width records with the NDVI across different spatial and temporal scales (Berner *et al.*, 2011; Bunn *et al.*, 2013; Vicente-Serrano *et al.*, 2016; Correa-Díaz *et al.*, 2019). However, less frequently, tree-ring density variables have also been explored (D'Arrigo *et al.*, 2000; Andreu-Hayles *et al.*, 2011; Beck *et al.*, 2013). From these studies, we can conclude that the photosynthetic activity and carbon allocation (e.g. MXD) are broadly linked although they deal with different aspects of plant growth.

Documented links between MXD and NDVI at northern latitudes showed that the summer NDVI (May and June) is an important driver of xylogenesis influencing the timing and vigor of early growing season phases on the cell differentiation process (D'Arrigo *et al.*, 2000; Andreu-Hayles *et al.*, 2011). However, we did not see the same pattern, indeed, previous winter to spring period showed a positive strong correlation (highest correlation in doy 065 – March) with NDVI at TLA but not at JOC (Figure 3. 7). This relationship implies that higher NDVI values during the first months of the year are traduced in denser woody tissues at the end of growing season but not all sites and variables are suitable to establish robust links. For example, we saw a lower correlation at JOC and with the LAI variable, thus, although both mountains are strongly temperature-limited, JOC is probably locally limited by another environmental factor. The negative correlation observed between NDVI and MID (highest correlation in doy 017 – January) indicates that high photosynthetic activity (NDVI) at this time is traduced with low MID. Perhaps because carbon allocation at the start of the growing season is primarily directed towards shoot growth (leaf area) and at the beginning of cambial activity, cell division and enlargement (i.e., wider xylem cells) have priority over cell wall thickening. Mäkinen *et al.* (2002)

reported a decrease in wood density when well-watered and optimal nutrients conditions are supplied.

The NDVI is an appropriate indicator of canopy vigor and thus the health status of plants (Kaufmann *et al.*, 2004). The fact that MXD time series at TLA mirrored the NDVI activity, capable to capture pointer years (i.e. droughts), reinforces the idea that more studies are needed to improve our understanding of the relationship between canopy and cambial activity at large spatio-temporal scale and the potential impact of climate change on forests tree growth and productivity.

3.7. Conclusions

We demonstrated that two high-elevation forest closely located, dominated by the same tree species (*Pinus hartwegii*) and even with statistically similar average density profiles, can adjust differently their xylogenesis to climate variability. These adjustments coupled with a decrease in productivity (previously reported) can provide early-warning signals of stressed forests. Moreover, conversely to widely-reported association between maximum latewood density-MXD to temperature, we reported a better association with minimum earlywood density-MID. A set of significant correlations between MXD and the normalized difference vegetation index-NDVI, makes this proxy suitable to evaluate xylogenesis spatially.

3.8. References

Andreu-Hayles, L., R. D'Arrigo, K. J. Anchukaitis, P. S. A. Beck, D. Frank and S. Goetz. 2011. Varying boreal forest response to arctic environmental change at the firth river, alaska. Environmental Research Letters 6.

AppEEARS, T. 2019. Application for extracting and exploring analysis ready samples (appeears). Ver. 2.27. NASA EOSDIS Land Processes Distributed Active Archive Center (LP DAAC), USGS/Earth Resources Observation and Science (EROS) Center, Sioux Falls, South Dakota, USA.

Astudillo-Sánchez, C. C., J. Villanueva-Díaz, A. R. Endara-Agramont, G. E. Nava-Bernal and M. A. Gómez-Albores. 2017. Climatic variability at the treeline of monte tlaloc, mexico: A dendrochronological approach. Trees 31: 441-453.

Babst, F., O. Bouriaud, D. Papale, B. Gielen, I. A. Janssens, E. Nikinmaa, A. Ibrom, J. Wu, C. Bernhofer, B. Köstner, T. Grünwald, G. Seufert, P. Ciais and D. Frank. 2014. Above-ground woody carbon sequestration measured from tree rings is coherent with net ecosystem productivity at five eddy-covariance sites. New Phytologist 201: 1289-1303.

Beck, P. S. A., L. Andreu-Hayles, R. D'Arrigo, K. J. Anchukaitis, C. J. Tucker, J. E. Pinzon and S. J. Goetz. 2013. A large-scale coherent signal of canopy status in maximum latewood density of tree rings at arctic treeline in north america. Global and Planetary Change 100: 109-118.

Berner, L. T., P. S. A. Beck, A. G. Bunn, A. H. Lloyd and S. J. Goetz. 2011. High-latitude tree growth and satellite vegetation indices: Correlations and trends in russia and canada (1982–2008). Journal of Geophysical Research: Biogeosciences 116: 1-13.

Blunden, J. and D. S. Arndt. 2018. State of the climate in 2017. Bulletin American Meteorology Society 99: 332.

Bouriaud, O., J. M. Leban, D. Bert and C. Deleuze. 2005. Intra-annual variations in climate influence growth and wood density of norway spruce. Tree Physiology 25: 651-660.

Bradley, R. S. 2015. Chapter 13 - tree rings. Paleoclimatology (third edition). Academic Press. San Diego. pp. 453-497.

Briffa, K. R., T. J. Osborn and F. H. Schweingruber. 2004. Large-scale temperature inferences from tree rings: A review. Global and Planetary Change 40: 11-26.

Briffa, K. R., F. H. Schweingruber, P. D. Jones, T. J. Osborn, S. G. Shiyatov and E. A. Vaganov. 1998. Reduced sensitivity of recent tree-growth to temperature at high northern latitudes. Nature 391: 678-682.

Bunn, A. G., M. K. Hughes, A. V. Kirdyanov, M. Losleben, V. V. Shishov, L. T. Berner, A. Oltchev and E. A. Vaganov. 2013. Comparing forest measurements from tree rings and a space-based index of vegetation activity in siberia. Environmental Research Letters 8.

Camarero, J. J. and E. Gutiérrez. 2017. Wood density of silver fir reflects drought and cold stress across climatic and biogeographic gradients. Dendrochronologia 45: 101-112.

Camarero, J. J., V. Rozas, J. M. Olano and J. M. Fernández- Palacios. 2014. Minimum wood density of juniperus thurifera is a robust proxy of spring water availability in a continental mediterranean climate. Journal of Biogeography 41: 1105-1114.

Cerano-Paredes, J., J. Villanueva-Diaz, L. Vazquez-Selem, R. Cervantes-Martinez, G. Esquivel-Arriaga, V. Guerra-de la Cruz and P. Z. Fule. 2016. Historical fire regime

and its relationship with climate in a forest of pinus hartwegii to the north of puebla state, mexico. Bosque 37: 389-399.

Cerrato, R., M. C. Salvatore, B. E. Gunnarson, H. W. Linderholm, L. Carturan, M. Brunetti, F. De Blasi and C. Baroni. 2019. A pinus cembra l. Tree-ring record for late spring to late summer temperature in the rhaetian alps, italy. Dendrochronologia 53: 22-31.

Chave, J., D. Coomes, S. Jansen, S. L. Lewis, N. G. Swenson and A. E. Zanne. 2009. Towards a worldwide wood economics spectrum. Ecology Letters 12: 351-366.

Chen, F., Y. Yuan, W. Wei, S. Yu, Z. Fan, R. Zhang, T. Zhang, Q. Li and H. Shang. 2012a. Temperature reconstruction from tree-ring maximum latewood density of qinghai spruce in middle hexi corridor, china. Theoretical and Applied Climatology 107: 633-643.

Chen, F., Y. J. Yuan, W. S. Wei, Z. A. Fan, T. W. Zhang, H. M. Shang, R. B. Zhang, S. L. Yu, C. R. Ji and L. Qin. 2012b. Climatic response of ring width and maximum latewood density of larix sibirica in the altay mountains, reveals recent warming trends. Annals of Forest Science 69: 723-733.

Correa-Díaz, A., L. C. R. Silva, W. R. Horwath, A. Gómez-Guerrero, J. Vargas-Hernández, J. Villanueva-Díaz, A. Velázquez-Martínez and J. Suárez-Espinoza. 2019. Linking remote sensing and dendrochronology to quantify climate-induced shifts in high-elevation forests over space and time. Journal of Geophysical Research: Biogeosciences 124: 166-183.

Cuny, H. E., P. Fonti, C. B. K. Rathgeber, G. von Arx, R. L. Peters and D. C. Frank. 2019. Couplings in cell differentiation kinetics mitigate air temperature influence on conifer wood anatomy. Plant Cell and Environment 42: 1222-1232.

Cuny, H. E., C. B. K. Rathgeber, D. Frank, P. Fonti and M. Fournier. 2014. Kinetics of tracheid development explain conifer tree- ring structure. New Phytologist 203: 1231-1241.

D'Arrigo, R. D., G. C. Jacoby, D. E. Bunker, C. M. Malmstrom and S. O. Los. 2000. Correlation between maximum latewood density of annual tree rings and ndvi based estimates of forest productivity. International Journal of Remote Sensing 21: 2329-2336.

D'Arrigo, R. D., G. C. Jacoby and R. M. Free. 1992. Tree-ring width and maximum latewood density at the north american tree line: Parameters of climatic change. Canadian Journal of Forest Research 22: 1290-1296.

Didan, K. 2015. Mod13q1 modis/terra vegetation indices 16-day l3 global 250m sin grid v006. Nasa eosdis land processes daac.

Dubroeucq, D., D. Geissert, I. Barois and M.-P. Ledru. 2002. Biological and mineralogical features of andisols in the mexican volcanic higlands. Catena 49: 183-202.

Eastman, J. 2016. Terrset manual. Clark University. 390 pp.

Fajardo, A. 2018. Insights into intraspecific wood density variation and its relationship to growth, height and elevation in a treeline species. Plant Biology 20: 456-464.

Franceschini, T., J.-D. Bontemps, P. Gelhaye, D. Rittie, J.-C. Herve, J.-C. Gegout and J.-M. Leban. 2010. Decreasing trend and fluctuations in the mean ring density of norway spruce through the twentieth century. Annals of Forest Science 67: 816-816.

Franceschini, T., J.-D. Bontemps and J.-M. Leban. 2012. Transient historical decrease in earlywood and latewood density and unstable sensitivity to summer temperature for norway spruce in northeastern france. Canadian Journal of Forest Research 42: 219-226.

García, E. 2004. Modificaciones al sistema de clasificación climática de koppen. 5th ed. Universidad Nacional Autónoma de México. México. 91 pp.

Gómez-Mendoza, L. and L. Arriaga. 2007. Modeling the effect of climate change on the distribution of oak and pine species of mexico. Conservation Biology 21: 1545-1555.

González-Cásares, M., J. I. Yerena-Yamallel and M. Pompa-García. 2016. Measuring temporal wood density variation improves carbon capture estimates in mexican forests. Acta universitaria 26: 11-14.

Govorčin, S., T. Sinković and J. Trajković. 2003. Some physical and mechanical properties of beech wood grown in croatia. Wood Research 48: 39-52.

Granda, E., J. J. Camarero, J. D. Galván, G. Sangüesa-Barreda, A. Q. Alla, E. Gutierrez, I. Dorado-Liñán, L. Andreu-Hayles, I. Labuhn, H. Grudd and J. Voltas. 2017. Aged but withstanding: Maintenance of growth rates in old pines is not related to enhanced water-use efficiency. Agricultural and Forest Meteorology 243: 43-54.

Hacke, U. G., J. S. Sperry, W. T. Pockman, S. D. Davis and K. A. McCulloh. 2001. Trends in wood density and structure are linked to prevention of xylem implosion by negative pressure. Oecologia 126: 457-461.

Hevia, A., R. Sánchez-Salguero, J. J. Camarero, J. I. Querejeta, G. Sangüesa-Barreda and A. Gazol. 2019. Long-term nutrient imbalances linked to drought-triggered forest dieback. Science of The Total Environment 690: 1254-1267.

Hochberg, Y. 1988. A sharper bonferroni procedure for multiple tests of significance. Biometrika 75: 800-802.

Holtmeier, F.-K. 2009. Mountain timberlines: Ecology, patchiness, and dynamics. Springer Science & Business Media. 421 pp.

IPCC. 2013. Climate change 2013: The physical science basis. Summary for policymakers. Cambridge University Press. London. 231 pp.

Ivković, M., W. Gapare, H. Wu, S. Espinoza and P. Rozenberg. 2013. Influence of cambial age and climate on ring width and wood density in pinus radiata families. Annals of Forest Science 70: 525-534.

Jenkerson, C., T. Maiersperger and G. Schmidt. 2010. Emodis: A user-friendly data source. U.S. Geological Survey Open-File Report 2010-1055: 10.

Kaufmann, R. K., R. D. D'Arrigo, C. Laskowski, R. B. Myneni, L. Zhou and N. K. Davi. 2004. The effect of growing season and summer greenness on northern forests. Geophysical Research Letters 31: L09205 09201-09204.

Kaufmann, R. K., R. D. D'Arrigo, L. F. Paletta, H. Q. Tian, W. M. Jolly and R. B. Myneni. 2008. Identifying climatic controls on ring width: The timing of correlations between tree rings and ndvi. Earth Interactions 12: 1-14.

Kiaei, M. 2012. Effect of site and elevation on wood density and shrinkage and their relationships in carpinus betulus. Forestry Studies in China 14: 229-234.

Körner, C. 2007. The use of 'altitude' in ecological research. Trends in Ecology & Evolution 22: 569-574.

Körner, C. 2012. Alpine treelines. Springer Basel. 220 pp.

Liang, E., L. Balducci, P. Ren and S. Rossi. 2016. Chapter 3 - xylogenesis and moisture stress a2 - kim, yoon soo. *In*: Funada R. and Singh A. P.s (eds.). Secondary xylem biology. Academic Press. Boston. pp. 45-58.

Mäkinen, H., P. Saranpää and S. Linder. 2002. Wood-density variation of norway spruce in relation to nutrient optimization and fibre dimensions. Canadian Journal of Forest Research 32: 185-194.

Martinez-Meier, A., M. E. Fernández, G. Dalla-Salda, J. Gyenge, J. Licata and P. Rozenberg. 2015. Ecophysiological basis of wood formation in ponderosa pine: Linking water flux patterns with wood microdensity variables. Forest Ecology and Management 346: 31-40.

McDowell, N. G. and C. D. Allen. 2015. Darcy's law predicts widespread forest mortality under climate warming. Nature Climate Change 5: 669.

Morgado-González, G., A. Gómez-Guerrero, J. Villanueva-Díaz, T. Terrazas, C. Ramírez-Herrera and P. H. de la Rosa. 2019. Wood density of pinus hartwegii lind. At two altitude and exposition levels. Agrociencia 53: 645-660.

Mothe, F., G. Duchanois, B. Zannier and J.-M. Leban. 1998. Microdensitometric analysis of wood samples: Data computation method used at inra-erqb (cerd program). Annales des Sciences Forestieres 55: 301-313.

Myneni, R., Y. Knyazikhin and T. Park. 2015. Mod15a2h modis/terra leaf area index/fpar 8-day l4 global 500m sin grid v006. NASA EOSDIS Land Processes DAAC.

Perry, J. P. 1991. The pines of mexico and central america. Timber Press. Portland, Oregon. 231 pp.

Pinheiro, J., D. Bates, S. DebRoy, D. Sarkar and R. C. Team. 2018. Nlme: Linear and nonlinear mixed effects models. R package version 3.1131.1.

Polge, H. 1978. Fifteen years of wood radiation densitometry. Wood Science and Technology 12: 187-196.

Pompa-García, M. and A. Venegas-González. 2016. Temporal variation of wood density and carbon in two elevational sites of pinus cooperi in relation to climate response in northern mexico. PLOS ONE 11: e0156782.

Rehfeldt, G. E., N. L. Crookston, C. Sáenz-Romero and E. M. Campbell. 2012. North american vegetation model for land-use planning in a changing climate: A solution to large classification problems. Ecological Applications 22: 119-141.

Ricker, M., G. Gutierrez-Garcia and D. C. Daly. 2007. Modeling long-term tree growth curves in response to warming climate: Test cases from a subtropical mountain forest and a tropical rainforest in mexico. Canadian Journal of Forest Research 37: 977-989.

Rojas-Garcia, F. and L. Villers-Ruiz. 2008. Estimation of the forest biomass of malinche national park, tlaxcala-puebla. Ciencia Forestal en Mexico 33: 59-86.

Rojas Garcia, F. and L. Villers Ruiz. 2005. Comparison of two methods for estimating the wood density of pinus hartwegii lindl. From la malinche volcano. Madera y Bosques 11: 63-71.

Rossi, S., A. Deslauriers, T. Anfodillo and V. Carraro. 2007. Evidence of threshold temperatures for xylogenesis in conifers at high altitudes. Oecologia 152: 1-12.

Rossi, S., A. Deslauriers, T. Anfodillo and M. Carrer. 2008. Age-dependent xylogenesis in timberline conifers. New Phytol 177: 199-208.

Rozenberg, P. 2019. Climate warming differently affects larch ring formation at each end of its altitudinal distribution

Sáenz-Romero, C., J.-B. Lamy, E. Loya-Rebollar, A. Plaza-Aguilar, R. Burlett, P. Lobit and S. Delzon. 2013. Genetic variation of drought-induced cavitation resistance among pinus hartwegii populations from an altitudinal gradient. Acta Physiologiae Plantarum 35: 2905-2913.

Schweingruber, F. H. 1996. Tree rings and environment dendroecology. Paul Haupt. 609 pp.

Topaloğlu, E., N. Ay, L. Altun and B. Serdar. 2016. Effect of altitude and aspect on various wood properties oforiental beech (fagus orientalis lipsky) wood. Turkish Journal of Agriculture and Forestry 40: 397-406.

Vicente-Serrano, S. M., J. J. Camarero, J. M. Olano, N. Martin-Hernandez, M. Pena-Gallardo, M. Tomas-Burguera, A. Gazol, C. Azorin-Molina, U. Bhuyan and A. El-Kenawy. 2016. Diverse relationships between forest growth and the normalized difference vegetation index at a global scale. Remote Sensing of Environment 187: 14-29.

Villanueva-Díaz, J., J. Cerano Paredes, L. Vázquez Selem, D. W. Stahle, P. Z. Fulé, L. L. Yocom, O. Franco Ramos and J. Ariel Ruiz Corral. 2015. Red dendrocronológica del pino de altura (*pinus hartwegii* lindl.) para estudios dendroclimáticos en el noreste y centro de méxico. Investigaciones Geográficas, Boletín del Instituto de Geografía 2015: 5-14.

Viveros-Viveros, H., C. Sáenz-Romero, J. J. Vargas-Hernández, J. López-Upton, G. Ramírez-Valverde and A. Santacruz-Varela. 2009. Altitudinal genetic variation in pinus hartwegii lindl. I: Height growth, shoot phenology, and frost damage in seedlings. Forest Ecology and Management 257: 836-842.

von Wilpert, K. 1991. Intraannual variation of radial tracheid diameters as monitor of site specific water stress. Dendrochronologia 9: 95-113.

Wang, L., S. Payette and Y. Bégin. 2002. Relationships between anatomical and densitometric characteristics of black spruce and summer temperature at tree line in northern quebec. Canadian Journal of Forest Research 32: 477-486.

Wang, T., A. Hamann, D. Spittlehouse and C. Carroll. 2016. Locally downscaled and spatially customizable climate data for historical and future periods for north america. PLOS ONE 11: e0156720.

Wang, T., A. Hamann, D. L. Spittlehouse and T. Q. Murdock. 2012. Climatewna—high-resolution spatial climate data for western north america. Journal of Applied Meteorology and Climatology 51: 16-29.

Wu, P., L. Wang and X. Shao. 2008. Reconstruction of summer temperature variation from maximum density of alpine pine during 1917-2002 for west sichuan plateau, china. Journal of Geographical Sciences 18: 201-210.

Yocom, L. L., P. Z. Fulé and P. Brando. 2012. Human and climate influences on frequent fire in a high-elevation tropical forest. Journal of Applied Ecology 49: 1356-1364.

Zang, C. and F. Biondi. 2015. Treeclim: An r package for the numerical calibration of proxy-climate relationships. Ecography 38: 431-436.

Zobel, B. J. 1965. Variation in specific gravity and tracheid length for several species of mexican pine. Silvae Genetica 14: 1-12.

Zubizarreta-Gerendiain, A., J. Gort-Oromi, L. Mehtätalo, H. Peltola, A. Venäläinen and P. Pulkkinen. 2012. Effects of cambial age, clone and climatic factors on ring width and ring density in norway spruce (picea abies) in southeastern finland. Forest Ecology and Management 263: 9-16.

CONCLUSIONS

We found that the multi-proxy approach developed here, including traditional dendrochronology, isotopic analysis, wood density traits, and remotely sensed variables; is robust enough to capture temporally and spatially forest responses to climate variability in central México. First, we showed that although warmer conditions observed in the study site after the year 1950, the *Pinus hartwegii* growth has been more dependent on ontogenic factors (i.e. age) and microsite conditions (e.g. soil humidity) rather than temperature. We did not find a growth stimulation on the upper elevation belt considering neither the NDVI trend analysis nor basal area increment trend analysis. Concordance between these metrics suggests that the greening effect detected in other studies should not be directly understood as gross primary productivity increase or major carbon sequestration.

The physiological processes that account for the photosynthetic activity and leaf gas-exchange showed an active response in *P. hartwegii* to the atmospheric composition change. The influence of combusted fossil C fuels and major climatic events (e.g. severe drought) were printed in the wood chemistry composition. Despite the observed rising intrinsic water use efficiency, forest growth not necessarily increased at tree-line ecotone. However, NDVI was strongly related to the wood isotopic composition providing a general methodological and conceptual frame for spatio-temporal studies of carbon and water cycling. Finally, we showed a contrasting adjustment on wood density traits in two high elevation forests closely located but related with denser rings after the year 1950, mainly with minimum earlywood density. These xylogenesis adjustments could provide a set of early-warning signals of possible forest dieback due to low hydraulic conductivity and/or carbon starvation.

Although the spatial links were constrained by the temporal availability (17 years), and spatial resolution (250 m) of remotely-sensed data, our findings can provide a general methodological and conceptual frame for detailed studies to establish robust connections between canopy activity (e.g. photosynthesis, leaf area index, chlorophyll content, etc.)

with different carbon allocation processes. However, in the near future, we expected that these approaches will be an effective way to monitor forest ecosystem's processes and functions.